JACOBS
UNIVERSITY

**Cloning, characterization and directed evolution of pyranose oxidase
from *Trametes versicolor* for biofuel cell applications**

by

Josefa Caballero Hernandez

A thesis submitted in partial fulfillment
of the requirements for the degree of

Doctor of Philosophy in Biochemical Engineering

Approved, Thesis Committee

Prof. Dr. Matthias Ullrich
Jacobs University Bremen

Prof. Dr. Alexander Lerchl
Jacobs University Bremen

Prof. Dr. Ana Linares Gil
University of Granada

Date of Defense: January, 12th 2011

School of Engineering and Science

To Jan-Gustav Strandenaes, as I promised;

And to María, my one-year old daughter,
who kindly went to bed at 9:00 every night, so that mom could accomplish this work...

…and deliver us, Oh Lord, from the wrath of the Norsemen…

Abstract

Chemical energy may be converted to electric energy using a biocatalyst (enzyme) or a whole cell. The respective device would require an anode, a cathode, a supporting electrolyte medium, and an external circuit to use the extractable power. In D-glucose-based biofuel cells, glucose oxidase (GOx) has become the prime enzyme used in the anodic compartment due to its high specificity and efficiency. Adam Heller and coworkers (2002) reported on a miniature biofuel cell based on glucose oxidation: One electrode was coated with GOx wired through a conducting polymer and striped the electrons from β-D-glucose to an external circuit. At the other electrode, another wired enzyme - bilirubin oxidase - added electrons to dissolved oxygen. According to the authors, the device produced about 1.9 microwatts, losing 6 % of its power per day, operating at a temperature and pH that resemble those of normal blood (37C, pH 7.2). These abiotic parameters are only suboptimal for most known GOxs from diverse microorganisms.

Prolonging the life span for such a biofuel cell battery is the main goal in developing implanted miniature biofuel cells. Such a device would be very attractive for diverse applications. Electrical output could be improved by tailoring GOx to optimally function at 37°C and pH 7. Alternatively, pyranose oxidase (POx) could be used. POxs show a broader substrate profile, a significantly higher affinity towards glucose and no anomeric preference. Their pH range of activity varies from 5 to 8, and at values superior to 7, the kinetics of the reaction over D-glucose is barely affected by the buffer composition. However, the catalytic efficiency needs to be improved. POxs are specially challenging since – in contrast to GOxs - there is little knowledge about POx structures, their structure-function relationships, electrochemical properties, and enzymatic stabilities. Only few relevant publications have been released in recent years and the first resolved POx structure was reported in 2004.

In the current work, POx from the basidiomycete *Trametes versicolor* was cloned from a cDNA library and was expressed in *Escherichia coli* as an intracellular active recombinant enzyme. Directed evolution via error-prone PCR-based random mutagenesis was used to generate mutant libraries, which were subsequently tested for improved catalytic efficiency of the recombinant POx variants. High-throughput screening using a

Abstract
_____

newly developed ABTS chromogenic POx assay and further cloning in a mutator *E. coli* strain led to a C-terminally truncated POx variant (trPOx), which had lost 208 of its 623 amino acid residues and exhibited a ~14-fold increased k_{cat} (from 5.5 to 78.2 s^{-1}). The apparent K_m value of trPOx decreased (from 4.5 to 0.85 mM) resulting in a ~78-fold improved catalytic efficiency (from 1.2 to 93.0 $mM^{-1}s^{-1}$). trPOx is the smallest active POx yet described.

Results of this study proved the applied directed evolution strategy to be successful at optimizing catalytic activities of POxs, which are alternative enzymes for the anodic compartment of implanted miniature biofuel cells. Simultaneously, a novel HTS assay based in the reaction of phenylhydrazine with 2-keto-glucose, the enzymatic product of POxs over D-glucose, was carefully studied. The main advantage of this assay is that POx activity relates directly to product formation and not to the formation of the cell toxic side product, H_2O_2. Moreover, this assay will allow correlating POx activity and O_2-independecy in future POxs studies. Further development of diverse screening systems, particularly ferrocenemethanol assay, was recommended in order to improve tailoring POxs for biofuel cell purposes.

ACKNOWLEDGEMENTS

First of all, I would like to thank the former Dean Professor Haerendel and Dean Professor Kramer, who gave me the opportunity to join Jacobs University Bremen and accomplish my doctoral studies, with the fantastic academic and personal intercultural experience that being a member of this institution represents.

My earnest acknowledgement goes to Professor Dr. Schwaneberg who gave me the opportunity to enter a very exciting scientific field and to join his working group. I would like to express my gratitude for his guidance and the many fruitful discussions. Thanks for the four years of supervision of my laboratory work.

My very special thanks go to Prof. Dr. Matthias Ullrich, Professor of Microbiology, first member of my PhD dissertation committee, for always being keen on assessing my work, providing stimulating suggestions as well as showing enormous patience and offering continuous encouragement and support. This thesis work would not have been possible without his outmost valuable contribution. I feel honored and extremely thankful by the way Prof. Ullrich turned the supervision of my PhD work into such a dedicated, serious and careful task.

I would like to thank the other members of my PhD committee: Prof. Dr. Alexander Lerchl, Professor of Biology at Jacobs University Bremen, and Prof. Dr. Ana Linares, Professor of Biochemistry and Molecular Biology at the University of Granada, who also serves as external reviewer, for their assessment and supervision. Also special thanks to Prof. Dr. Fernandez-Lahore, Professor of Biochemical Engineering, for assisting me with his professional guidance, informed opinions, friendship and support.

Thanks to Dr. Anke Allner, assistant to the Dean, who, despite her obligations and tight schedule, always found a moment and listened carefully, showing tolerance and dedicated support. Thanks to Amina Oezelsel, Students Counselor, for her devoted dedication to such an essential task.

CONTENTS

Contents

LIST OF ABREVIATIONS AND SYMBOLS

ABTS	2,2'-azino-bis(3-ethylbenzothiazoline-6-sulfonic acid) diammonium salt
Atm	atmosphere
BOD	billirubin oxidase
bp	base pair
cm	centimeter
CV	coefficient of variation
2,6-DCPIP	2,6 dichlorophenolindophenol
DMSO	dimethylsulfoxide
DNA	deoxyribonucleic acid
e	electron
epPCR	error prone polymerase chain reaction
ET	electron transfer
FAD	flavin adenine dinucleotide
FMN	flavin mono nucleotide
g	gram
GMC	glucose–methanol–choline (family of flavin adenine dinucleotide (FAD)-dependent oxidoreductases)
Glu	glucose
h	hour
His	histidine
HPLC	high pressure liquid chromatography
HRP	horseradish peroxidase
Ip	isoelectric point
KDa	kilodalton
LB	Luria-Bertani
mBC	minituarized biofuel cell
ml	milliliter
min	minute
M	molar
mM	milimolar
MW	molecular weight
nm	nanometer
OD	optical density
PAGE	poyacrylamide gel electrophoresis
PCR	polymerase chain reaction
PDB	protein database
POx	pyranose oxidase
rpm	rotation per minute
SD	standard deviation
SDS	sodium dodecyl sulphate
sp	species
UV	ultraviolet

1. INTRODUCTION

1.1. Pyranose oxidase

1.1.1. Natural occurrence

Pyranose 2-oxidase (POx; P2Ox; pyranose: oxygen 2-oxidoreductase; glucose 2-oxidase; EC 1.1.3.10) is a H_2O_2-producing flavoenzyme that participates in ligninolytic processes by wood-degrading basidiomycete fungi (Daniel et al. 1994; Eriksson et al. 1986; Leitner et al. 2003; Volc et al. 1985). It is located in the hyphal periplasmic space and, unlike glucose oxidase (GOx; D-glucose:oxygen oxidoreductase; glucose 1-oxidase; EC 1.1.3.4), catalyzes the oxidation in position 2 of D-glucose and other aldopyranoses (D-xylose, D-galactose, and L-arabinose) to the corresponding 2-keto derivatives (Janssen and Ruelius 1968). Oxidation in position 3 occurs to a smaller extend in certain substrates such as 2-deoxy-D-glucose, 2-keto-D-glucose and methyl-β-D-glucosides (Freimund et al. 1998; Volc et al. 1988; Volc et al. 2003). The reaction occurs with concomitant reduction of molecular oxygen to hydrogen peroxide (Giffhorn et al. 2000; Volc et al. 2003) which is subsequently used by lignin peroxidases for wood degradation in fungi (Daniel et al. 1994). POxs show typical FAD absorption maxima at 456, 345 and 275 nm (Halada et al. 2003; Leitner et al. 2001).
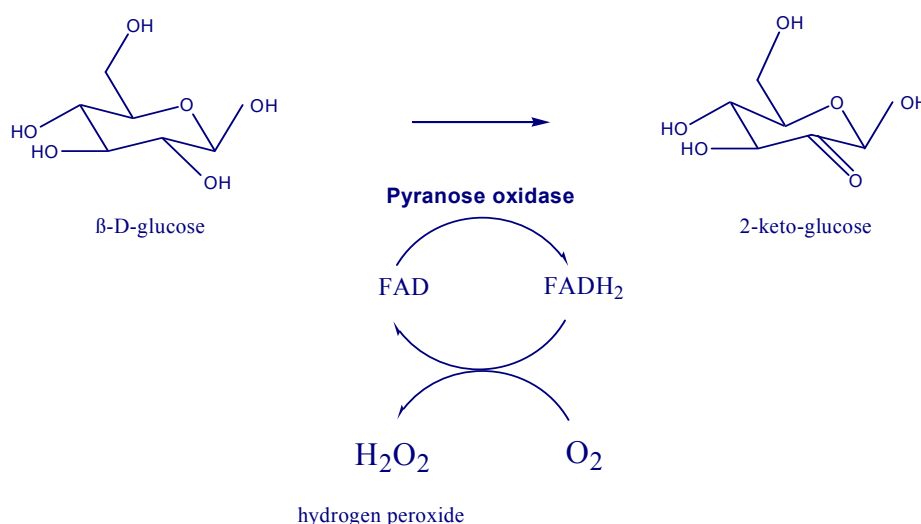
Fig 1 Oxidation of β-D-Glucose by pyranose oxidase with concomitant reduction of oxygen to water. The reaction is mediated by FAD cofactor.

Regeneration of oxidized FAD is achieved by oxygen or other substances produced during lignin degradation such as benzoquinones and radicals.

In lignin degradation, a redox cycle sustained by oxidoreductases and laccases accelerates the process. The mechanism is based on reducing quinoid or radical intermediates thus preventing their repolymerization (Ander 1994; Ander et al. 1990). Since POxs are capable of reducing several redox mediators: 1,4 benzoquinone, FMN and PSMN and 2,6 DCPIP (Huwig 1997; Machida and Nakanishi 1984; Shin et al. 1993, Yamada et al. 1967), their involvement in such systems have been suggested (Gifforn 2000).

Further reported functions of POxs comprise antifungal activity (*Tricholoma matsutake*: Takakura et al. 2003), formation of the antibiotic cortalcerone (Baute et al. 1987; *Panerochaete crysosporium*: Koths et al. 1992; Volc et al. 1991), and detoxification of compounds such as benzoquinones and radicals (Leitner et al. 2001).

POxs have been isolated from various fungal organisms including *Trametes multicolor* (synonym *Trametes ochracea*; Leitner et al. 2001), *Polyporus obtusus* (Janssen and Ruelius 1975)*, Coriolus versicolor* (Machida and Nakanishi 1984; Taguchi et al. 1985), *Panerochaete chrysosporium* (Artolozaga et al. 1997; Volc et al. 1991)*, Peniophora gigantea* (Danneel et al. 1993), *Pleurotus ostreatus* (Shin et al. 1993), *Phlebiosis gigantea* (Schaefer et al. 1996) and *Tricholoma matsusake* (Takakura and Kuwata 2003).

Fig 2 Two examples of natural occurrence of pyranose oxidases: **A** *Coriolus sp.*, **B** *Panerochaete chrysosporium*

The level of expression of sugar oxidases varies in ligninolytic cultures. GOx and POx occurred in *P. chrysosporium* (Kelley and Reddy 1986), thus making it uncertain until recent years, which enzyme GOx or POx was the major source of H_2O_2. Evidence has been shown that POxs have a major role in lignin degrading fungi. Unlike GOxs, POxs occur in a wide variety of fungal species (Baute and Baute 1984; Daniel et al. 1992, Izumi et al. 1990; Volc et al. 1985; Daniel et al. 1994) and acts on D-glucose and D-xylose, the major sugars derived from wood (Daniel et al. 1994). A cooperative function between GOxs and POxs has been discarded (Volc et al. 1996). However, cooperation has been suggested with Mn-peroxidases also located in the hyphal periplasmic space (Daniel et al. 1994).

1.1.2. POxs family and structure

Until 2004 there were no data available on POx structure. Research on these enzymes was long being performed with no knowledge on the topology of the active site, with no substrate-binding model, nor POx oligomerization pattern, etc

Only in 2004, crystal structures of native *T. multicolor* POx (Hallberg et al. 2004) and of recombinant *Peniophora sp.* POx (Bannwarth et al. 2004, 2006) were solved. MALDI spectrometry data indicated that *T. multicolor* POx is a homotetrameric enzyme with a molecular mass of 270 kDa. Each subunit is flavinylated and has a mass of 67.3 (±0.2) KDa (Leiner et al. 2001). *Peniophora sp.* POx forms a symmetric homotetramer with its four subunits interconnected via respective tetramerization loops.

Each subunit consists of a substrate binding domain, a FAD binding domain and a collar region. The FAD molecule is covalently bound to N3 of a histidine residue at position 167, via the 8α-methyl group of the cofactor (Halada et al. 2003). From a spacious central cavity formed in the tetramer, the substrate can access one of the four catalytic centers by penetrating glucose-sized pores and a highly mobile peptide loop in each of the monomers (Bannwarth et al. 2004).
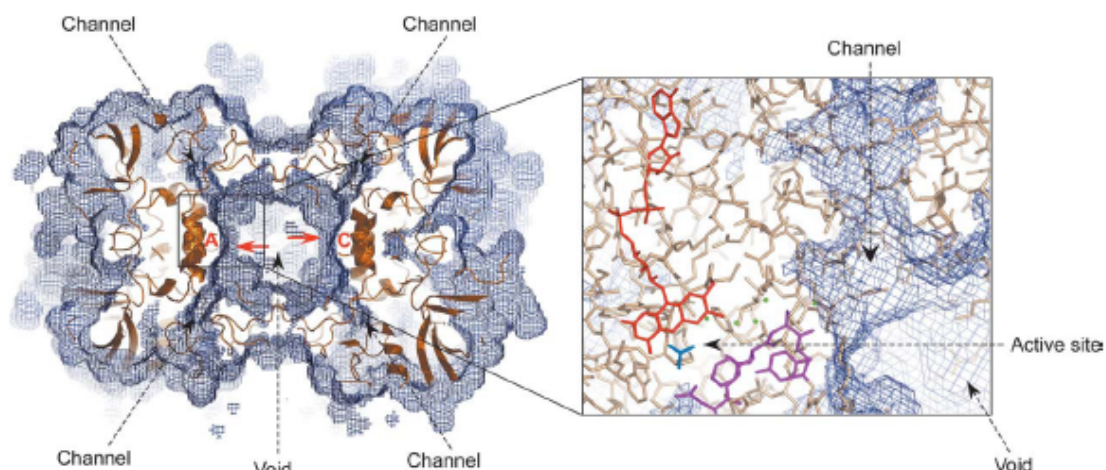
Fig 3 Cross-section of the water-accessible surface calculated for *Trametes multicolor* POx tetramer (Hallberg et al, 2004). Two subunits of the enzyme, A and C shown as a cartoon (orange), are visible in this projection and active-site entrance is indicated by red arrows. The inset to the right shows the relative location of the active site in subunit A and the top left void channel. The FAD cofactor (red), the active site loop (violet), and an acetate molecule (blue) are highlighted. Water molecules are shown as green spheres delineating the path from the void into the active site. The water-accessible surface (calculated with VOIDOO[62] using a probe radius of 1.4 Å) shows that access to the active site from the void is closed off by the active-site loop.

Hallberg et al. suggested that α-D-glucose, which is the predominant (98 %) form of D-glucose in solution (Funcke et al. 1979), would accumulate in the central cavity of the tetramer, where two the amino acid residues -Asp124 or Glu542 - could serve as the catalytic base for α-D-glucose to β-D-glucose conversion (Bannwarth et al. 2006). According to these authors, α-anomer of D-glucose cannot be oxidized directly since the respective 1-hydroxyl group would sterically collide with specific residues of the active site -Val546 and Phe474- (Bannwarth et al. 2006).

Studies on sequence similarity (Albrect and Lengauer 2003) have suggested that POx belongs to the glucose–methanol–choline (GMC) family of flavin adenine dinucleotide (FAD)-dependent oxidoreductases (Cavener 1992) which include *Aspergillus niger* glucose 1-oxidase (GOx), *Brevibacterium sterolicum* cholesterol oxidase (ChOx), and the flavoprotein domain (DHcdh) of *P. chrysosporium* cellobiose dehydrogenase (CDH).

Structural comparisons within the GMC family indicated close structural relationships between glucose oxidase, hydroxynitrile lyase, cellobiose dehydrogenase, cholesterol

oxidase and POxs (Albrect and Lengauer 2003). Despite low sequence identity values (14-22 %) to other GMC oxidoreductases, sequence alignments revealed the conservation of structurally and functionally important residues in POxs (Albrect and Lengauer 2003). Structural relationships are rather close since more than 70% of all residues align within a 3 Å distance for C-α atoms (Bannwarth et al. 2004).

Hydroxynitrile lyase, cellobiose dehydrogenase, and cholesterol oxidase are monomeric, glucose oxidase is a dimer and POx occurs as a tetramer. The tetrameric structure of POx is formed through a dimer of dimers. A dimeric subunit of POx has similar surface areas of protein-protein interactions as GOx. The interface areas are however not highly conserved. Superimposition of GOx and POx dimers showed deviations in the range of 10 Å between the respective C-α backbones (Bannwarth et al. 2004).

It has been suggested that POxs together with the entire GMC family are derivatives of a primordial FAD-binding domain that developed large insertions at the same positions as glutathione reductase and numerous other members of the family (Bannwarth et al. 2004; Dym and Eisenberg, 2001).
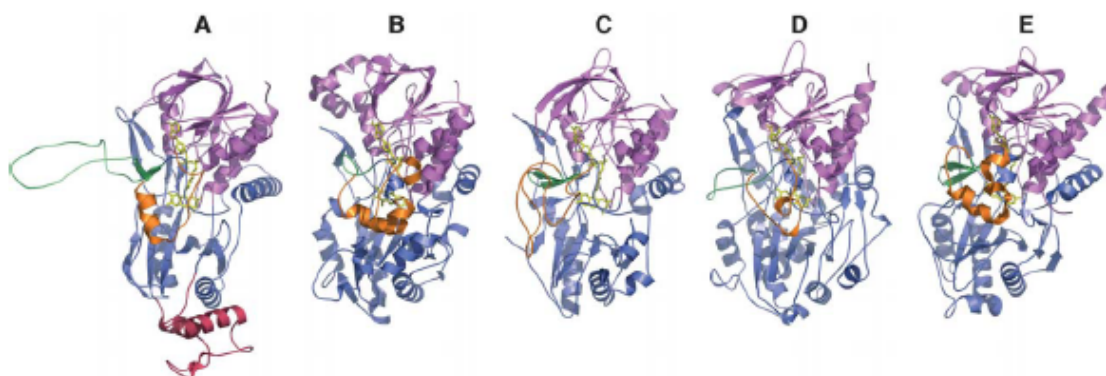
Fig 4 Comparison of the subunit structure of POx with related GMC enxymes. **A**, *T. multicolor* POx, **B** *P. chrysosporium* DH_{cdh,} **C**, *B. sterolicum* ChOx, **D**, *A. niger* GOx, **E**, *P. dulcis* FAD-HNL. Secondary structures belonging to the Rossman domain, substrate binding domain and head domain, are colored in violet, blue and red, respectively. The oligomerization loop and arm are shown in orange and green, respectively. The FAD cofactor is shown in yellow (Hallberg et al., 2004)

Specific insertions of POx are residues 115-148 which form a long loop involved in dimer formation, and a compact sequence 372-427, which is likely involved in binding to the wood surface promoting its degradation. A similar loop for the same function exists in cellobiose dehydrogenase (Bannwarth et al. 2004). In POx of *T. multicolor* the protrusion sequence (368-430) has been reported being involved in POx oligomerization due to its planar structure (Hallberg et al. 2004).

The central part of the GMC family fold is the FAD binding subdomain consisting of a five stranded parallel β-sheet featuring a Rossmann fold that includes the βαβ mononucleotide binding motif (Bannwarth et al. 2004, Rossmann et al 1975; Schulz et al. 1982; Schulz et al 1978; Wierenga et al. 1983; Wierenga et al. 1986). In POxs these β-sheets have central residues 276-73-50-316-578 and, together with the connections between β-strands, are considered the FAD domain (Hallberg et al. 2004). Using the FAD domain as reference, two large insertions can be found in POx: one that is located at the FAD domain and is formed by five loops dispersed over the entire chain fold and a second consisting of six antiparallel β-sheets with central residues 237-436-448-472-363-539 postulated to be required for substrate binding (Bannwarth et al. 2004; Hallberg et al. 2004).
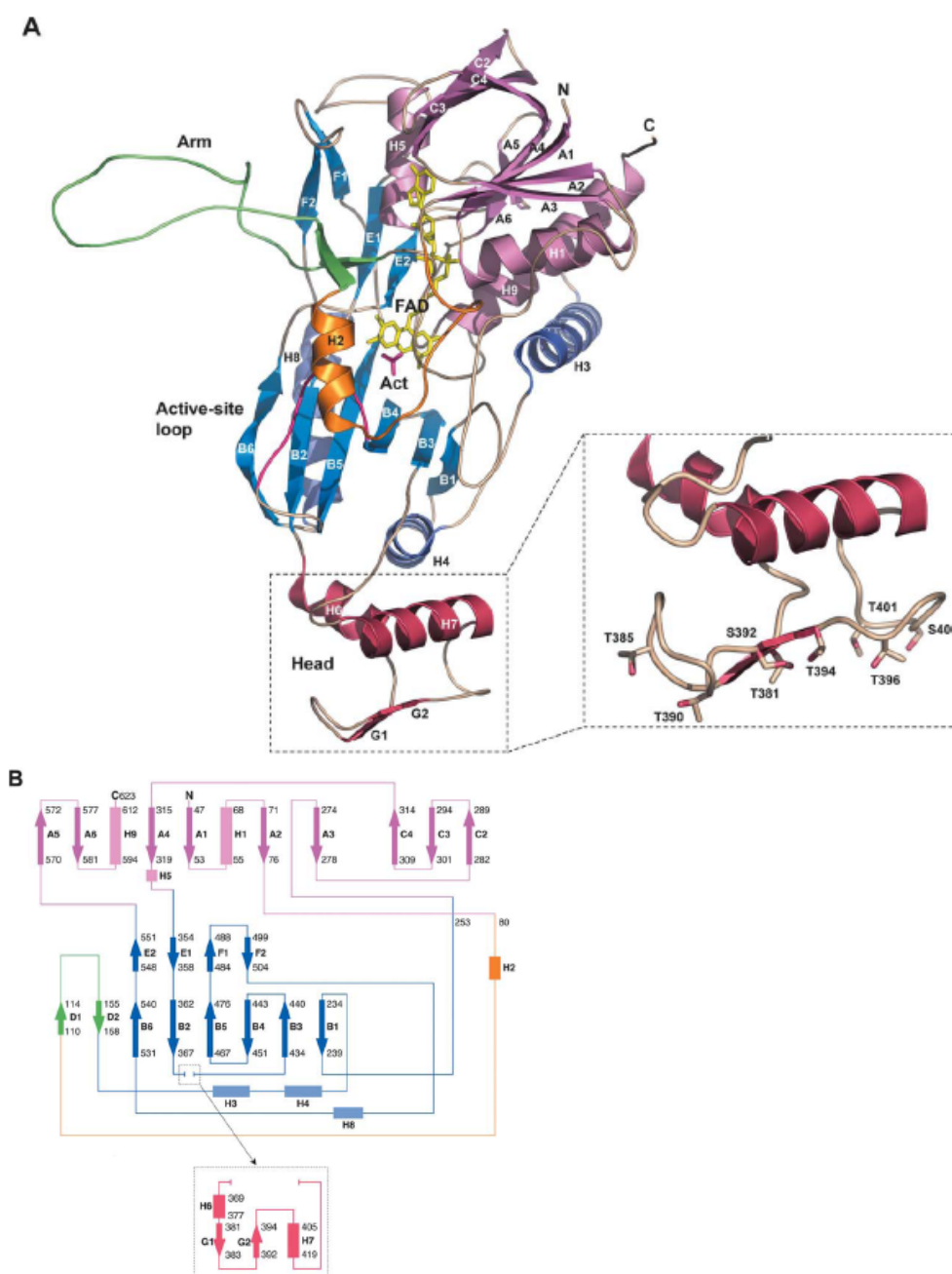
Fig 5 Structure of *Trametes multicolor* POx subunit. **A**, ribbon diagram: The FAD cofactor is shown in yellow and the head domain is shown as a picture inset. **B**, topology diagram. The head domain is shown in a picture inset. Secondary structure elements are denoted H for α-helix, and A, B or C for β-strands, and the numbering according to that used previously for DH_{cdh}[Hallberg et al, 2002]. The core β sheet in the Rossmann domain is denoted A, and the β meander is denoted C. The core β sheet in the substrate binding domain is denoted B. Additional β structures include sheets D, E, and F. Secondary structure elements belonging to the Rossmann domain, substrate-binding domain, and head domain are colored violet, blue and red, respectively. Oligomeriztion loop and oligomerization arm are shown in orange and green, respectively. Partitioning of the domains: Rossmann domain, residues 43-79, 254-353, 552-619, substrate-binding domain, residues 80-253, 354-551, head domain, 368-430, oligomeriztion loop, 80-109, oligomerization arm, 110-158 (Hallberg et al. 2004).

1.1.3 Pyranose oxidase catalytic metabolism

Lacking information on POxs structure, several studies were performed based on the reactivity of various POxs on D-glucose, L-sorbose, D-xylose, maltose and D-glucono-1,5 lactone to produce the corresponding 2-keto sugars and H_2O_2 and comparing the structures of the substrates with those of unreactive sugars. As a result, a common structure of the substrate was proposed (Janssen and Roelius, 1968). The reactive substrate would be a pyranose ring with fixed structure and conformation at positions C-2, C-3 and C-4.

Further studies showed diverse POx capabilitity of conversion of several monosaccarides and could identify the subsequent keto products (Volc et al. 1980; Daneel et al. 1993; Eriksson et al. 1986; Gabriel et al. 1993, 1994; Machida and Nakanishi 1984; Volc et al. 1991). Later studies demonstrated *P.gigantea* and *T. versicolor* POxs capability to oxidize the disaccharides melibiose and gentibiose to their 2-keto products (Freimund et al. 1998; Huwig 1997; Volc et al. 1999). A procedure with an immobilized operational improved variant of *P. gigantea* POx served to a throughout study of its catalytic capacity (Freimund et al. 1998; Huwig 1997; Huwig et al. 1997) providing data on apparent catalytic efficiencies and yields of bioconversions. Extensive chemical characterization of the products was also performed. Correlating kinetic quantitative data to structural features of the substrates, an interaction model of minimum requirements between enzyme and substrate was suggested (Giffhorn 2000). Two different modes were proposed for the regioselective C-2 and C-3 oxidation.

According to this model, the ring oxygen and the equatorial OH at C-2 have essential roles, since substituted analogues are non reactive. Passive binding occurs between oxygen and the enzyme whereas active binding occurs at C-2 for oxidation (Freimund et al., 1998, Huwig 1997). From data showing reduced activities on deoxy derivates, it was suggested that OH groups at C-1 and C-6 contribute to stabilize the enzyme-substrate complex. Although equatorial OH groups at C-3 and C-4 do not seem to intervene in binding, they were confirmed to be restricted positions in space. In fact, a bulky methyl

substitution at position 3 or axial OH at position C-3 or C-4 caused steric hindrance. As for the oxidation at position C-3, the authors proposed a partially rotated positioning of the substrate, so that free oxygen electrons could still interact with the enzyme and C-3 remains exposed to a similar distance for catalytic action (Giffhorn, 2000).

Recent structural studies on *Trametes multicolor* POx (Hallberg et al. 2004) provide a more specific model of reaction. Using docking of D-glucose and derived chrystallographic data, the authors proposed in 2004 the following conformations for C-2 and C-3 oxidation:

A   **B**
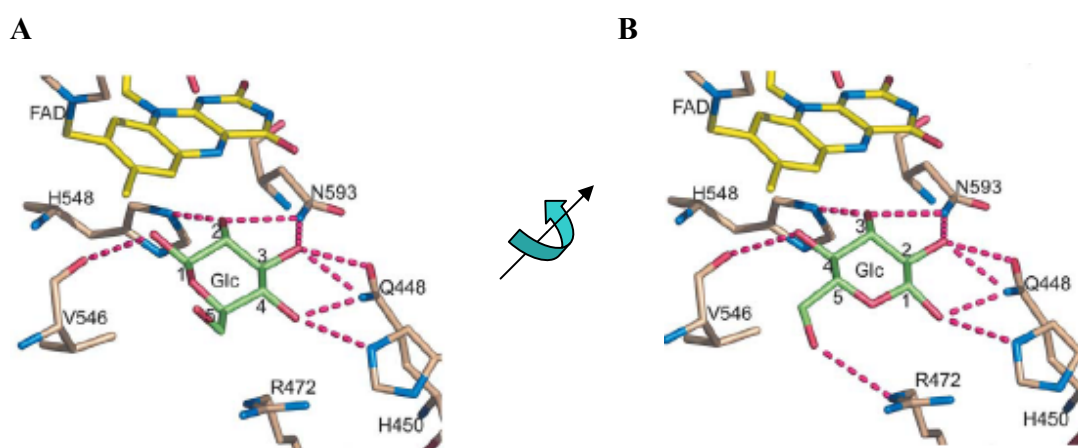
Fig 6 Docking of β-D-glucose to *Trametes multicolor* POx active site. A and B show glucose oriented for oxidation at C-2 and C-3 respectively. Broken lines depict distances < 3.3 Å, which is the typical length for hydrogen bonds. A 180º rotation of glucose about an axis as shown between the figures changes the oxidation position from C-2 to C-3, with a similar hydrogen bonds pattern. Atom coloring scheme: carbon, beige (protein), yellow (FAD), green (glucose), nitrogen is shown in blue and oxygen in red. (Hallberg et al. 2004) Note: The active site loop 452-461 has been deleted for clarity in the docking model

1.1.4 POx catalytic site

Recent structure studies showed the binding mode of the oxidized product 2-keto-glucose in the catalytic center of *Peniophora sp.* POx (Bannwarth et al. 2006). Interestingly, the mobile loop 454-461 at the active center has essentially the same conformation in the complex as in the substrate-free crystal (Bannwarth et al. 2004). Only Phe454, which

move away during sugar passage, undergoes a slight side chain displacement. However, the 2-keto-glucose binding structure at pH 6.0 (Bannwarth et al. 2006) shows a drastic conformational change in the loop 454-461 at the active center compared to that of the close homologous *T. multicolor* POx solved at pH 4.5 with a bound acetate inhibitor (Hallberg et al. 2004).
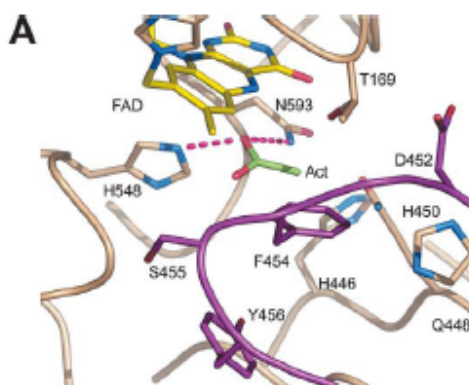
Fig 7 Acetate binding in *Trametes versicolor* POx active site. Key residues are shown. The active site loop (residues 452-456) that blocks the catalytic site from substrate access is highlighted in purple. Atom coloring scheme: carbon, beige (protein), yellow (FAD), green (acetate), nitrogen is shown in blue and oxygen in red. For clarity of the picture, water molecules were not included. (Hallberg et al. 2004)

These findings suggested that the highly mobile loop (residues 453-461, Banwarth et al, 2006; residues 452-456, Hallberg et al. 2004) functions as a gatekeeper which translocates to allow glucose pass to the active center (Bannwarth et al. 2004, 2006). The strictly conserved and mobile Phe474 forms a tight 3.8 Å non polar contact with the α-face of glucose pushing the sugar towards the flavin at the catalytic center therefore closing like a lid on the substrate. The same work suggested that the α-anomer of D-glucose, which is the predominant (98 %) form of D-glucose in solution (Funcke et al. 1979), cannot be converted since the respective 1-hydroxyl group would sterically collide with Val546 and Phe474 (Bannwarth et al. 2006). The authors explain that α-D-glucose would undergo a conversion to β-D-glucose in the central void of the tetramer prior to

reaction at the catalytic site. The conversion would occur via the catalytic bases Asp124 or Glu542 in the central void of the tetramer (Bannwarth et al. 2006).

1.1.5 Catalytic mechanism of POx

Using a chromogen in a coupled assay, spectrophotometric reading has been used to determine POx activity (Artolozaga et al. 1997; Daneel et al. 1993; Schaefer et al. 1996). ABTS has been a preferred chromogen in studies on POxs. However, assays have been performed at different temperatures and in non-saturating O_2 concentration thus making it difficult to compare POx activity data (Giffhorn, 2000). An O_2 electrode can alternatively be used to correlate O_2 consumption as POx activity (Artolozaga et al. 1997; Daneel et al. 1993; Schaefer et al. 1996). Such a kinetic study was provided for POx from *P. chrysosporium*, which has been analyzed under an O_2 saturated atmosphere (Artolozaga et al. 1997). The authors proposed a ping-pong Bi-Bi mechanism for the substrates D-glucose and O_2.

Interestingly, the kinetics of D-glucose oxidation remained unaffected by pH and buffer composition at pH values equal or above 7. Both factors have been demonstrated to affect POx kinetics at pH values below 7 (Artolozaga et al. 1997).

1.1.6 Potential applications

Since its first characterization, the importance of POx for various biotechnical applications has been recognized and many patents concerning POx have been granted (Freimund et al. 1998; Roeper et al. 1991) The numerous POx applications for patents range from analytical applications in clinical chemistry (Chusney et al. 1995; Fukumura et al. 1994; Namba et al., 1994; Taguchi et al. 1985; Tanabe et al. 1994) to monitoring of industrial processes (Eberhardt et al. 1999), or applications in synthetic chemistry (Giffhorn 2000). A novel application, subject of study of this PhD is the potential application of POxs in biofuel cells.

1.1.6.1 Applications in synthetic chemistry

Reviews on the biotechnical applications of POxs put special emphasis on bio-transformations of carbohydrates to produce various important sugar-derived intermediates for the synthesis of rare sugars, fine chemicals, and drugs (Bastian et al. 2005; Giffhorn 2000).

It is well-known that the unfavorable chemical properties of 2-keto-aldoses together with the relatively low yields and many by-products of their synthesis (Bayne and Fewster, 1956; Fischer 1889; Haas and Schlimmer 1972; Linberg and Theander 1968) make them unsuitable as starting products for chemical synthesis. Keto-sugars, which are very efficiently produced by POx (Freimund et al. 1998; Gabriel et al. 1994.; Huwig et al. 1994; Koths et al. 1992; Leitner et al. 1998; Liu et al. 1983; Volc et al. 1999), prove more useful for industrial synthesis of important compounds (Freimund et al. 1996, 1998; Gabriel et al. 1994; Geigert et al. 1983; Haltrich et al. 1998; Koths et al. 1992; Leitner et al. 1998; Volc et al. 1995).

POx also possesses a glycosyl-transfer potential and is able to produce disaccharides from β-glycosides of higher alcohols. Most substrates are oxidized in C-2 position but several are converted into the 3-keto derivatives. Using POx from *Peniphora gigantean,* Giffhorn et al, have proposed combined strategies of biotechnical and chemical methods for the production of sugar-derived syntons, rare sugars and fine chemicals (Giffhorn et al., 2000).

The enzyme product, 2-keto glucose, is also an intermediate compound in the synthesis of the antibiotic cortalcerone (Baute et al. 1987; Volc et al. 1991). Finally, POxs could also play an important role in industrial production of fructose (Neidleman et al. 1981; Shaked and Wolfe 1998).

1.1.6.2 Applications in clinical chemistry and monitoring of industrial processes

The quantitative analysis of D-glucose in blood and in glucose biosensors are potential application areas due to the low K_m value of POx for glucose ($K_m \sim 1\text{-}7$ mM for most POxs compared to $K_m \sim 11\text{-}40$ mM for *Aspergillus niger* GOx, the most comprehensively studied). This treat significantly improves the response time of the POx reaction (Taguchi et al. 1985). Furthermore, POxs convert α- and β-anomers of D-glucose which is an advantage compared to GOx, only active with β-D-glucose (Suye and Inuta1991).
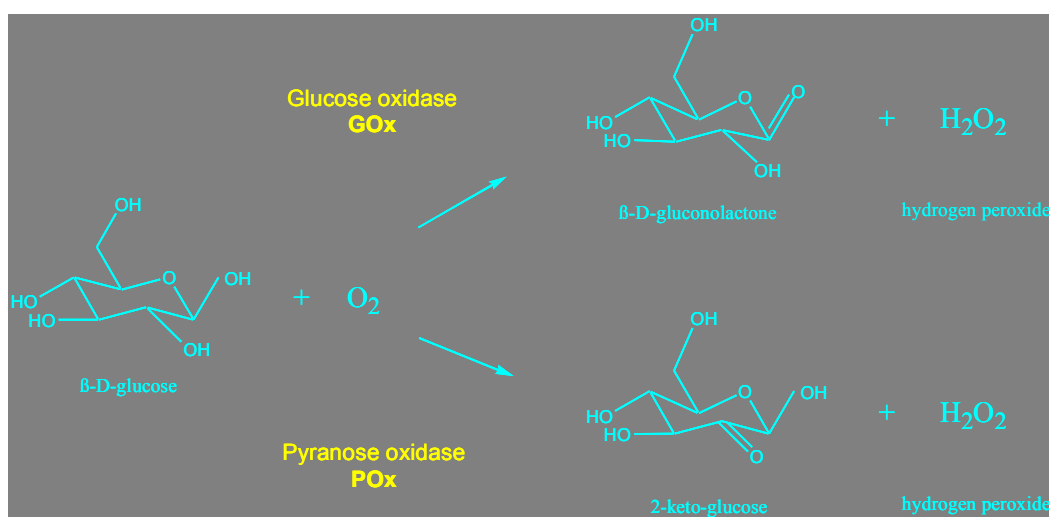
Fig 8 Different catalytic oxidation of the substrate D-glucose by GOxs and POxs.

In a recent study, different types of POx (fungal wild type, recombinant wild type with a hexa-histidine tag and mutant form E542K with a hexa-histidine tag) from *Trametes multicolor*, and recombinant POx from *Coriolus sp.* overexpressed in *Escherichia coli* as well as of pyranose dehydrogenase (PDH) from *Agaricus meleagris* and *Agaricus xanthoderma* were wired electrically on graphite electrodes and tested as glucose biosensor. Wild type POx from *T. multicolor* based biosensor, showed, together with PDH from *A. meleagris* biosensor, the best characteristics in terms of linear range, detection limit and sensitivity, and were therefore further investigated for their selectivity for a number of different sugars (Tasca et al. 2007)

POxs further convert 1,5-anhydro-D-glucitol, a diagnostic marker for Diabetes mellitus. 1,5-anhydro-D-glucitol is found in human cerebrospinal fluid and in serum and its depletion in serum is associated with hyperglycemia or renal dysfunction. Several assays have been proposed to use POx for the quantitative determination of 1,5-anhydro-D-glucitol in body fluids (Chusney et al. 1995; Fukumura et al. 1994; Kiba et al. 1993; Nakamura et al. 1986; Namba et al. 1994; Taguchi et al. 1985; Tanabe et al. 1994; Yabuuchi et al. 1989).

1.1.6.3 POx for biofuel cell applications

Chemical energy may be converted to electric energy using a biocatalyst (enzyme) or a whole cell. This type of device requires an anode, a cathode, a supporting electrolyte medium and an external circuit to use the extractable power. A biofuel cell converts biochemical energy into electrical energy. Enzymes like glucose oxidase have traditionally been used in the anodic compartment of biofuel cells

A hypothetical biofuel cell based on POx and bilirrubine oxidase (bilirrubine:oxygen oxidoreductase) could be represented as follows:
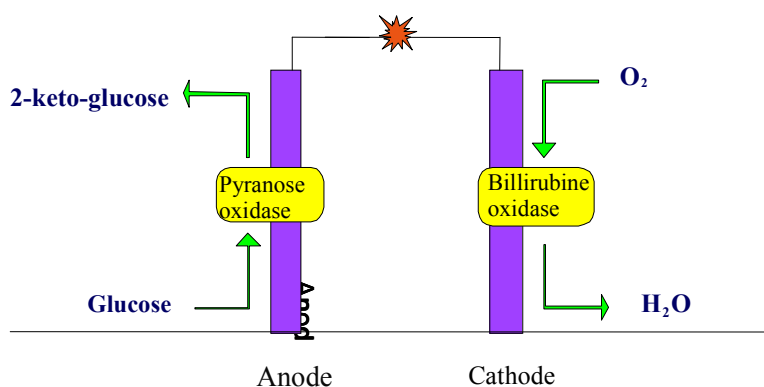
Fig 9 Scheme of proposed biofuel cell: Electron transfer during the electro-catalytic oxidation of glucose and reduction of O_2. The enzymes are immobilized in an electron-conducting redox-polymer

Catalytic oxidation of D-glucose takes place in the anode whereas in the cathode bilirubine oxidase reduces O_2 to H_2O.

In D-glucose based biofuel cells, GOx has become the prime enzyme used in the anodic compartment due to its high specificity and efficiency. Adam Heller group reported a miniature biofuel cell consisting of two carbon fibers (2cm long, 7 10^{-3} mm wide) that is based on glucose oxidation. One electrode is coated with GOx wired through a conducting polymer and strips the electrons from β-D-glucose to an external circuit. At the other electrode another wired enzyme –laccase- adds electrons to dissolved oxygen.

According to the authors, the device produces about 1.9 μwatts, approximately the power of a wristwatch battery, losing 6 % of its power per day, at a temperature and pH that resemble those of normal blood (37°C, pH 7.2), which are non-optimal for GOxs. Further causes of decay may include the instability of GOx to buffer components (salinity) and enzyme damage caused by H_2O_2.

There is no doubt, that prolonging the life of such a battery is a main goal in developing implanted minituarized biofuel cells. Such a device would result very attractive for diverse applications. Electrical output could be improved by tailoring GOx to optimally function at 37°C and pH 7. Or by using POx, which offers optimal treats to work under these conditions.
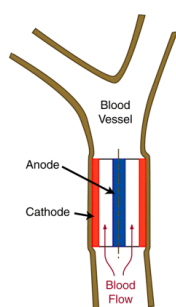
Fig 10 Scheme of a miniaturized biofuel cell implanted in a blood vessel
Source: http://www.darpa.mil/dso/thrust/ md/energy/pa_uta.html

POxs show a broader substrate profile and a significantly higher affinity towards glucose, and no anomeric preference. Their pH range of activity varies from 5 to 8, and at values superior to 7, the kinetics of the reaction over D-glucose is barely affected by buffer composition (Artolozaga et al. 1997; Bastian et al. 2005; Giffhorn 2000).

POxs are therefore extremely suitable for biofuel cells applications intended to function under physiological conditions. However, catalytic efficiency, a basic weakness that POxs present compared to GOxs, should be improved. Other major handicap of POxs is the very little knowledge about their structure, structure-function relationships, electrochemical properties and stability. In fact, only a few relevant publications have started been released in the recent years about these enzymes with the first POx resolved structure released in 2004 (Bannwarth et al. 2004).

A general obstacle in applying redox enzymes on electrodes is the inhibition of electrochemical communication between the redox enzyme and the electrode due to the buried electroactive site of the enzyme (Pishko et al. 1990; Moser et al. 1992). In fact, distance between electron donor and electron transfer is a limiting factor of the electron transfer rate

$$k_{et} \propto e^{-\beta(d - d_0)} * e^{\frac{(-\Delta G^o + \lambda)^2}{4RT\lambda}} \quad (1)$$

Where ΔG^0 is the free energy associated with electron transfer and generation of redox products
λ is the reorganization energy
d_0 is the Van-der Waals distance
d actually distance between donner and acceptor
β is the electronic couple coefficient

Several strategies can nevertheless be used to overcome this obstacle and gain a more efficient electron transfer. They mainly fall into two categories: chemical modification of the enzyme or genetic modification. Within the first category, several strategies have been developed for GOxs. Among them, the use of mediators to assist electron transfer between active site and electrode surface or the wiring of the enzyme by means of conducting polymers, are methods widely studied. Still, research has been extensively done for GOxs but not for POxs.

Electrochemical properties of POxs are little investigated. *Pleurotus ostreatus* POx was able to reduce several redox mediators such as 1,4 benzoquinone, FMN and 2,6-DCPIP (Shin et al. 1993). Another study shows that mediators as ortho and para-quinones, benzoquinone imines, cation radicals such as ABTS, redox dyes such us phenothiazines or phenoxazines and iron complexes, can shuttle electrons from cellobiose deshydrogenase/pyranose oxidase and laccase (Baminger et al. 2001).

Concerning immobilization of POxs, it mostly has been studied for their use in sensing applications for D-glucose, D-xylose, D-galactose, L-sorbose, 1,5-anhydroglucitol and L-lactate and to assist the synthesis of fine chemicals (Vandamme et al. 1995).

POxs have been immobilized onto a cellulose acetate membrane in a sensor that proved usable for 70 days (Suye et al. 1991). Using glutardialdehyde, diazo, and carbdiimide methods in a glass beaded support, POx conserved 10-23 % residual activity (Olsson et al. 1991). Onto nylon net, POx remained stable for 8 months at 4°C (Petrivalsky et al. 1994). POxs have also been immobilized on toresylate-poly (vinyl alcohol) beads (Kiba et al. 1997) and co-immobilized in carbon paste with horseradish peroxidase (Liden et al. 1998).

More recently, in a study of sugars biosensors from 2007, different types of POx were successfully wired electrically on graphite electrodes using an osmium redox polymer (poly(1-vinylimidazole)12-[Os(4,4′-dimethyl-2,2′-dipyridyl)2Cl2]2+/+)) (Tasca et al. 2007).

Since enzymes did not evolve in nature to work in circuitry, all biofuel cells face considerable challenges. For a biofuel cell thought to function under physiological conditions, POxs represent a very good anodic candidate but improvements should be done mainly in its catalytic efficiency (Freimund et al. 1998).

1.1.7 Directed evolution of enzymes

Directed evolution allows tailoring enzymes to operate in industrial processes. Mimicking natural evolution by generating genetic diversity and screening for improved variants, laboratory evolution of enzymes represents a valuable tool to address improvements in stability, catalytic efficiency, solubility and specificity of biocatalysts. Furthermore, it assists elucidation of structure-function relationships (Kuchner and Arnold 1997; Tao and Cornish 2002).

Mutagenesis and recombination of one or more parent sequences are frequently used to generate genetic diversity. The resulting gene is subsequently cloned into a vector which is then introduced into a suitable expressing host (*E. coli*). By using selection and screening methods, improved variants are identified and isolated, and then included for the next round of the directed evolution experiment.

The typical laboratory evolution experiment on POx, as performed in this PhD work, could be outlined as follows:

pyranose oxidase gene

Error prone PCR

pyranose oxidase mutated genes

Ligation into the pASK- IBA 3

Repeat the procedure

Transformation into *E. coli*

Transfer of clones into 96-well
- cell growth
- replication
- protein expression

Selection of the improved variants

Assays to check the property of interest

- cell growth
- master plate
- storage in the freezer
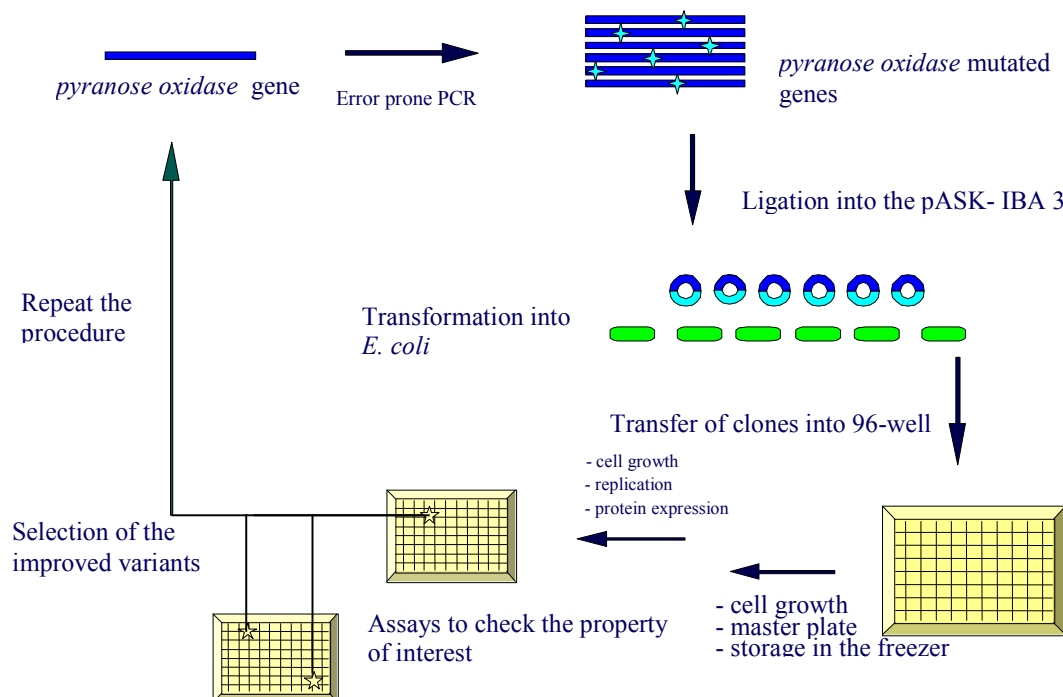
There are four basic requirements for a successful directed evolution experiment: there should be a physically possible path to bring us from the starting point of the enzyme to the improved variant. Second, the intermediate and final improved variants should be biologically feasible. Third, research tools should allow producing libraries – in suitable expressing organisms- that may include rare beneficial mutations. Fourth, a rapid screening system for the desired property should be available (Kuchner and Arnold 1997).

Laboratory evolution methods have not yet been used to improve e^- transfer rates of GOxs and POxs, These enzymes are highly regulated to operate under physiological conditions, so that there is a high probability of bypassing barriers created by regulatory units.

A directed evolution experiment consists of two major steps:

- Creating genetic diversity in the target gene
- Screening effectively for the desired treat in the enzyme
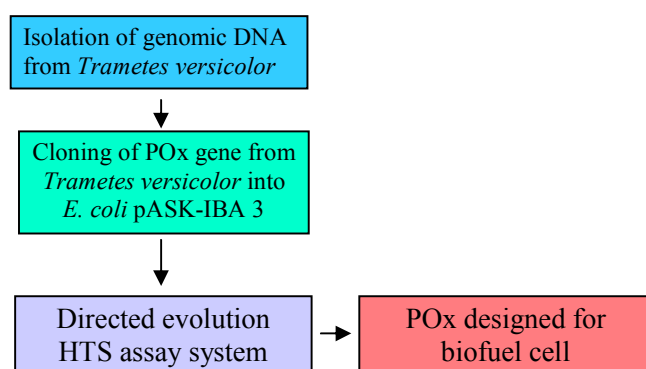
1.1.7.1 Generating genetic diversity

a) Error-prone Polymerase Chain Reaction

By varying Mn^{2+} or Mg^{2+} concentration in the reaction mix, the frequency of random errors occurring during polymerase chain reaction may be modulated. In a directed

evolution experiment, epPCR is normally performed at moderate to low frequency of errors in order to warrant a high percentage of active clones (Cadwell and Joyce, 1992).

An ideal mutagenesis method would allow the replacement of any amino acid residue in the polypeptide derived from the gene by any of the other 19 possible amino acids. Furthermore, probability of all possible variants should be equal and the level of expression in the host would not be affected (Wong et al. 2004).

The redundancy of the genetic code and the biased mutational spectra of polymerases make epPCR fall far from this ideal. In order to overcome this, new methods have been developed. Some authors propose the use of diverse low fidelity polymerases whose biased spectra of mutagenesis partially complement (Vanhercke et al. 2005). The authors further propose a combination of methods - epPCR followed by DNA shuffling of close related genes – as a strategy to generate unbiased libraries; alternatively, conditions at each step can be adjusted to produce a desired degree of mutational bias (Vanhercke et al. 2005).

Stratagene offers an "in vivo" replication system (XL1-Red Competent Cells) which contains deficient polymerases that add mutations in all the genetic material during the organism's growth (Radman 1980; Scheuerman et al. 1983; Cox 1976). Other authors propose an "in vivo" system (Mutazyme II Polymerase Kit from Stratagene) that allows mutagenesis in the gene of interest and preservation of genomic DNA by operating with a sloppy polymerase and a precise polymerase expressed in two different plasmids (Camps et al. 2003).
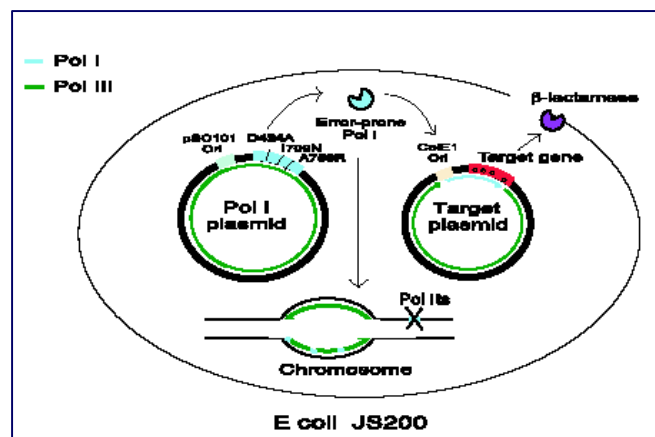
Fig 11 Two-plasmid system for *in vivo* mutagenesis; Plasmid I carries the *polA* gene under control of the *tac* promoter; it is a low-copy plasmid with a pSC101 origin of replication and carries a cm-resistance marker. Plasmid II carries the target gene placed in close proximity downstream of a pUC19 (ColE1-type) origin of replication; it is high-copy and carries a kan-resistance marker. Error-prone Pol I is expressed from plasmid I and initiates replication of plasmid II; it has been reported that Pol I synthesizes the first 400–500 nt before a switch to the more accurate and processive Pol III. Pol III is the main replicative polymerase and is responsible for replicating the majority of chromosomal DNA. Sequences synthesized by Pol I and Pol III, are indicated in light blue and green, respectively (Camps et al. 2003).

b) Saturation mutagenesis

In a more specific manner, saturation mutagenesis can be used to introduce all possible aminoacids substitutions in a certain position of the protein sequence or in positions adjacent to it, thus providing more comprehensive information and overcoming the major drawbacks of random mutagenesis. However, certain knowledge on the enzyme sequence and structure-function relationships are crucial for applying this method to explore the possibilities of improvement by acting on key sites.

c) Site-directed mutagenesis

In site-directed mutagenesis, a designed synthetic DNA fragment that includes a mutation, is extended and copied by PCR. The fragment may later be cloned thus perpetuating the mutation deliberately introduced. This method allows targeted single aminoacid substitutions thus providing a tool for studying gene expression and structure-function relationships (Cedrone et al. 2000; Bolon et al. 2002).

1.1.7.2 Screening POxs libraries

Developing a sensitive and reliable screening system that detects improved activity of the variants generated by mutagenesis methods is a major task in directed evolution of enzymes. In studies about POxs methods comprise three major groups: measurement of

oxygen depletion, detection of the by-product H_2O_2 or measurement of the product 2-keto-glucose.

```
                    ┌─────────────────┐
                    │      Assay      │
                    │   development   │
                    └─────────────────┘
```
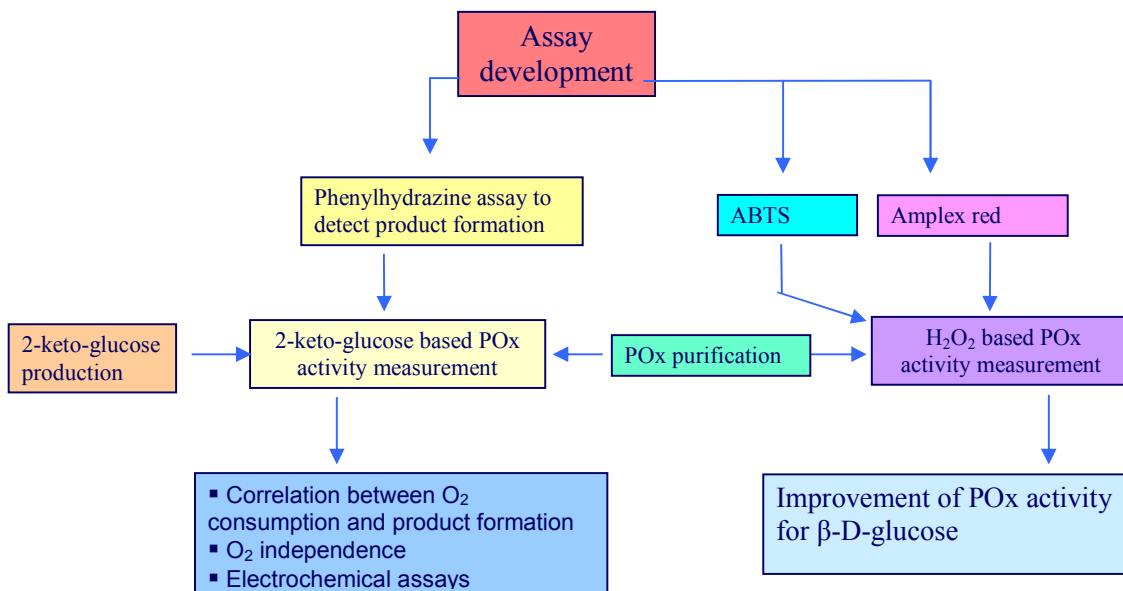

a) Measurement of oxygen depletion

POxs oxidize D-glucose to 2-keto-glucose with the concomitant reduction of molecular oxygen to hydrogen peroxide. Oxygen consumption is therefore directly proportional to POx activity. Analysis on POx activities has successfully been performed using an oxygen electrode (Artolozaga et al. 1997; Daneel et al. 1993; Schaefer et al. 1996). Alternatively, oxoplates (PreSens GmbH, Regensburg, Germany), might be used. These plates are prepared for a single use thus becoming a hardly affordable method for screening applications.

b) Determination of the by-product H_2O_2

Coupled colorimetric assays that allow determining H_2O_2 are the most widespread methods of measuring POx activity. They are based in the reaction of peroxidase with H_2O_2 and a chromogen to render a colored product. Most widely used chromogens are 2,2'-azino-bis(3-ethylbenzothiazoline-6-sulfonic acid) (ABTS) (Bateman et al. 1995; Chance and Maehly, 1955), o-dianisidine, and 3,3',5,5'-tetramethylbenzydine (TMB)

(Yamaguchi et al. 2001) with a clear preference for ABTS (Artolozaga et al. 1997; Daneel et al. 1993; Schaefer et al. 1996). ABTS is oxidized in presence of H_2O_2 and Horseradish peroxidase (HRP) to a colored compound which is determined by photometric reading at 414 nm.
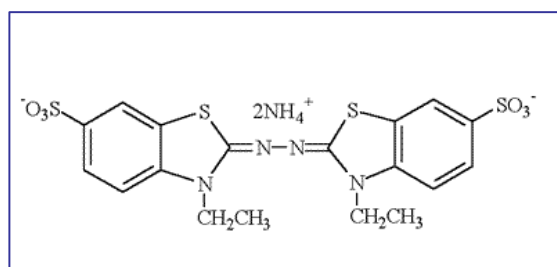
Fig 12 ABTS (2,2′-azino-bis-(3-ethylbenzothiazoline-6-sulfonic acid), diammonium salt)

These assays are very sensitive and specific due to the peroxidase but the variable quantity of dissolved oxygen in solution and the fact that H_2O_2 can also be produced during the cells metabolism, are inherent handicaps. Futhermore, o-dianisidine and ABTS have been reported to be carcinogenic (Voogdt et al. 1980) and TMB is labile in aqueous buffer.

Fluorimetric assays using have also been proposed. Colorless Amplex Red (10-acetyl-3,7-dihydroxyphenoxazine) has been reported to be oxidized in presence of H_2O_2 and peroxidase to a red-fluorescent compound –resofurin- which is determined by fluorescence reading at 587 nm (excitation at 563 nm) (Mohanty et al. 1997; Zhou et al. 1997).

Amplex Red

HRP, H_2O_2

Resorufin
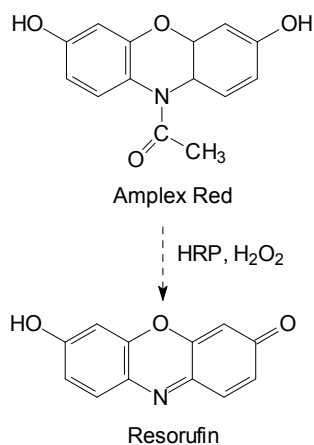
Fig 13 Reaction of Amplex Red with H_2O_2

c) Determination of the product 2-keto-glucose

Principle of this novel assay is the reaction of phenylhydrazine with 2-keto-glucose, the product of the action of POxs over D-glucose, to form a yellow colored compound which is determined by photometric reading at 390 nm. The main advantage of this assay is that product formation relates directly to POx activity. Furthermore, contrary to H_2O_2, concentrations of 2-keto-glucose are very stable in solution and unaffected by external conditions. However, the yellowish background of the samples demands increased POx activity values for a reliable and sensitive assay system.
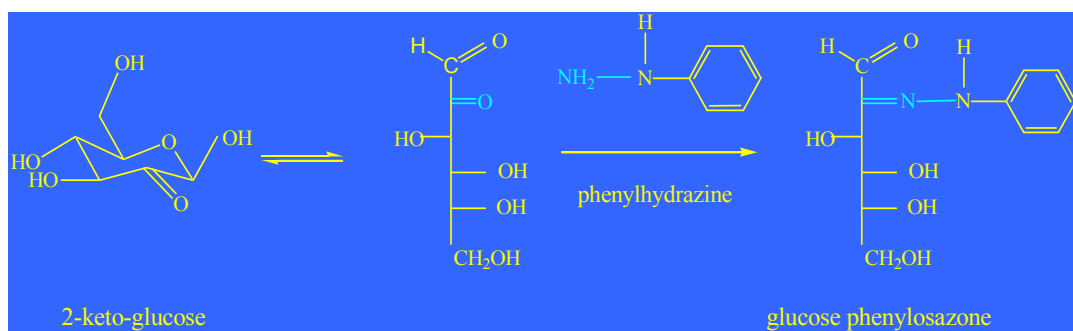
Fig 14 Reaction of 2-keto-glucose with phenylhydrazine to produce the yellow glucose phenylosazone

d) Determination of POx activity on D-glucono-1,5-lactone.

The in vivo substrates of POx are D-glucose, D-galactose, and D-Xylose. In adition, POx also exhibits significant activity with a number of other carbohydrates, including L-Sorbose, D-glucono-1,5-lactone and D-Allose. This may serve to develop a novel assay for assessing POx activity.

2-keto-D-gluconate reductases catalyze the oxidation of D-gluconate to 2-dehydro-gluconate with the concomitant reduction of the cofactor NADP+ to NADPH + H+ (Ameyama and Adachi, 1982; Pitt and Mosley, 1984).

2-keto-D-gluconate reductases

D-gluconate + NADP$^+$ $\rightleftharpoons$ 2-dehydro-gluconate + NADPH + H$^+$

This reaction is reversible in most of the cases and can be followed by spectrophotometric reading of NADPH production at 340 nm or fluorescent emission reading at 445 nm after excitation at 340nm. The idea would be to develop an enzymatic essay in which production of 2-dehydro-gluconate via POx oxidation of the D-glucono-1,5-lactone would be followed by decrease of the spectrophotometric / fluorescent reading values as the oxidized NADP+ is produced, after 2-keto-D-gluconate reductase activity. A novel HTS to assay POx activity could be developed. The scheme would be as follows:

D-glucono-1,5-lactone

POx

2KG reductase

D-gluconate + NADP$^+$ $\rightleftharpoons$ **2-dehydro-gluconate + NADPH + H$^+$**

Absorbance reading at 340 nm / Fluorescence reading at 445 nm
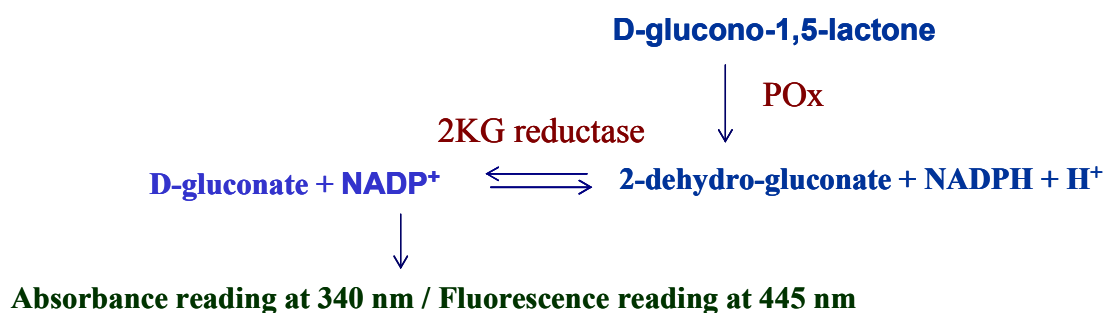
Fig 15 Reactions scheme for a pyranose oxidase screening method based in 2-KG-reductase

Several 2-keto-gluconate reductases from different organisms are considered. Most of them show a pH preference for the oxidation or reduction reaction: the first is favored at high pH values in the range from 10 to 12, whereas the latter occurs at lower values, in the range from 4 to 9. This feature make them suitable for testing POx activity due to two reasons: pH optimum of POx is 7 which turns advantageous in terms of sensitivity, and a pH shift for the assay would be unnecessary thus simplifying the protocol.

Organism	Best substrate	Natural product	Cofactors	K_m value (mM substrate)	K_m (mM NADPH)	pH optimum	Temp optimum
Acetobacter ascendens	2-dehydro-D-gluconate	D-gluconate	NADP+ NADPH	5,3	0.0074	6 (4,5 - 8,5)	55 (40 - 55)
Acetobacter rascens	2-dehydro-D-gluconate	D-gluconate	NADP+ NADPH	-	-	6 (5 – 9,2)	50 (35 - 65)
Gluconobacter liquefaciens	2-dehydro-D-gluconate	D-gluconate	NADP+ NADPH	-	-	6	-
Gluconobacter suboxydans	2-dehydro-D-gluconate	D-gluconate	NADP+ NADPH	-	-	6	-
Brevibacterium ketosoreductum	2-dehydro-D-gluconate	D-gluconate	NADP+ NADPH	-	0,01	6	-
Penicilium notatum	2-dehydro-D-gluconate	D-gluconate	NADP+	-	-	-	-
Escherichia coli	2-dehydro-D-gluconate	D-gluconate	NADP+	-	-	-	-

Table 1 Main parameters of 2-keto-gluconate reductases from different organisms. Source: BRENDA

According to their substrate specificity, affinity (Km value for 2-keto-gluconate), optimum pH and temperature, as well as pH and temperature ranges of activity (Chiyonobu et al. 1976; Shinagawa et al. 1978; Adachi et al. 1978; Yum et al. 1998), 2-keto-gluconate reductases from *Acetobacter ascendens* and *Acetobater rascens* seem to be the best candidates.

e) Screening POx electrochemical properties:

Oxygen independent POxs are interesting in order to avoid the drawbacks of producing the byproduct H_2O_2. An assay system meant to assist directed evolution to improve this treat should be able to react to the electron transfer in the reaction. Firm candidates to develop electrochemical assays are water soluble electrochromic polymers such as polypyrrol and polythiophenes derivatives. These compounds undergo color change during redox reaction.
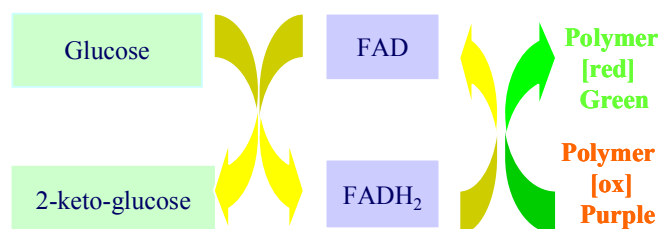
Fig 16 Scheme of a POx electrochemical assay system based on electrochromic polymers

Alternatively to the use of a conducting polymer to screen electrochemical properties of POx, diffusional relays or electron transfer mediators whose absorbance changes when undergoing reduction might be used. Some are related below:

Electron acceptor	Relative activity (%)	K_m (mM)	K_{cat} (s^{-1})	K_{cat}/K_m (mM^{-1} s^{-1})
Oxygen	100	0.090	71	790
1,4 benzoquinone	300	0.31	210	690
1,4 benzoquinone (pH 4,5)	380	0.30	270	900
methyl-1,4 benzoquinone	250	0.40	180	440
methyl-1,4 benzoquinone (pH 4,5)	330	0.35	230	670
2,6 dimethyl-1,4 benzoquinone	170	2.1	120	58
2,6 dimethyl-1,4 benzoquinone (pH 4,5)	290	0.83	210	250
tetrafluoro-1,4 benzoquinone	900	0.22	640	2900
tetrachloro-1, 4 benzoquinone	1100	0.088	750	8600
tetrabromo-1,4 benzoquinone	400	0.090	280	3100

Table 2 Apparent kinetic constants of POx from *Trametes versicolor* for several electron acceptors, determined at 30°C by using 100 mM glucose as a substrate at pH 6.5 (Leitner et al. 2001).

Little research has been done on artificial mediators that could replace molecular oxygen as electron acceptor for POxs. And, as shown by extensive studies done on the GOxs reaction with diverse mediators candidates, to build up an efficient mediator-based screening system is not easy, basically due to limitations of the mediator - poor stability and pH dependence- or of the assay itself - poor color or fluorescence development. Organometallic redox compounds, such as ferrocene derivatives behave well

electrochemically and exhibit rapid kinetics for enzyme oxidation (Luong et al. 1994). Cass et al. reported in 1984 a GOx based glucose biosensor that used ferrocene to mediate the electron transfer between GOx redox site and an electrode surface. Cass et al. reported in 1984 a GOx based glucose biosensor that used ferrocene to mediate the electron transfer between GOx redox site and an electrode surface. The oxidative and reductive half-reactions can be represented as follow:
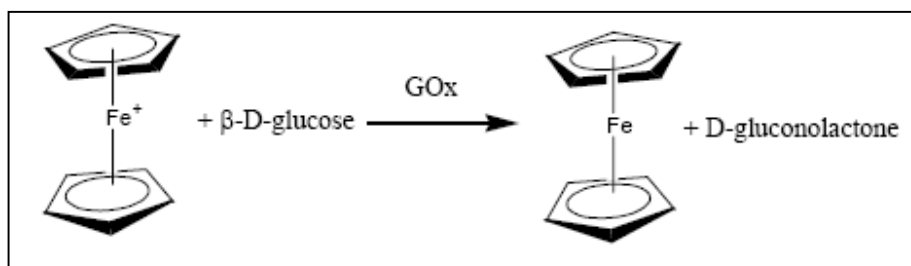
Fig 17 Ferrocenium ion reduction during oxidation og D-glucose by GOx, Ziwei Zhu PhD thesis.

Since the β-D-glucose/ D-glutonate and $FADH_2/FAD$ couples are $2e^- + 2H^+$ systems, and ferrocenes are one-electron oxidizing systems, two equivalents of ferrocene and ferrocenium are involved in the reaction. It has been reported that the oxidation rate constant at pH 8 in presence of ferrocenium ion is larger than that observed with dioxygen so that GOx accepts ferrocenium ion instead of dyoxygen as electron acceptor at that pH value (Bourdillon et al. 1993). The same principle could be used to test driving POxs. Indeed, due to their convenient and cheap preparation, artificial electron acceptors are interesting to develop a high throughput screening assay. However, oxygen competition and selection of the redox potential are major concerns in testing alternative electron acceptors.

1.1.8 Cloning of POx

Several POx have been cloned and expressed in active form. POx gene sequences are available from *C. versicolor* (Nishimura et al. 1996), *Trametes hirsuta* (8), *T. matsutake* (Takakura and Kuwata, 2003), *Peniophora species* (Heckmann-Pohl et al., 2006), *T. ochracea* (Vecerek et al. 2004), *Panerochaete chrysosporium* (de Koeker et al. 2004), *P.*

gigantea (Bastian et al. 2005), *Trametes pubescens* (Maresova et al. 2005) and *Lyophyllum shimeji* (Takakura et al., unpublished).

1.1.9 Engineering of pyranose oxidase

Data on POx engineering are scarce. Previously engineered POxs include *C. versicolor* POx (Masuda-Nishimura et al. 1996) *P. gigantea* POx (Bastian et al. 2005) and *Peniophora sp.* POx (Heckmann-Pohl et al. 2006).

A directed evolution approach led to the *C. versicolor* POx variant E542K exhibiting improved stabilities and K_m values for D-glucose (from 1.4 to 0.74 mM) and 1,5-anhydro-D-glucitol (from 35.3 to 1.4 mM) (Masuda-Nishimura et al. 1996). A dual approach of site-directed mutagenesis and directed evolution was used to engineer recombinant *P. gigantea* POxB (Bastian et al. 2005). The resulting variant, which included amino acid residues substitutions E540K, K312E and a C-terminal His_6-tag, showed slightly improved thermal and pH stabilities compared to native POx. The temperature optimum was increased (from 44°C to 50°C) and the catalytic efficiencies improved (269.08 $mM^{-1}s^{-1}$ compared to 50.46 $mM^{-1}s^{-1}$ for the WT; a ~5.4 fold increase). Site directed mutagenesis has been used to produce the T158A, E540K variant on recombinant *Peniophora sp.* POx (Heckmann-Pohl et al. 2006). The mutant, which also included a C-terminal His_6-tag, showed improved thermo-stability (up to 60°C compared to 45°C for the recombinant WT), lower apparent K_m value towards D-glucose (reduced from 5.0 to 0.47 mM) and a significantly increased catalytic efficiency k_{cat}/K_m towards D-glucose (284.03 $mM^{-1}s^{-1}$ compared to 1.89 $mM^{-1}s^{-1}$ for the WT; a ~230-fold increase). The precedent E540K variant is thermo-stable up to 65°C, shows apparent K_m value of 1.5 mM and a catalytic efficiency k_{cat}/K_m towards D-glucose of 19.39 $mM^{-1}s^{-1}$ (a ~10-fold increase).

1.2 Objectives

The main objectives of this PhD work were to prepare a c-DNA library from freshly extracted *Trametes versicolor* RNA, to clone the *pox* gene, and to express POx in *Escherichia coli* as an intracellular active recombinant enzyme. Further goals comprised the development of a proper POx purification protocol and to study POx optimum storage conditions. Finally, this thesis work aimed at establishing an assay based on ABTS, which will serve to fully characterize *Trametes versicolor* POx in terms of activity, kinetic parameters, thermo-stability, pH stability, chloride resistance and, thus, evaluate its possible use in the anodic compartment of biofuel cells.

Additional objectives focussed on tailoring POx for its possible use in implanted miniaturized devices. For this purpose, methods of directed evolution needed to be set-up and tested on *Trametes versicolor* POx. Aiming to improve POx catalytic efficiency and to search for O_2 independent POx variants, various mutagenesis methods were considered. Special emphasis was also set on developing rapid screening systems for the properties of interest, a basic requirement of a directed evolution experiment. In this respect, the ABTS assay was aimed to be further developed to a highthroughput screening system. Two novel assays–one based on phenylhydrazine and another based 2-keto-reductase- were proposed and studied. Furthermore, the possibility of developing a fluorescence-based assay and a ferrocenemethanol assay to assess activity of POx was explored.

The phenylhydrazine assay, which directly measures product formation, was of special interest since searching for O_2-independent POx was per se a goal of the project. The final acceptor of electrons was to be the anode and not occasional free oxygen, a strong competitor that may be present. Furthermore, H_2O_2 formation, and its pernicious effect specially considering the final goal of incorporating POx to an implanted device, was eventually aimed to be prevented. The combination of ABTS and phenylhydrazine assays would allow correlating POx activity and O_2-independecy.

Finally, agar plate pre-screening assays were to be tested, and the use of permeabilizers in high throughput screening assays had to be studied as means of speeding up the screening process.

2. MATERIAL AND METHODS

2.1. Chemicals

All chemicals used were of analytical reagent grade or higher quality and were purchased from Sigma–Aldrich Chemie (Taufkirchen, Germany) and Applichem (Darmstadt, Germany). Toyopearl DEAE-650S chromatographic resin was purchased from TOSOH BioScience GmbH (Stuttgart, Germany). If not stated otherwise, nucleotides and enzymes were purchased from Fermentas (St. Leon-Rot, Germany). PCRs were performed in thin wall 0.2 mL PCR tubes (Multi-Ultra, Carl Roth, Germany) using a thermal cycler (Mastercycler gradient, Eppendorf, Hamburg, Germany).

2.2. Organisms, growth conditions, and plasmids

The white rot fungus *T. versicolor* (DSM 1977), was grown at 28°C in malt extract peptone agar (Medium 90) and in glucose-yeast extract agar. The bacterial strains were grown in LB broth under appropriate selective conditions (Sambrook et al. 1989).

T. versicolor (DSM 1977) was purchased from the DMSZ collection (Germany). *E. coli* strain XL2-Blue and XL1-Red Competent Cells were purchased from Stratagene (Hycor Biomedical, Kassel, Germany). pGEM-T Easy plasmid was purchased from Promega GmbH (Mannheim, Germany) and used to construct a cDNA library from mRNA of *T. versicolor*. pASK-IBA3 vector was purchased from IBA GmbH (Göttingen, Germany) and used for POx expression. Plasmids expressing several chaperones to assist correct folding were purchased from Takara Bio Inc (Shiga, Japan).

Malt Extract Peptone Agar	3% malt extract	0.3% Soya peptone			1.5 % Agar	1000 ml distilled water

Glucose-Yeast extract Agar	2% glucose	1 % malt extract	0.5 % yeast extract	0.1 % K_2HPO_4 0.01 % $MgSO_4$ 7 H_2O 0.001 % $FeSO_4$ 7 H_2O	15 g Agar	1000 ml distilled water
LB media		1.0 % Soya peptone	0.5 % yeast extract	1.0 % NaCl		1000 ml distilled water

Table 3 Composition of cultivation media

2.3. Preparation and treatment of RNA

Trametes versicolor mycelium was frozen in liquid nitrogen and disrupted in a grinding mortar. Total RNA was extracted according to a novel protocol (Schenk et al. 2008) and treated with RNase-free DNase I (Ambion Europe, Cambridgeshire, UK). A phenol/chloroform/isoamylalcohol (25:24:1) and successive chloroform/isoamylalcohol (24:1) extraction step was used to remove DNase I. The RNA was recovered from the aqueous phase by precipitation using ammonium acetate (0.5 M final concentration) and 2.5 volumes of pure ethanol followed by incubation at (-80°C, 1 h) and centrifugation (4°C, 16,100×g, 20 min). To remove residual phenol traces, the pellet was washed twice by adding 1 mL 75 % ethanol and centrifuging (4°C, 16,100×g, 10 min). The RNA was resuspended in RNase-free water and RNA concentration was determined photometrically.

2.4. Synthesis and amplification of Trametes versicolor POx cDNA

Synthesis of cDNA was performed according to the manufacturer's instructions, using SuperScript II Reverse Transcriptase (Invitrogen, Karlsruhe, Germany). The reaction mix contained 5 µg of DNA-free total RNA, 250 ng of reverse primer r1 (Table 4) and SUPERASE-In (Ambion, Cambridgeshire, UK). The reverse primer had been derived from the c-DNA sequence of *C. versicolor* POx (Nishimura et al. 1996). The cDNA

obtained was used for PCR amplification of the POx open reading frame by using the forward and reverse primers f1, r1 (Table 4). PCR reactions were conducted in 50 µL reaction volume containing 20 pmol of each primer, 10 nmol of each dNTP, 0.1 µg of cDNA, and 3U of Taq DNA polymerase. PCR amplifications were performed in a gradient thermal cycler and had the following conditions: 94°C for 3 min, 1 cycle; 94°C for 1 min/ 55°C for 1 min/ 72°C for 2.25 min, 30 cycles; 72°C for 10 min, 1 cycle. The obtained 1,872 bp long PCR product was gel extracted and cloned into the pGEM-T Easy.

For sequencing	
A. f 1 (-7)	5'-GGAATTCATGTCTACTAGCTCGAGCGAC- 3'
B. f 2 (543)	5'-GTTGCTCGTGAAGGACGACCAGGACGTGACG- 3'
C. f 3 (1173)	5'-CAGCGTCACGTACACACGCCCGGCGCGGAGAC- 3'
D. r 1 (1850)	5'-ATGCCATGGCATGGGTTACAGCCTGATCTGTGAAAG-3'
E. f 4 (513)	5'-GACGCCCCGCTTTGGACCGCGAGCAGCG-3'
F. f 5 (255)	5'-GATCGGTGCCCACAAGAAGAACACTGTCG- 3'
G. f 6 (1143)	5'-CATCAGGGGCAAACCCTGGTGATCGGGGG- 3'
J. r 2 (648)	5'-CCGCGAGCTTGTTGAGCACGAGGTTGTGGCGGATC-3'
I. f 8 (820)	5'-CGCTTCAACCTCTTCCCCGCGGTCGCATGT- 3'
M. f 9 (1) pASK-IBA3	5'-CCATCGAATGGCCAGATGATTAATTCCC-3'
Site-directed mutagenesis	
K. f 10 (130) pASK-IBA3	5'-GGGCAAAAAATTGGAGACCGCCG-3'
L. r 3 (130) pASK-IBA3	5'- CGCGGTCTCAATTTTTTGCCC-3'
N. r 4 (1250)	5'-CATGCCATGGCATGTTATGTGGTTCTCCACCTTCTCG-3'
K338 → E338	5'-GCTTTGAAATCGAAGCAGACGTG-3'
S627 → K627	5'-GCAATGTCGCAAACGATCAAG-3'
Ligase-free method	
O. f 11 (24) ligase free	5'-CCCTCGAGGTCGACCTGCA*G*GATGTCTACTAGCTCG-3'
P. r 5 (1851) ligase free	5'-GACCATGGTCCCCCTGCAG*G*TCTTACAGCCTGATCTG-3'

Table 4 Oligonucleotides designed for the various PCR reactions at studying pyranose oxidase gene

2.5. Construction of POx expression plasmids

T. versicolor POx cDNA was amplified by PCR using the similar reaction conditions as described above, but with 0.2 µg of cloned cDNA template and 2.5 U of *Taq* DNA polymerase. The PCR products generated by using the primers pair f1, r1 (Table 4) were digested with EcoRI/NcoI. The digested DNA fragment was isolated from agarose gels with QIAquick Gel Extraction Kit (Qiagen, Hilden, Germany) and cloned into EcoRI/NcoI digested ATTpASK IBA3 vector resulting in plasmid p_{wt}POx.

A classical ligation method was used for the cloning. The reaction mix contained typically 1x T4 DNA ligase buffer, ~500 ng insert, ~50 ng of plasmid and 0.5U of T4 DNA ligase, in 15 µL of final volume. The reaction mix was incubated at room temperature for 1 hour and kept at 4°C overnight.

E. coli XL-2Blue was transformed with 2 µL of ligation product by electroporation using an Electroporator 2510 (Eppendorf, Hamburg, Germany) and transformants were selected on LB_{amp} (0.1 mg/mL of ampicillin in LB media) agar plates. Clones harboring *pox* genes were inoculated in tubes containing 4 mL LB_{amp} media and grown overnight (37°C, 220 rpm, 12 h). Purified plasmids were isolated from *E. coli* using QIAprep Spin MiniPrep Kit (Qiagen, Hilden, Germany) and were sequenced (MWG-Biotech AG; Ebersberg, Germany) using the primers f1, f2, f3, r2 (Table 4).

Re-ligation of the pASK IBA3 plasmid, a major drawback in the generation of mutant libraries, was corrected by introducing a further step of electrophoresis separation preceding the transformation of *E. coli*. A preliminary transformation was nevertheless necessary in order to increase DNA yields. Plasmids were then extracted from *E. coli* cells with QIAprep Miniprep Kit (Qiagen). The re-ligation band was analyzed by standard agarose electrophoresis and removed whereas vectors containing the insert were extracted from the gel and purified using QIAquick Gel Extraction Kit (Qiagen). This plasmid preparation was used to transform *E. coli* cells via electroporation to generate mutant libraries.

2.6. Generation of epPCR mutant library of POx

p_{wt}POx was used as template for mutant library generation by error-prone PCR (epPCR). epPCR was performed using a thermal cycler and had the following conditions: 94°C for 3 min, 1 cycle; 94°C for 1 min/ 55°C for 1 min/ 72°C for 2.25 min, 30 cycles; 72°C for 10 min, 1 cycle. PCR mix had a total volume of 50 μL and consisted of 0.2 mM dNTP mix, 40 ng pASK-IBA3 POx template, 0.05 mM $MnCl_2$ and 10 pmol of each primer f1, r1 (Table 4). PCR was hot started when the reaction mix reached 94°C by adding 2.5 U *Taq* polymerase. PCR template was digested with 0.2 U/μL Dpn I (37°C, 3h). PCR product was purified using QIAquick PCR Purification Kit (Qiagen, Hilden, Germany). PCR product was digested with the EcoRI/NcoI pair and subsequently cloned into pASK-IBA3 vector. Transformation into *E. coli* and selection of clones were done as described above.

2.7. Generation of mutant libraries by epPCR and ligase-free method

ATTpASK IBA3 plasmid harboring the POx insert was used as a template. epPCR was performed using a thermal cycler and had the following conditions: 94°C for 6 min, 1 cycle; 94°C for 1 min/ 55°C for 1 min/ 72°C for 2.25 min, 30 cycles; 72°C for 10 min, 1 cycle. PCR mix had a total volume of 50 μL and consisted of 0.2 mM dNTP mix, 40 ng pASK-IBA3 POx template, 0.05 mM $MnCl_2$ for adjusting the mutation frequency and 10 pmol of ligase free primers f11, r5 (Table 4). Nucleotides marked with a * contained a phosphorothioate bond which terminates T7 Gene Exonuclease digestion (Zhou and Hatahet, 1995). PCR was hot started when the reaction mix reached 94°C by adding 2.5 U *Taq* polymerase. PCR product was purified using QIAquick PCR Purification Kit (Qiagen, Hilden, Germany).

Cloning of *pox* variants into pASK IBA3 vector was performed according to a ligase free cloning method (Zhou et Hatahet, 1995). Firstly, 100 μg pASK IBA3 plasmid was linearized by Pst I digestion (5U/μg DNA, 6 h, 37°C), separated by agarose electrophoresis and purified with QIAquick Gel Extraction Kit (Qiagen). Secondly, 3 μg

of *pox* PCR product and 200 ng of linearized pASK IBA3 plasmid were treated with T7 Gene Exonuclease (5 U/µg DNA, 15 min, 37°C) in order to generate overhangs of ~20 nucleotides. T7 Gene 6 Exonuclease was subsequently inactivated by heat treatment (10 min, 80°C) and this reaction fully terminated with 50 µL of 50 mM EDTA pH 8.

Ligation was then performed by mixing digested PCR product and linearized pASK IBA3 plasmid in a ratio 15:1 (3 µg: 200 ng). The ligation mix was heated (10min, 75°C) and slowly cooled down to room temperature during 30 min before transforming into XL2-Blue *E. coli* strain using electroporation.

2.8. Site-directed mutagenesis

QuikChange Site-Directed Mutagenesis Kit (Stratagene, Hycor Biomedical, Kassel, Germany) and the primers f10, r3 (Table 3) were used to remove the start codon contained in the pASK IBA3 sequence. The same kit and the primers pair f1, r4 (Table 4) were used to include into the *T. versicolor* WT *pox* beneficial mutations of reported improved variants. PCR protocols and program were conducted according to the manufacturer's instructions. Successful nucleotide exchanges were confirmed by DNA sequencing of the purified plasmid preparations using the primers f9 and f4 (Table 4) respectively.

2.9. Generation of further POx variants using a mutator strain: XL1-Red Cells

p_{wt}POx was transformed into XL1-Red Competent Cells following standard protocols (Sambrook et al. 1989). Clones selected on LB$_{amp}$ plates were picked with toothpicks, inoculated in 4 mL LB$_{amp}$ media and grown overnight (37°C, 250 rpm) using a Multitron II incubator shaker (Infors, Einsbach, Germany). 50 µL of inoculum were transferred to 500 mL shaking flasks containing 100 mL of LB$_{amp}$ growth media and left for growth over seven days (37°C, 250 rpm). From second day on, 1 mL of the culture was

transferred to a 500 mL shaking flask containing 100 mL fresh media. Each day, a 4 mL aliquot of the culture was taken and used for plasmid extraction. Plasmid preparations were used to transform XL2-Blue *E. coli* cells by electroporation (Sambrook et al. 1989) producing seven POx libraries.

2.10 Preparation of electro-competent E. coli

A single colony of *E. coli* from a fresh agar-plate was inoculated into a 100 mL flask containing 10 mL LB. Overnight incubation is performed in vigorous aeration (37°C, 250 rpm). 500 mL of pre-warmed LB in a 2L flask were inoculated with the overnight culture. Incubation was performed (37°C, 250 rpm) and the OD_{600} of the growing bacterial cultures checked every 20 minutes. When the OD of the cultures reached 0.6-0.8, the flask was rapidly transferred to an ice-water bath for 10-15 minutes. Even cooling was ensured by occasional swirl.

In preparation for the next step, centrifuge bottles were placed in an ice-water bath. For maximum efficiency of transformation, temperature of the bacteria should never rise above 4°C at any stage of the protocol.

The culture was transferred to ice-cold centrifuge bottles and the cells harvested by centrifugation (Eppendorf 5810R, 4°C, $2,100 \times g$, 15 min). Supernatant was decanted and the cell pellet resuspended in 250 mL of ice-cold pure H_2O. Cells were newly centrifuged (4°C, $2,100 \times g$, 15 min), the supernatant decanted and the pellet resuspended in 200 mL of ice-cold pure H_2O. After a further centrifugation (4°C, $2,100 \times g$, 15 min) the supernatant is decanted and any drop of water removed by pipetting out. The cell pellet is resuspended in 400µL o f ice cold 20% glycerol. 50 µL aliquots of the cell suspension were dispensed into sterile, ice-cold microfuge tubes, drop into a bath of liquid nitrogen and store into at -80°C.

2.11. Electroporation

50 µL of electrocompetent cells were mixed with 0.1-0.5 µL of plasmid DNA and exposed to electric shock in a previously chilled cuvette with an Electroporator 2510 (Eppendorf, Hamburg, Germany) set at 2.500 V. 1 mL of LB media was added to the cuvette immediately after the pulse. The cells were incubated (37°C, 250 rpm, 60 min) and plated onto LB_{amp} agar plates. Plates were incubated overnight at 37°C until colonies were visible.

2.12. Cultivation and expression of POx in E. coli libraries

Colonies grown on LB selective agar plates containing ampicillin were picked with toothpicks, inoculated into 96-well plates (BRAND, Wertheim, Germany), containing 1 mL LB_{amp} growth media and grown overnight (37°C, 900 rpm) in a Multitron II incubator shaker. Using a 96-pin Duetz System replicator tool (Steinbrenner, Wiesenbach, Germany), ~5 µL of culture were transferred to a 2 mL 96-well plate containing 500 µL LB_{amp} media and incubated (37°C, 900 rpm) until an OD_{578} value of 0.5-0.6. Recombinant POx production was induced by adding 0.05 mg of anhydrotetracycline (10 µL of 0.01 mg/mL stock solution of anhydrotetracycline in N,N-dimethylfolmamide) followed by incubation (30°C, 500 rpm, 18 h).

When performing expression of the chaperones set GroES-GroEL to assist the proper folding of expressed POx (Takara Kit, Takara Bio Inc, Shiga, Japan), the expression protocol was slightly modified: Colonies grown on LB selective agar plates ($LB_{amp/cm}$: 0.1 mg/mL of ampicillin and 0.04 mg/mL of chloramphenicol in LB) were picked with toothpicks, inoculated into 96-well plates containing 1 mL $LB_{amp/cm}$ and incubated overnight (37°C, 900 rpm). Using the 96-pin replicator tool, ~5 µL of culture were transferred to a 96-well plate containing 500 µL $LB_{amp/cm}$ media and left for growth (37°C, 900 rpm) until OD_{578} value reached 0.4. Expression of chaperones genes was first induced by adding arabinose (0.5 mg/mL) (6.25 µL per well of 40 % arabinose stock

solution) and after incubation (37°C, 900 rpm, 2 h), expression of recombinant POx was induced by adding 0.05 mg of anhydrotetracycline and incubating the cells overnight (30°C, 500 rpm, 18 h).

2.13. Whole cell ABTS HTS assay

A modified ABTS assay protocol was used to determine POx activity. Cells were centrifuged (Eppendorf 5810R, 4°C, 2,100×g, 10 min), supernatants were decanted and pellets were washed with 300 µL of 10 mM K_xPO_4 buffer pH 7. After a second centrifugation and removal of washing buffer cells were resuspended with 300 µL of 60 µM polymyxin B solution (in 10 mM K_xPO_4 buffer pH 7) and allowed to stand for 5 min. 200 µL of cells were transferred to a 96-well flat-bottom microplate (Greiner Bio-One (Greiner Bio-One, Essen, Germany), 100 µL of 100 mM D-glucose was added to each well (33.3 mM D-glucose final concentration) and the plate was incubated (45°C, 2 h). After centrifugation (4°C, 2,100×g, 10 min), 200 µL of the supernatant were transferred to a new 96-well flat-bottom microplate. Color development reaction was initiated by adding 50 µL of ABTS mix (50 mM ABTS, 30 U/mL horseradish peroxidase (HRP), 10 mM K_xPO_4 pH 4 buffer). After incubation (45°C, 2 h), the change in absorbance was measured by photometric reading at 414 nm using a FLASHScan S12 microplate reader (Analytik Jena, Jena, Germany).

2.14. Standard ABTS HTS assay

Definitive tests of activity were performed via ABTS assay on supernatants of samples after cell disruption via homogenization. 200 µL of the supernatants separated by centrifugation after cell disruption (4°C, 2,100×g, 10 min) were transferred to a 96-well flat-bottom microplate (Greiner Bio-One, Essen, Germany), 100 µL of 100 mM D-glucose was added to each well (33.3 mM D-glucose final concentration) and the plate was incubated (45°C, 2 h). 200 µL of sample were taken for color development reaction which was initiated by adding 50 µL of ABTS mix (50 mM ABTS, 30 U/mL horseradish peroxidase (HRP), 10 mM K_xPO_4 pH 4 buffer). After incubation (45°C, 2 h), the change

in absorbance was measured by photometric reading at 414 nm using a FLASHScan S12 microplate reader (Analytik Jena, Jena, Germany).

After introducing chaperones to assist the expression and proper folding of POx variants, the ABTS HTS assay could be reduced to a single step protocol: 150 µL of the supernatants separated by centrifugation after cell disruption were transferred to a 96-well flat-bottom microplate (Greiner Bio-One, Essen, Germany), 100 µL of 100 mM D-glucose was added to each well (33.3 mM D-glucose final concentration) and color development reaction was initiated by adding 50 µL of ABTS-HRP mix (50 mM ABTS, 30 U/mL horseradish peroxidase (HRP), 10 mM K_xPO_4 pH 4 buffer). After incubation (45°C, 2 h), the change in absorbance was measured by photometric reading at 414 nm using a FLASHScan S12 microplate reader (Analytik Jena, Jena, Germany).

Apparent standard deviation was calculated based on absorbance values obtained. The whole procedure was repeated using supernatant of cells that did not contain the insert. Absorbance values obtained were considered as background absorbance. True standard deviation was calculated after subtracting the background absorbance.

Substrate profile for FAD catalysis of POx wild-type and generated POx variants was performed using D-glucono-1,5-lactone and 5-thio-D-glucose. Regioselective oxidation was determined using 2-fluoro-2-deoxy-D-glucose as substrate.

2.15. Standard Phenylhydrazine assay

Tests of activity via product formation were performed via phenylhydrazine assay on supernatants of samples after cell homogenization or chemical lysis. Cultivation and expression of POx had been performed as described above. 100 µL of the supernatants separated by centrifugation after cell disruption (4°C, 2,100×g, 10 min), were transferred to a 96-well flat-bottom microplate (Greiner Bio-One, Essen, Germany), 50 µL of 100 mM D-glucose was added to each well (66.6 mM D-glucose final concentration) and the plate was incubated (45°C, 2 h). POx reaction is stopped and color-development reaction

initiated by adding 100 µL of 20 mM phenylhydrazine hydrochloride solution. After incubation (45°C, 2 h), the change in absorbance was measured by photometric reading at 390 nm using a FLASHScan S12 microplate reader (Analytik Jena, Jena, Germany).

2.16. Ferrocenemethanol based assay

100 µL of clear POx containing supernatant were transferred from each well of the deep plate into a 96-well flat-bottom microplate (Greiner Bio-One, Essen, Germany) and 100 µL oxidized ferrocenemethanol pH 8 (100 mM K_xPO_4) added to each well (see oxidized ferrocenemethanol preparation in Appendix 1). The conversion was initiated by supplementing 100 µL D-glucose pH 8 (333 mM, 100 mM K_xPO_4) and reaction kinetics was followed by photometric reading at 625nm using a FLASHScan S12 microplate reader (Analytik Jena, Jena, Germany). For molar extinction coefficient calculation and linear detection range determination of ferrocenemethanol based assay see Appendix 2 and 3, respectively).

2.17. Chemical lysis of E. coli cells

Cells were pelleted by centrifugation (4°C, 2,100×g, 10 min), media was decanted and pellets washed with 300 µL KxPO$_4$ buffer pH 7. After a new centrifugation (4°C, 2,100×g, 10 min), cells were resuspended with 1 mL 10mM phosphate buffer pH 7. 100 µL of the resuspension were transferred to 96-well flat-bottom microplate and 200 µL of B-PER (Bacteria Protein Extraction Reagent, Perbio Science, Deutschland GmbH, Bonn, Deutschland) reagent were added, cells resuspended and left 10 min at room temperature for cell disruption. Supernatant and membrane fragments were separated by centrifugation (4°C, 2,100×g, 10 min).

2.18. Homogenization of E. coli cells

Cells were collected in 50 mL Falcon tubes (Greiner Bio-One, Essen, Germany) and centrifuged (4°C, 2,100×g, 10 min). Pellets were washed with 25 mL K_xPO_4 pH 7 buffer and centrifuged again. The cells were then resuspended in 15 mL K_xPO_4 pH 7 and homogenized by 1 cycle at 1,200 bar (13,404 psi), at a working flow of 3 L/h in a Homogenizer Emulsi-Flex C3 (Avestin, Mannnheim, Germany). Cell debris was removed by centrifugation (4°C, 2,100×g, 10 min).

2.19. Sonication of E. coli cells

Cells were collected in 50 mL Falcon tubes (Greiner Bio-One, Essen, Germany) and centrifuged (4°C, 2,100×g, 10 min). Pellets were washed with 25 mL K_xPO_4 pH 7 buffer and centrifuged again. The cells were then resuspended in 15 mL K_xPO_4 pH 7 and sonicated -always on ice- for three cycles of 30s at 50% amplitude. Samples are centrifuged (4°C, 2,100×g, 10 min) and supernatants kept to proceed to POx activity determination.

2.20. Recovery and purification of commercial, native and recombinant POx

XL2-Blue cells transformed with $p_{wt}POx$ and $p_{tr}POx$ were grown to an OD_{578} of 0.6 in 1 L shaking flasks containing 200 mL of $LB_{amp/cm}$ (37°C, 250 rpm). Gene expression was induced by addition of 40 µL of 1 mg/ml anhydrotetracycline and incubation overnight (30°C, 250 rpm, 18 h). Cells were collected in 50 mL Falcon tubes (Greiner Bio-One, Essen, Germany) and centrifuged (4°C, 2,100×g, 10 min). Pellets were washed with 25 mL K_xPO_4 pH 7 buffer and centrifuged again. The cells were then resuspended in 15 mL K_xPO_4 pH 7 and homogenized by 1 cycle at 1,200 bar (13,404 psi), at a working flow of 3 L/h in a Homogenizer Emulsi-Flex C3 (Avestin, Mannnheim, Germany). Cell debris was removed by centrifugation (4°C, 2,100×g, 10 min).

The recombinant POx was purified from the supernatant by anion-exchange chromatography using a Toyopearl DEAE-650S (TOSOH BioScience GmbH, Stuttgart, Germany) packed 15/125 mm column (KronLab, Sinsheim, Germany) in an AKTA purifier (Amersham Pharmacia Biotech, Freiburg, Germany). Pre-equilibration of the DEAE-650S column was performed at pH 7.0 with 10 mM K_xPO_4 buffer (flow rate 5 mL/min). After loading POx-containing supernatant, non-absorbed proteins were washed out with 10 column volumes of the same buffer. POx was eluted via step gradient with 400 mM KCl 10 mM K_xPO_4 pH 7 buffer (Nishimura et al. 1996). Elution of the POx-containing fractions was monitored via photometric reading at 280 nm, 345 and 456 nm (Leitner et al. 2001) and checked via ABTS assay. The POx-containing fractions were lyophilized (Christ Alpha 1-2 LD, Osterode, Germany) and stored at -20°C.

2.21 Separation of protein using PAGE

SDS-polyacrylamide gel electrophoresis was conducted according to the method of Laemmli (1970) using 10 % separating gel and 5 % stacking gel containing 1 % SDS. Purified rPOx extracted from *E. coli* was heated at 95°C for 5 min in tris-glycine buffer containing 2 % SDS. 0.1 % bromophenol blue and 100 mM dithiotheitol. Electrophoresis was carried out at a constant current of 10 mA for 2 h using a running buffer of tris-glycine containing 1 % SDS. After electrophoresis, the gel was stained with 0.025 % Comassie Brilliant Blue R-250 solution (4h, room temperature) and was finally distained in methanol: acetic acid solution (8h, room temperature and changing the solution three times).

2.22. Silver staining of POx

Silver staining was performed over polyacrylamide SDS gels according to the method described by (Nesterenko et al. 1994), as summarized in the table below

Steps	Solution	Time
1 Fixation	60 mL acetone stock[b], 1.5 TCA stock[b], 25 μL 37% HCHO	5 min
2 Rinse	dd H_2O	3 x 5s
3 Wash	dd H_2O	5 min
4 Rinse	dd H_2O	3 x 5s
5 Pretreat	60 mL acetone stock[b]	5 min
6 Pretreat	100 μL $Na_2S_2O_3$ 5 H_2O stock[b] in 60 mL dd H_2O	1 min
7 Rinse	dd H_2O	3 x 5s
8 Impregnate	0.8 mL $AgNO_3$ stock[b], 0.6 mL 37% HCHO, 60 mL dd H_2O	8 min
9 Rinse	dd H_2O	2 x 5s
10 Develop	1.2 g $NaCO_3$, 25 μL 37% HCHO, 25 μL $Na_2S_2O_3$[b] 5 H_2O stock, 60 mL dd H_2O	10-20 s
11 Stop	1 % glacial acetic acid in dd H_2O	30 s
12 Rinse	dd H_2O	10 s

[a] All steps are performed in glass or plastic containers on a shaker at room temperature (approx. 23C). The volumes of all solutions were 60 mLs for minigels 0.75 mm thick

[b] Stock solutions 50% acetone in dd H_2O, 50 % TCA in dd H_2O, 20% $AgNO_3$ in dd H_2O (store in dark, shelf-life up to 4 months), 10% $Na_2S_2O_3$ 5 H_2O in dd H_2O (shelf-life up to 4 months).

[c] A brown precipitate may appear upon contact with the developer. It can be dissolved by vigorous shaking.

Table 5 Silver staining protocol

2.23. Zymogram

A zymographic activity determination method was developed for POx. It was based on the ABTS assay which detects formation of the by-product H_2O_2. Purified POx samples were run on native PAGE gels: neither SDS nor dithiotreitol were added and no heating of the samples was performed. The gel was then covered with a cellulose membrane which had previously been soaked for 10 min in 20 mL of the assay reaction mix (50 mM

D-glucose, 25 mM ABTS, 5 U/mL HRP). The preparation was incubated for 4 hours at room temperature. During incubation, the membrane was kept humid but drained. This involved addition of 250 μL of reaction mix from time to time in order to avoid drying of the membrane. Color development could be observed at the migration height of the POx bands with a characteristic dark green of oxidized ABTS. Color intensity increased with time, reaching full development after incubation overnight.

2.24. Active POx-band extraction. Protein and FAD photometric reading

Bands containing POx were cut out from the zymogram for enzyme extraction. POx was extracted by incubation of the polyacrylamide gel piece in 450 μL of buffer solution containing 10 mM K_xPO_4 pH 7, 100 mM NaCl and 2 % mercaptoethanol (25°C, 16 h). The solution was then used for photometric reading of protein content at 280 nm and oxidized FAD at 345 and 456 nm (Leitner et al. 2001) as well as for subsequent SDS-PAGE electrophoresis. Micro electrophoresis was performed using an Agilent Bioanalyzer 2100 (Agilent Technologies Deutschland, Böblingen, Germany).

2.25. Determination of kinetic parameters of β-D-glucose conversion

Maximum reaction rate (v_{max}), Michaelis–Menten constant (K_m) and turnover number (k_{cat}) were determined for β-D-glucose using the ABTS assay, total protein content determination and a Michaelis–Menten model. ABTS-based kinetic measurements of purified wild-type POx and mutated variants were performed identically to the ABTS assay in 96-well format, except that final concentrations of β-D-glucose ranged between 0 and 300 mM. The reactions were performed at room temperature. Total protein determination was performed according to BCA_{TM} assay kit (Pierce, Bonn, Germany). Data were used to estimate kinetic constants.

2.26. Thermostability

Thermostability of wtPOx and variants was assessed in 10 mM $KxPO_4$ buffer pH 7 by measuring initial activity and residual activity over the temperature range 25-75 °C. The same amount of wtPOx and variants were incubated at each temperature for 30 min in a thermal cycler and cooled down to room during 15 min before proceeding to ABTS assay in 96-well microtiter plate.

Simultaneously, the same amount of purified wtPOx and variants were aliquoted in PCR tubes and incubated in a thermal cycler at each specific temperature. Aliquots were taken at various time intervals from 1 to 7 hours and cooled down to room temperature for 15 min before they were assayed by ABTS assay in a 96-well microtiter plate.

2.27. pH stability

Pure wtPOx and POx variants samples in 10 mM $KxPO_4$ buffer pH 7 were aliquoted, diluted to 1:10 with specific pH buffers (Table 3) in order to assess a pH range from 3 to 10 and were incubated for 2 hours at room temperature. Initial and residual activities were measured using ABTS assay.

Buffer	pH value
100 mM Phosphate	3
100 mM Acetate	4
100 mM Acetate	5.5
100 mM Phosphate	7
100 mM Phosphate	8
CHES	9
CHES	10

Table 6 Buffer solutions used to study pH profile of pyranose oxidase activity

2.28. Chloride resistance

Pure commercial POx and purified recombinant wtPOx and POx variants were tested in 10 mM KxPO$_4$ buffer pH 7 with varying Cl$^-$ concentrations ranging from 0 to 170 mM by measuring their initial and residual activities using ABTS assay.

3. RESULTS

3.1 Cloning of Trametes versicolor pox

Amplification of the cDNA from *T. versicolor* POx yielded a 2,064-bp PCR product which included the 1,872-bp long open reading frame encoding for *T. versicolor* POx (wt POx). The cloned *T. versicolor pox* gene had a G+C content of 60 % and was predicted to encode a polypeptide of 623 amino acid residues with an estimated molecular mass of 69.4 (±0.2 KDa), which showed high similarities to other pyranose oxidases.

3.2 Site-directed mutagenesis of plasmid pASK-IBA3

Site-directed mutagenesis (Quick Change) was used to remove the codon ATG from the vector sequence. Thus, recombinant POx would be produced starting with the amino acid Met encoded in the gene and extra undesired amino acid residues will be avoided. Following the producer instructions and using the primers f10, r3 (Table 4, Material and Methods) the following PCR product was obtained:
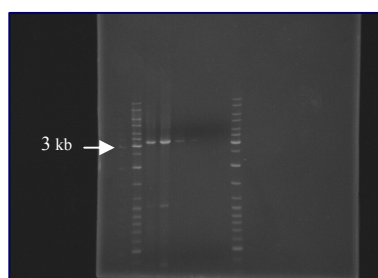
Fig 18 Purified site-directed mutagenesis product:
ATT pASK-IBA 3 at 3.2 kb

After cloning the ATT pASK-IBA3 plasmid in *E. coli*, four of the positive clones were selected for plasmid extraction. Electrophoresis of the samples showed an unexpected size thus suggesting the presence of supercoiled DNA. Subsequent digestion of the plasmid preparations with Nco I led to the expected 3.2 kb values. Presence of the desired mutation in two of the clones was proven after sequencing.

50
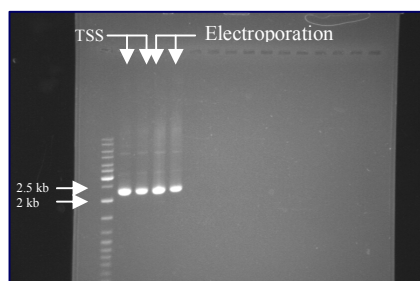
Fig 19a Positive clones after transformation in *E. coli.*
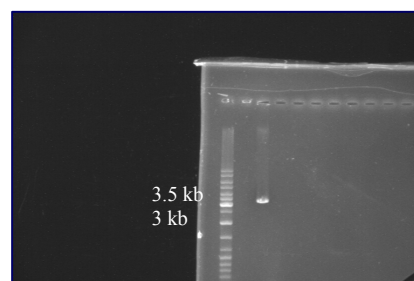
Fig 19b Clone 1 after digestion with Nco I

3.3 Gene cloning of pox in the plasmid ATTpASK-IBA 3

By means of reverse polymerase reaction using the mRNA extracted from *Trametes versicolor* cDNA of POx was obtained. PCR was used to amplify the cDNA. Cloning of the gene into *E. coli* using the modified ATTpASK-IBA 3 plasmid resulted in two positive clones confirmed by electrophoresis after plasmid extraction.
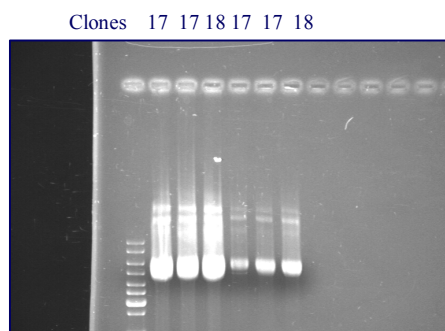
Fig 20 POx from *Trametes versicolor* cloned in *E. coli*

Gene cloning methods was performed as described in the section of Material and Methods.
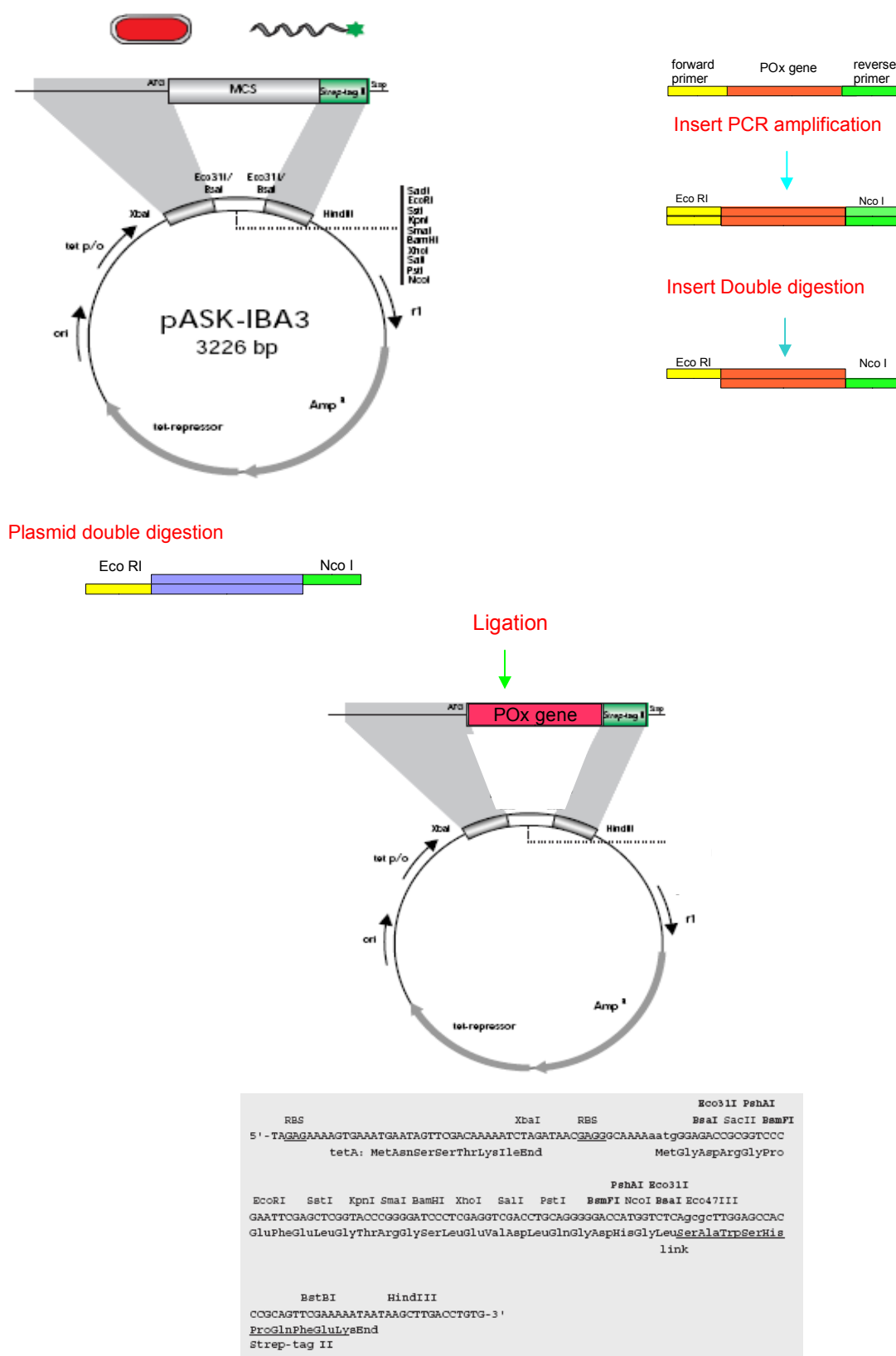
Fig 21 Scheme of the selected POx pASK-Iba III cloning system

3.4 Optimizing POx expression

First experiments on expression of POx by *E. coli* showed no activity in the samples. SDS Page electrophoresis of both pellets and supernatants after cell disruption showed a band around 65 kD indicating POx expression, which was significantly enhanced in the pellets fractions. POx in form of inclusion bodies which aggregates to membrane fragments could be detected as an enhanced band at 69 KDa in pellets from recombinant POx expressing clones when compared to control cells pellet. Supernatants showed very similar band patterns in both POx clones and control cells.

Lowering the temperature of induction from 37°C to 30°C led to a significant reduction of the inclusion bodies formation, which was then corroborated by ABTS assay in the supernatants which showed oxidase activity.

Conditions for POx expression in *E. coli* were assayed in order to optimize the protocol. Thus, different temperatures and duration of induction as well as various concentration values of the inducer, anhydrotetracycline for pASK-IBA 3 and IPTG for pPRME, were tested. Simultaneously, different methods for cell disruption were tried in order to maximize POx yield. These assays were performed by measuring expressed POx activity by ABTS assay. Samples were the following: obtained clones (17 and 18 for POx from *Trametes versicolor*), negative control (*E. coli* with no insert containing the modified plasmid ATTpASK-IBA3) and POx containing pPMRE 10 mutant from the Japanese company Kikkoman.

Assayed values	Optimum induction values for POX expressing pASK-IBA 3 clones	Optimum induction values for pPRME10 clone
Incubation temperature: 37°C 35°C 30°C 28°C 25°C	(37° C)* 28° C, 30° C (low values) 25° C	30° C
Incubation time: 4 hours, 6 hours, overnight	(4 hours)* overnight	overnight

Inducer concentration (Anhydrotetracycline: five values ranging from 2.5 to 50 µL/100 mL culture, IPTG)	10 µL/100 mL of 2mg/ml anhydrotetracycline solution in DMF	1mM final concentration of IPTG
Method for cell disruption: Sonication, B-PER lysis, lysozyme	B-PER buffer (4:1) No lysozyme	B-PER buffer (4:1) No lysozyme

* Inclusion bodies are produced

Table 7 Results summary of assaying different induction and cell disruption conditions to maximize active POx expression as determined by ABTS assay on supernatant samples

The use of lysozyme for cell disruption led to lower values of POx activity in the samples. Lysozyme could be degrading POx.

Bradford method was used to determine the protein yield obtained by the different means of cell disruption showing that the use of the lysis buffer Bacteria Protein Extraction Reagent (B-PER, Perbio Science Deutschland GmbH) led to higher yields of protein than sonication (Material and Methods). The difference ranges from 25 to 100 % depending on the volume of B-PER used. Optimum disruption was observed when the volume of phosphate buffer used to re-suspend the cells was minimized and B-PER added in a ratio 4:1.

POx activity of commercial available samples was proved not being affected by lysis buffer B-PER. Bacteria Protein Extraction Reagent was initially adopted as general method for cell disruption on 96-well plate format.

3.5 Designing a POx purification protocol

Purification of commercial POx was performed by HPLC through a DEAE 650S packed column using 10 mM KxPO4 buffer pH 7 for elution in a growing gradient (0-1 M) of KCl.

The protein eluted at a salt concentration of 0.26 M as shown at the corresponding chromatogram. Lyophilisate of the POx containing fractions was tested for POx activity.
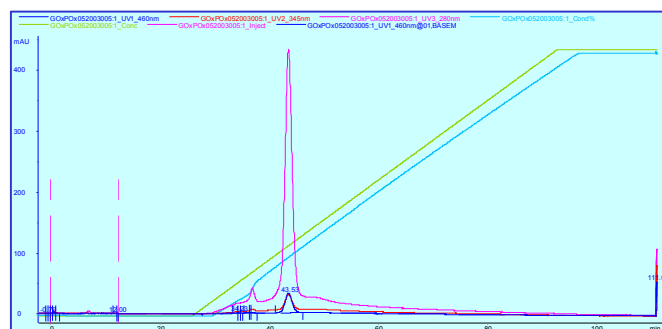
Fig 22 Purification demonstrated optimal by HPLC through a DEAE 650S packed column using 10 mM KxPO$_4$ buffer pH 7 for elution in a growing gradient 0-1 M KCl. POx eluted at 0.26 M KCl

This method was subsequently used to purify recombinant POx.

3.6 Commercial POx characterization

Assays as to evaluate temperature and pH profile as well as Chloride resistance were performed on purified commercial POx

Temperature	Activity (μmol glucose/mg lyophilisate)
25°C	31.85
30°C	34.76
35°C	28.25
40°C	(20.76)
45°C	23.72
50°C	23.57
55°C	15.38

Table 8 Activity of POx enzyme at different temperature values. Assay performed at 30 mM β -D-glucose by phenylhydrazine system

Temperature	Activity (µmol glucose/mg lyophilisate)
25°C	63.81
30°C	67.04
35°C	68.51
40°C	73.48
45°C	75.80
50°C	70.91
55°C	62.85

Table 9 POx activity at different temperature values. Assay performed with 20 mM β-D-glucose by phenylhydrazine assay and letting the samples cool down before measerument

[Chloride] (mM)	Activity (µmol glucose/mg lyophilisate)
0	31.85
10	34.26
30	39.03
50	32.16
70	29.89
90	32.86
110	28.60
130	24.82
150	29.29
170	30.09

Table 10 POx activity at different concentrations of chloride, pH 7 and 25 ˚C. Assay performed by phenylhydrazine system.

Ultrafiltration of DEAE HPLC purified fractions via Amicon filters (Millipore) with a cut-off of 30,000 MW to remove Chloride showed no significant difference (95%) in POx activity in the samples.

3.7 Optimizing the conditions for directed evolution of POx

Various values of $MnCl_2$ concentration were tried in a first epPCR to optimize mutational ratio and viability of the library clones during Directed Evolution experiments. Best yield of PCR product was obtained when 0.025 mM $MnCl_2$ was used.
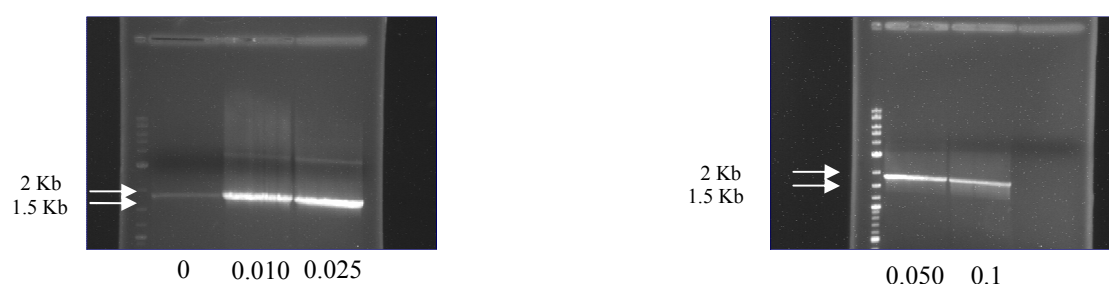
Fig 23 epPCR product yields according to the various $MnCl_2$ concentration values used

epPCR product was subsequently cloned and recombinant POx expressed. Activity was checked by ABTS. Results showed that higher 18 % of active transformants was obtained at 0.05 mM $MnCl_2$
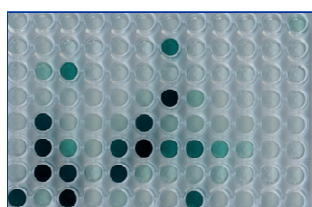
Fig 24 Clones obtained by Directed Evolution using 0.05 mM $MnCl_2$

In order to increase the number of mutants obtained a slight modification of the ligation protocol was introduced: Digested insert and plasmid were mixed and incubated at 72°C for 8 min and then left to cool down at room temperature before proceeding to add the rest of the components of the ligation mixture, then incubating for an hour and leaving at 4°C overnight. Samples treated as described led to a higher number of transformants than those following the usual ligation protocol.

In a second directed evolution experiment to optimize the percentage of active variants obtained 0.05 and 0.07 mM $MnCl_2$ concentration values were tried. The use of 0.07 mM $MnCl_2$ led to a higher ratio of active variants. Nevertheless, most of significantly improved variants -in terms of activity- were observed when 0.05 mM $MnCl_2$ was used.
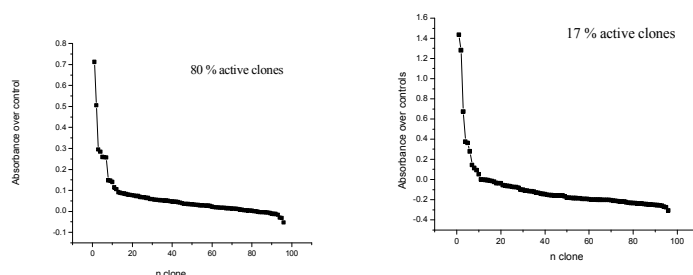
Fig 25 Percentage of active clones obtained by 0.07 mM $MnCl_2$ epPCR. Each graph corresponds to 96 clones of the *E.coli* library harboring ATT-pASK-IBA3 containing *pox* gene. POx activity checked via ABTS assay. Values of absorbance are over *E. coli* controls containing the plasmid but not the insert
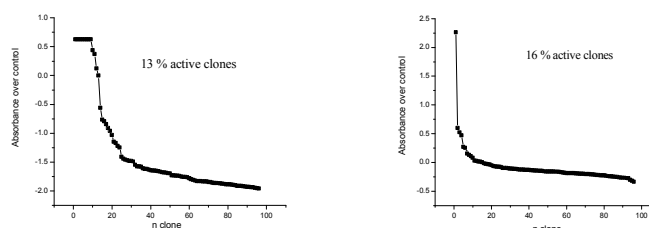
Fig 26 Percentage of active clones obtained by 0.05 mM $MnCl_2$ epPCR. Each graph corresponds to 96 clones of the *E.coli* library harboring ATT-pASK-IBA3 containing *pox* gene. POx activity checked via ABTS assay. Values of absorbance are over *E. coli* controls containing the plasmid but not the insert

3.8 Directed Evolution of POx

As a result of two experiments of directed evolution, a library of 1152 clones (12 x 96-well plates) was obtained. They were tested by ABTS assay for increased POx activity. Initial candidates were then re-screened in 3-4 repeats to remove false positives produced by the handling involved. In a last test, only best mutants are selected for the next round of directed evolution
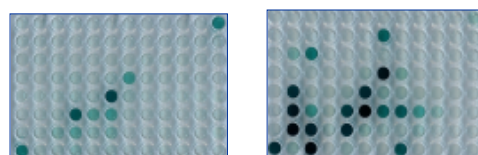
Fig 27 Plates (e) and (f). 0.05 mM MnCl$_2$ epPCR. POx WT controls in the corners in plate (e) and diagonally in the center in plate (f)

After the second round, three clones showed a 2-3 fold increased activity. Clone 70c was selected for a third round of Directed Evolution.

70 c

d 65

17

control

f 56
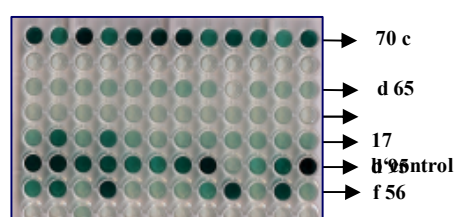
Difference to control			Ratio to WT		
17 b'		5.65	17 b'		1
Clone 0.07 c 70		15.15	Clone 0.07 c 70		2.68
Clone 0.05 d 95		13.37	Clone 0.05 d 95		2.37
Clone 0.05 f 56		8.20	Clone 0.05 f 56		1.45

Fig 28 Relative activity values of selected POxs variants after 2nd round of Directed Evolution

The classic DNA cloning procedure used - epPCR products, enzymatic restriction of inserts and vector pASK IBA 3, followed by ligation and subsequent transformation into *E. coli* cells for expression - suffered from certain limitations among which availability of unique restriction sites in both insert and vector and specially, poor ligation of the insert were the most remarkable.

3.8.1 DE of POx using ligase free cloning method

An alternative ligase-free cloning method for POx and ATTpASK-IBA3 was developed (Zhou et al, 1995, Li et al, 1997). The POx insert could be extended in a length of around 20-25 nucleotides at each end, in a sequence complementary to the vector at both sides of a specific restriction site. Pst I was the restriction enzyme selected to cut the vector

ATTpASK IBA3. The action of an exonuclease, both in the PCR product and on the sequence of the linearized vector would thus provide sticky ends that will match at a certain temperature and with no need of ligase.

The exonuclease, which only acts in direction 5'3', stops digesting at the phosphorothioate bond.
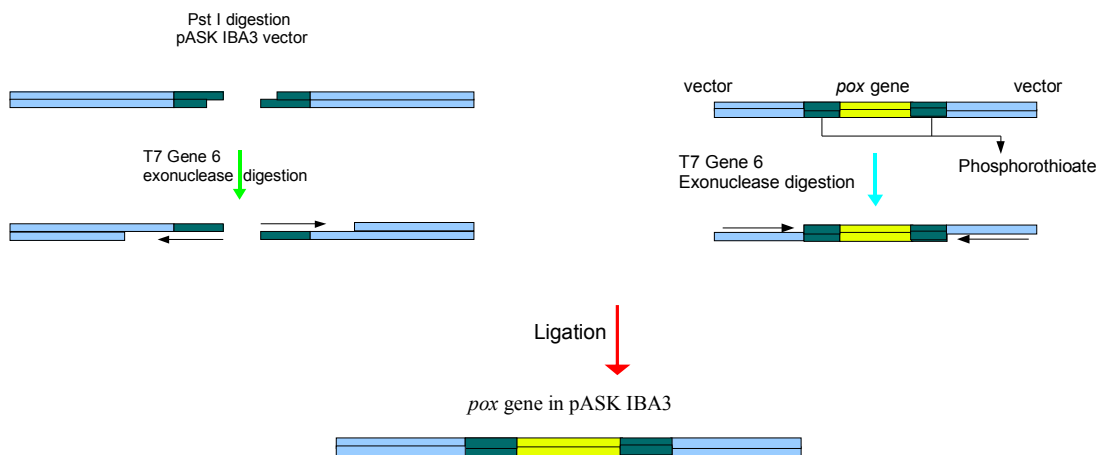
Ligase free method primers were designed for POx and ATTpASK-IBA3.

Forward primer   5'CCC TGC AGG TCG ACC TGC A*G*G ATG TCT ACT AGC TCG 3'
Reverse primer   3'GCT TAG TCC GAC ATT CT G*G* ACG TCC CCC TGG TAC CAG 5'

Plasmid restriction site: CC TGC AGG
                          GG ACG TCC

Pst I

Pst I

3 kb

Fig 29 Pst I digested pASK-IBA 3 plasmid separation
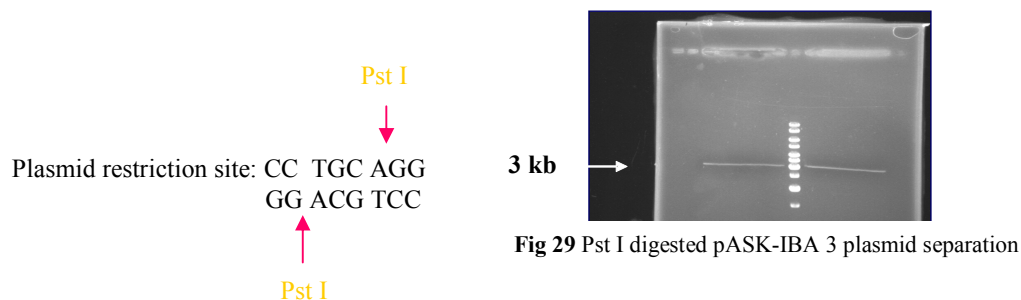
epPCR on the plasmid of the 70 c variant was performed using the described oligos. Amplified product was purified and digested with exonuclease. Pst I digested ATTpASK-IBA3 plasmid was gel extracted and digested with exonuclease. Insert and plasmid were

ligated via incubation for 10 minutes at 75°C. Ligation product was used to transform *E. coli.*

This ligase-free cloning method with T7 Gene 6 Exonuclease showed higher transformation efficiency compared to the classic method and was successfully used for creating large libraries (1814 clones in 20 x 20 cm plates), but colony PCR still showed a high percentage of religation of the plasmid without the insert. This result was confirmed by ABTS assay.

Testing different Pst I and exonuclease digestion conditions did not help. No amplified product of the inserts was observed in many clones after colony PCR.

The persisting problem of religation could finally be minimized by including in the protocol a further plasmid extraction, gel electrophoresis separation and subsequent extraction followed by transformation: the religated product was separated by electrophoresis, whereas plasmids harboring the *pox* gene were gel extracted and used to transform *E. coli*. The number of active clones boosted about a 20 % by this method.

Directed Evolution via ligase free method led to some variants showing increased activity compared to wild type

Confirmation	Relative activity to wild type
Clone 2 d	3.67
Clone 3 d	3.08
Clone 6 d	4.07
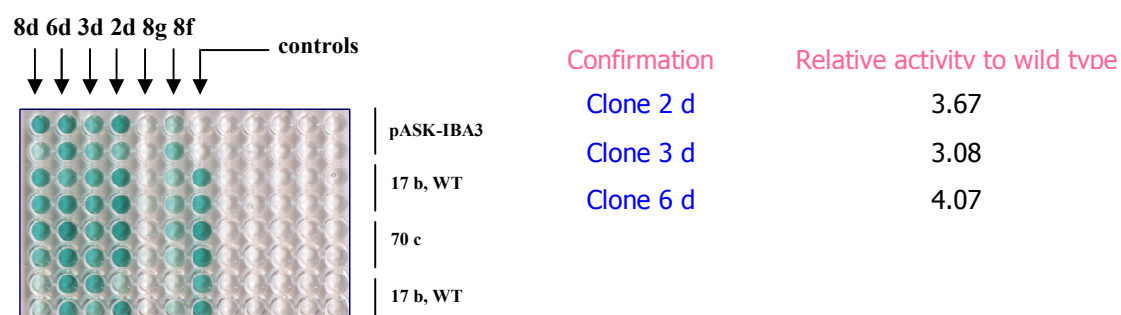
Fig 30 Relative activity values of selected POxs variants after 4th round of Directed Evolution via ligase free method

Plasmid of the best clone from the 4th round of DE (6d showing activity 4.07 fold WT) was extracted and was used as a template for the 5th round via ligase free method.

61

Supercoiled 6d variant plasmid

6d variant plasmid after 3h of Pst I digestion at 37°C.
The fade band at 5 kb indicates the linearized plasmid

ep PCR products on the 6d variant

Separation of the epPCR products
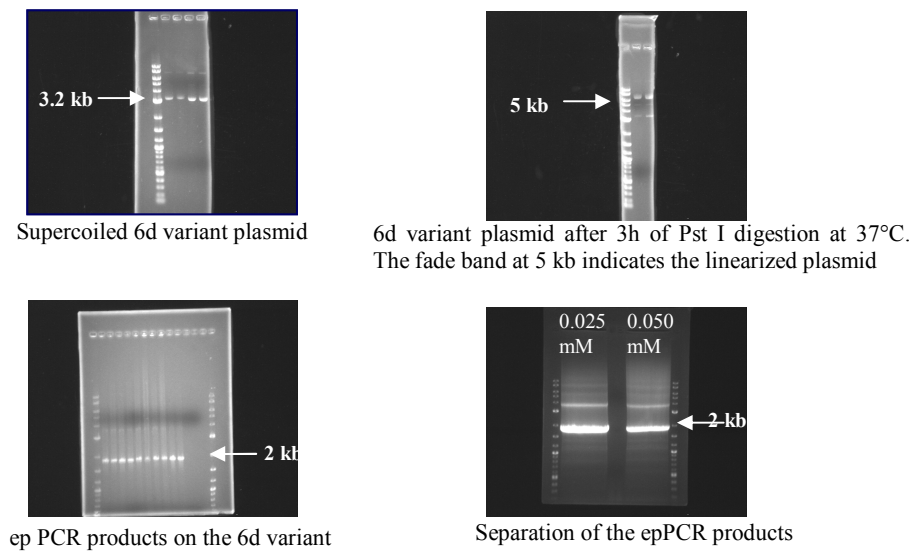
Fig 31 Diverse steps of checking the 6d2 POx variant which is further used as a new epPCR template

The free-ligase method was performed as described before except for the ligation step, slightly modified to reduce religation. Ligation was performed as follows:

- Insert: plasmid ratio was increased from 3:1 to 14:1
- Ligation was performed via incubation for 10 minutes at 80°C
- Mixture was left 30 min to cool down at room temperature
- T4 ligase and the corresponding buffer were added and samples incubated for 3h at 37°C
- Ligation was left to run overnight at room temperature before proceeding to transform *E. coli*

Colony PCR of the transformants obtained showed the presence of the POx insert in 37.5% of the clones, which confirmed the improvement of the modified ligation protocol. ABTS assay on 6 x 96 (576) clones showed the presence of active ones, not improved variants though.

In an attempt to further reduce religation, plasmids are extracted from a pool of fresh transformants and the 5kb band, which contained the POx insert, used for a new

transformation of electrocompetent *E. coli*. This way 18 x 96 clones (1728), initially containing the POx insert, were obtained. In total, a library of 2304 clones was screened. None of them was nonetheless confirmed as an improved variant in the 2nd ABTS test to remove false positives (Data not shown)

The idea of trying other Polymerase systems to overcome the possible bias occurring due to Taq Polymerase limitations started to be considered.

3.8.2 Reducing mutational bias

The use of Mutazyme II polymerase, which displays different mutational spectra to Taq polymerase, was considered.

No bias	Taq Pol	Mutazyme II Pol
Ts/Tv= 0.5	0.8	0.9
AT→GC/GC→AT	2	0.6
A→N, T→N	75.9 %	50.7 %
G→N, C→N	19.6 %	43.8 %

Table 11 Mutational spectra of Mutazyme II and Taq DNA Polymerases

The Mutazyme Kit from Stratagene, which combines the use of the two enzymes, was chosen. The basics of the method were described in the paper by Vanhercke et al, 2005.

According to these authors, the success of protein optimization through DE depends to a large extent on the size and quality of the displayed library. Current low-fidelity DNA polymerases that are commonly used display strong mutational preferences, favoring the substitution of certain nucleotides over others. The result is a biased and reduced functional diversity in the library under selection. In an effort to reduce mutational bias, the authors combined two different low-fidelity DNA polymerases, Taq and Mutazyme, which have opposite mutational spectra.

As reported by the authors, random mutants of the *Bacillus thuringiensis* cry9Ca1 gene were generated by separate error-prone PCRs with each of the two polymerases. Subsequent shuffling by staggered extension process (StEP) of the PCR products resulted in intermediate numbers of AT and GC substitutions, compared to the Taq or Mutazyme epPCR libraries. This strategy allowed generating unbiased libraries or libraries with a specific degree of mutational bias by applying optimal mutagenesis frequencies during epPCR and controlling the concentration of template in the shuffling reaction while taking into account the GC content of the target gene.
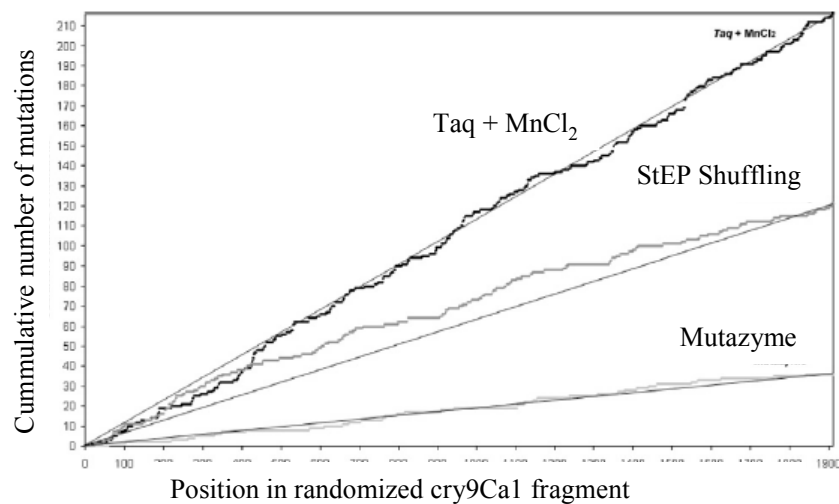
Fig 32 Distribution of random mutations in 10 clones after ep PCR with Taq polymerase, epPCR with Mutazyme DNA polymerase, or subsequent StEP shuffling. Straight lines represent an ideal distribution without mutational hot spots and are based on the total number of mutations in 10 sequenced clones of each library (Vanhercke et al. 2005)

Simultaneously, checking the possibilities of establishing an „in vivo" mutagenesis system via a mutated Polymerase I was considered (Camps et al, 2003). The authors reported a two-plasmid system for *in vivo* mutagenesis in JS200 (*polAts*). See the Introduction section.

3.8.3 DE of POx using Mutazyme Kit (Stratagene)

A new epPCR was performed using the Mutazyme Kit from Stratagene. The template was an equimolar mix of the 70 c (2,68 x WT), 2d (3,67 x WT) and the 6d (4,07 x WT) clones' plasmids. Several conditions were tested for optimization. Amount of template and number of cycles are the main parameters determining the mutation frequency: the higher the amount of template, the lower the mutation frequency. The same effect has a decreasing number of PCR cycles.

High, medium and low amount of template were tested, as well as PCR protocols of 20 and 30 cycles. Optimum yields were obtained by using medium amount of template (100 ng) and 20 cycles.

Mutation rate	Mutation frequency (Mut/kb)	Initial target amount (ng)
Low	0 - 4,5	500-1000
Medium	4,5 - 9	100-500
High	9 - 16	0.1-100
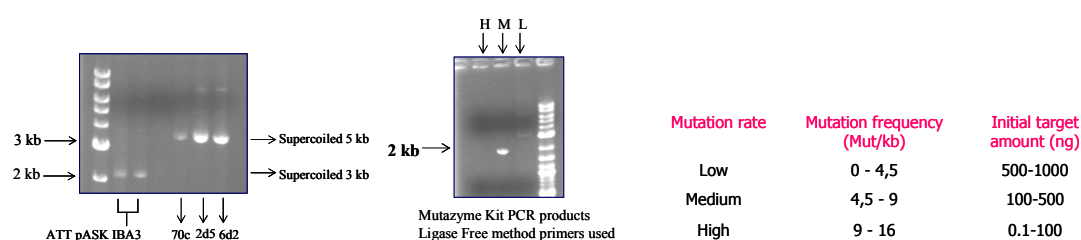
Fig 33 Results of Mutazyme Kit epPCR performed on a template of equimolar mix of 70 c (2,68 x WT), 2d (3,67 x WT) and 6d (4,07 x WT)

Ligation followed the improved Ligase Free method. Colony PCR of randomly selected transformants showed the presence of the POx insert in 20% of the clones.

14 x 96 clones (1344) were picked up, inoculated and tested for improved POx activity via ABTS HTS. 45 clones (3.35 %) showed apparently higher activity than the wild type and went for a 2nd ABTS test to remove false positives.

After performing a second round of DE according to the indications of the producer, several improved variants were found: 7A14, 10 C14, 12C14, 11F14, 7A13, 4F6, 4G6, 10G3, 6C5, 5E7.

Clone	Relative Activity (to 70 c)	Relative Activity (to WT)
5'	1,34	3,6
6C5	2,50	6,7
7A14	1,62	4,3
10C14	3,54	9,5
11F14	1,95	5,2
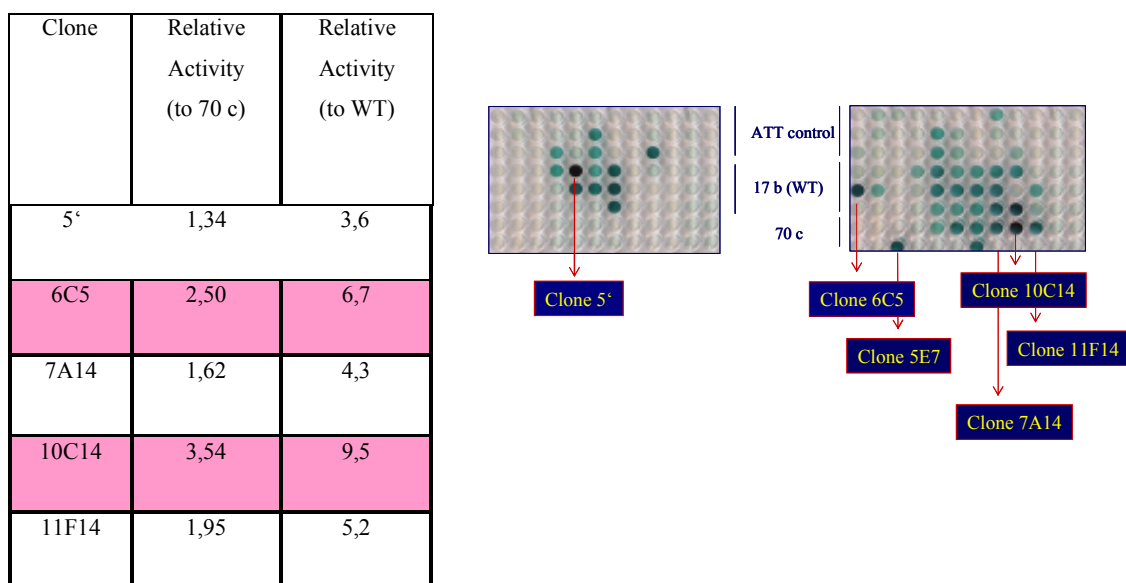
Fig 34 Relative activity values of selected POxs variants after Mutazyme round of Directed Evoltution

3.8.4 A defective Pol I system, used to introduce further mutations: XL-1 Red Competent Cells (Mutator Strain)

XL1-Red Competent Cells (Stratagene) were used for introducing random mutations in the POx gene. The method involves propagating the POx gene into this *Escherichia coli* strain, which is deficient in three of the primary DNA repair pathways: The mutS (error-prone mismatch repair), mutD (deficient in 3´- to 5´- exonuclease of DNA polymerase III) and mutT (unable to hydrolyze 8-oxodGTP).

A library of 846 clones was obtained. Best results were observed for transformants with plasmids from days 1, 2, 3 & 4 were a higher number of active clones and increased POx activity values were observed. Transformants with plasmids from days 5, 6 & 7 led to most of the clones not expressing active POx.

3.9 Improving POx expression: Use of Chaperones (Takara Kit)

Molecular chaperones have been demonstrated to be involved in the protein folding process. Takara's Kit chaperone plasmids carry an origin of replication derived from pACYC and a chloramphenicol resistance gene (Cmr). This arrangement allows their use with POx expression systems: *E.coli* / pASK-IBA3 (Iba-Göttingen) showing ampicillin resistance. For the chaperone genes situated downstream of the araB promoter, expression of chaperones and POx (mediated by tet promoter) can be induced separately.

GroEL (around 60 kDa)
GroES (around 10 kDa)
DnaK (around 70 kDa)
DnaJ (around 40 kDa)
Tf (around 56 kDa)
GrpE (around 22 kDa)
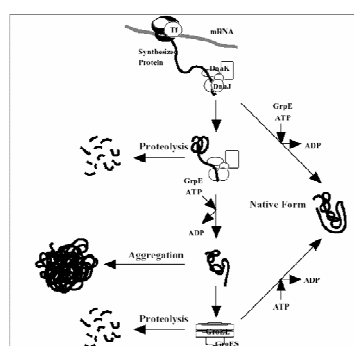
No.	Plasmid	Chaperone	Promoter	Inducer	Resistant Marker
1	pG-KJE8	dnaK-dnaJ-grpE	*araB*	L-Arabinose	Cm
		groES-groEL	*Pzt1*	Tetracyclin	
2	pGro7	groES-groEL	*araB*	L-Arabinose	Cm
3	pKJE7	dnaK-dnaJ-grpE	*araB*	L-Arabinose	Cm
4	pG-Tf2	groES-groEL-tig	*Pzt1*	Tetracyclin	Cm
5	pTf16	tig	*araB*	L-Arabinose	Cm

Fig 35 Description of Takara Kit sets of chaperones plasmids

Using the Takara kit, a total of five plasmids sets and their corresponding induction conditions were tested for POx expression as described in Material and Methods (Thomas et al, 1997; Nishihara, et al 1998; Nishihara et al, 2000).

WT POx expresed in combination with 5 sets of chaperones

Ch 1   Ch 2   Ch 3   Ch 4   Ch 5
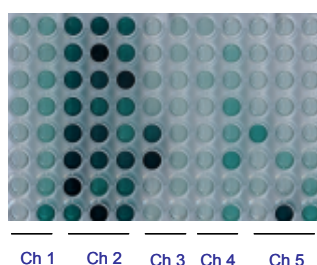
Fig 36 Results of recombinant POx expression in 96 well format using
five different sets of plasmids provided by Takara Kit

Set 2, pGro7 encoding <u>groES-groEL</u> proteins (araB, L-Arabinose, Cm), showed the best results in terms of activity and reproducibility: active POx expression got **highly reproducible** and a **two-fold increased POx expression** was obtained.
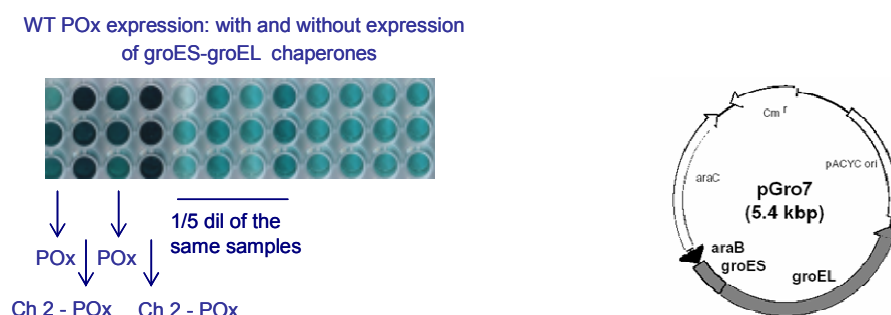
Fig 37 Set 2 of Takara Kit chaperone proteins –named Ch 2 in the picture- proved significant improvement in recombinant active POx expression. Ch 2 contained groES-groEL proteins encoded in pGro7 plasmid (araB, L-Arabinose, Cm).

This set of plasmids was from then on used to establish the Phenylhydrazine system and to further express POxs variants.

3.10 Use of Site-Directed Mutagenesis to simulate other reported improved variants

Site-directed mutagenesis was used to produce a mutant with two substituted amino acids which has been described to show improved kinetic parameters (Heckmann-Pohl et al, 2005).

Using the specifically designed oligos we proceed to the two following substitutions in *Trametes versicolor* POx:

❖ K338 → E338   Oligo: GC TTT GAA ATC GAA GCA GAC GTG

❖ S627 → K627   Oligo: G CAA TGT CGC AAA CGA TCA AG

In each case a previous gradient PCR is performed. Transformants obtained after cloning the PCR product are tested by ABTS HTS searching for higher POx activity values
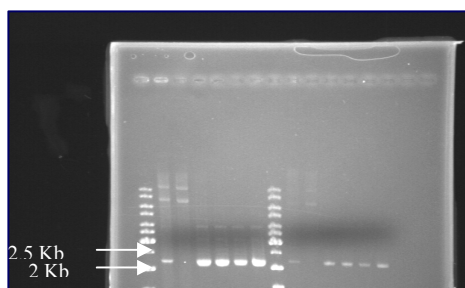
Fig 38 K 627 QuikChange Site-Directed mutagenesis transformants. Extracted plasmids are supercoiled

Over the S627K plasmids, the second mutation K338E was performed. ABTS tests on the transformants led to two improved mutants -5A and 3B- which initially showed higher POx activity. Sequencing results combined with kinetic studies on these clones will give structure-function insights on POx from *Trametes versicolor.*

3.11. Screening methods for POx reaction over glucose

3.11.1 Based on the detection of H_2O_2

    a) ABTS system
    b) Amplex Red assay

3.11.1.1 Designing the ABTS assay for determining POx activity

ABTS is oxidized in presence of H_2O_2 and HPR (Horseradish peroxidase) to a colored compound which is determined by photometric reading at 414 nm. Preliminary tests were performed to design the assay protocol and to establish de dynamic linear range for measurement.

Tests were initially performed in test tubes using commercial POx, varying buffers to be used, volumes of reaction, concentration of glucose, horseradish peroxidase (HRP), pH,

order of addition, time of reaction, etc. After scaling down the study in Eppendorf tubes, and further adapting the parameters to work in 96 well multititer plates, a proper preliminary protocol of the assay could be established. Finally the protocol was tested using recombinant POx expressed in 96 well multititer plates.

The assay proved valid and was subsequently used to evolve POx. The test conditions were also adapted to screen glucose oxidase. The assay system thus developed proved efficient to assist directed evolution of glucose oxidase and became an essential tool for the success of other coworkers (Zhu et al, 2006).
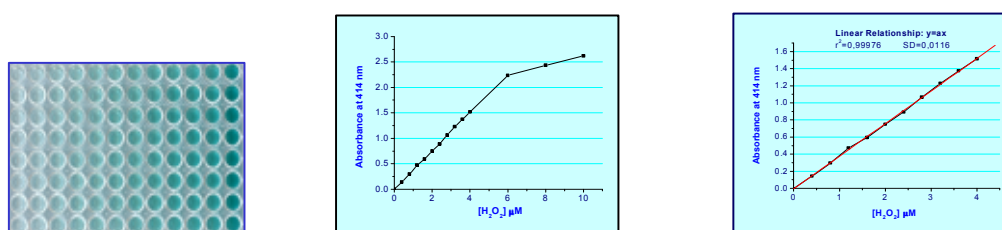
Fig 39 Study of the dynamic linear range for the ABTS system: sensitive at 0 to 6 µM of H_2O_2

3.11.1.2 Establishing the ABTS system as HTS assay

In order to develop the ABTS assay as an HTS system, clones of *E. coli* expressing POx from *Trametes versicolor* were inoculated in 2 ml deep well multititer plates containing 1mL LB_{amp}, let for growth and induced with anhydrotetracycline. Cells were then pelleted by centrifugation, resuspended in phosphate buffer pH 7 and disrupted by B-PER. Supernantants were then transferred to standard 96-well plate for POx activity by ABTS assay.

0.0025   0.01   0.05   0.25

    0.005   0.025   0.1   0.5
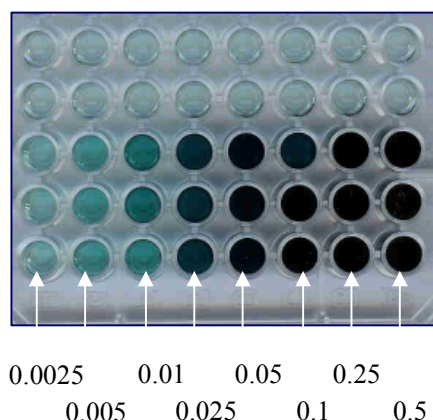
Fig 40 Color development in ABTS system (POx activity in U/mL)

In a repeat of the experiment, only wild type clone 17b was inoculated. Replication in a deep well multititer plate using the replicator tool showed improved assay results when compared to inoculation of a certain volume of culture, which led to too high cells concentration.

ABTS assay on the supernatants of the induced cells showed homogeneous color development as expressed by the obtained values of true standard deviation (9.4%).
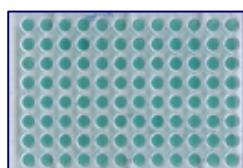
Fig 41a ABTS assay for POx activity expressed in *E. coli.* SD: 9.94 %
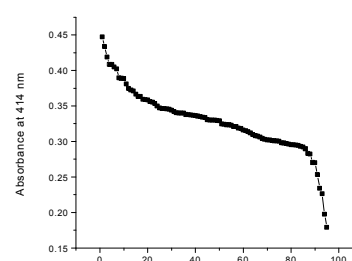
Fig 41b SD for the ABTS assay on recombinant POx expressed in *E.coli*

An experiment was performed with clone 17b expressing wild type *T. versicolor* POx to check if whether acidic or basic conditions were better to stop the color development reaction. 10 µl of 2.5 M HCl were sufficient for that purpose.

The value of SD (9.5%) permitted establishing a protocol for ABTS HTS assay (Materials and Methods)

3.11.1.3 Testing permeabilizers

A whole cell assay, which allows saving centrifugation steps, turned to be very an interesting in order to reduce the time required per measurement. Therefore comparative experiments were performed by using EDTA as permeabilizer showing that this approach is actually viable at certain concentration values and shows even increased sensitivity.
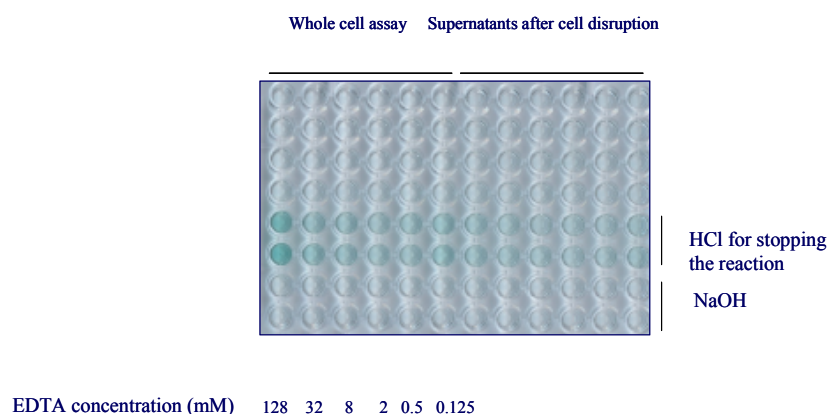
Fig 42 EDTA used as a permebilizer to develop a whole-cell assay system

In view of the results, other permeabilizers - Polyethylenimine, DHMP (dihydroximetaphosphate), Polymyxin B and EDTA - were tested. Polymyxin B performed well and was further studied testing at different concentrations ranging from 5 to 30 µM and compared to:

- using EDTA in a whole cell assay system.
- activity-test performed on supernatants after chemical lysis with B-PER

Simultaneously, different procedures were tried out in a six plates experiment in order to:

- minimize the time required per test
- obtain the lowest standard deviation

72

- gain highest color contrast between controls and samples
- achieve reasonably stable measurements

Parameters to test and optimize were:

- Time for POx reaction (ranging from 15 min to 4 h)
- Time for ABTS color development reaction (ranged from 0 to 2 h)
- Order in which reagents for POx reaction and ABTS color development reaction are added

The results indicated that

➢ Polymyxin B acts better than EDTA as permeabilizer
➢ Optimum Polymyxin B concentration 5 µM
➢ Both permeabilizers led to increased sensitivity for POx activity detection if compared to tests on the supernantants after lysis with B-PER
➢ Best procedure:

- 15 min for POx reaction
- Stop the reaction with HCl
- ABTS + HRP for color development reaction
- Measurement at 414 nm
- Values keep stable for 4 hours

Using polymixin B as a permeabilizer, ABTS HTS SD values were around 9%. As a result, a protocol for whole cell ABTS HTS could be established (See Materials and Methods).

In a last test, a comparison experiment was run with several POx variants, in which activity was tested

A) By ABTS assay in the supernatant after chemical cell disruption

B) By ABTS assay in the whole cell using the Polymyxin B as permeabilizer

Fig 43a Color development in supernatants after cell disruption. ABTS assay for POx expressed in *E. coli.*
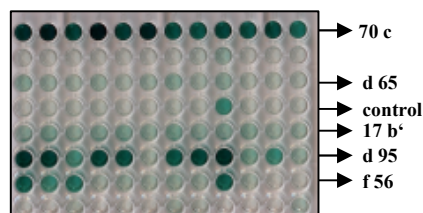
Fig43b Color development in permeabilized cells using 60 µM Polymyxin B. ABTS assay for POx expressed in *E. coli.*

ABTS HTS assay in supernatant and using permeabilized cells correlated well. The latter showed lower sensitivity but reduced SD when compared to ABTS HTS in supernatant of disrupted cells. Aiming to reduce the costs derived from using B-PER buffer for screening, the observed differences were considered acceptable. A protocol based on the use of Polymyxin B as permeabilizer was established and used as routine protocol (Material and Methods).

3.11.2 Based on the detection of the enzyme product 2- keto-glucose:

a) Phenylhydrazine system
b) Gluconate reductase-based assay system

3.11.2.1 Developing a novel assay: Phenylhydrazine system

Phenylhydrazine system: 2-keto-glucose reacts with phenylhydrazine forming a colored compound which is determined by photometric reading at 390 nm

2-Keto-glucose

Glucose phenylosazone

74

Preliminary tests were performed to design the assay protocol and to establish de dynamic linear range for measurement.

Fig 44 Study of the dynamic linear range for the phenylhydrazine system: sensitive at 0 to 12 µM D-glucose.

At saturating conditions of glucose (20 mM glucose, POx K_m towards glucose around 1.5 mM) other variables of the assay were tested.
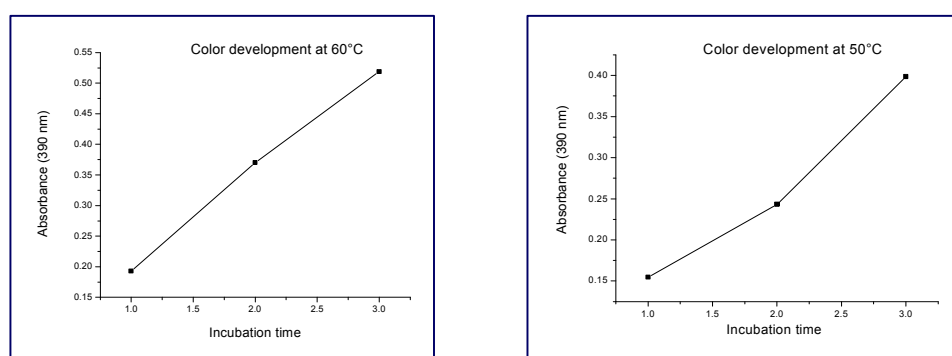
Fig 45 Study of the incubation time and temperature for the phenylhydrazine assay system. Experiments were performed at 20 mM β-D-glucose, with a 1.4 ml total volume.

Values at 50°C showed to be acceptable whereas values at 40 and 35°C showed to be in the very low range. In order to scale down the assay smaller volumes of reaction and lower values of temperature were tried in order to diminish the evaporation effect on multititer-plate well conditions.
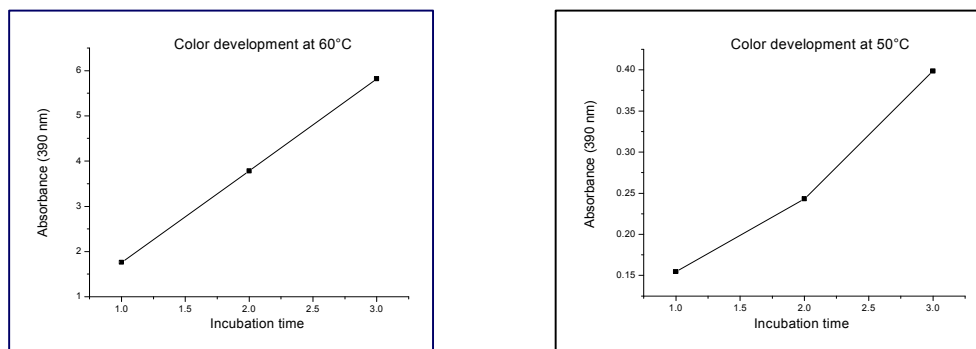
Fig 46 Study of the incubation time and temperature of the phenylhydrazine assay at 60°C and 50°C respectively. Experiments were performed at 20 mM β-D-glucose, with a 0.32 ml total volume.
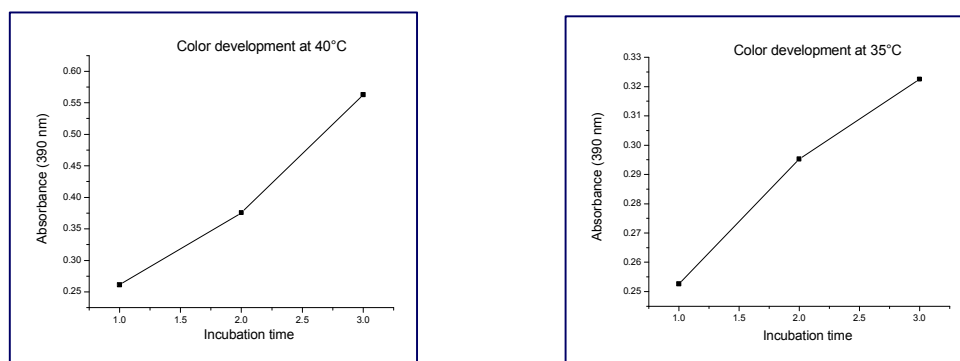
Fig 47 Study of incubation time and temperature of the phenylhydrazine assay at 40°C and 35°C respectively. Experiments were performed at 20 mM β-D-glucose, with a 0.32 ml total volume.

Values at 40°C and 35°C were acceptable. The evaporation effect was significantly reduced. Nevertheless, color saturation was not reached. Time-course for color saturation run at 45°C and 60°C respectively confirmed this result.
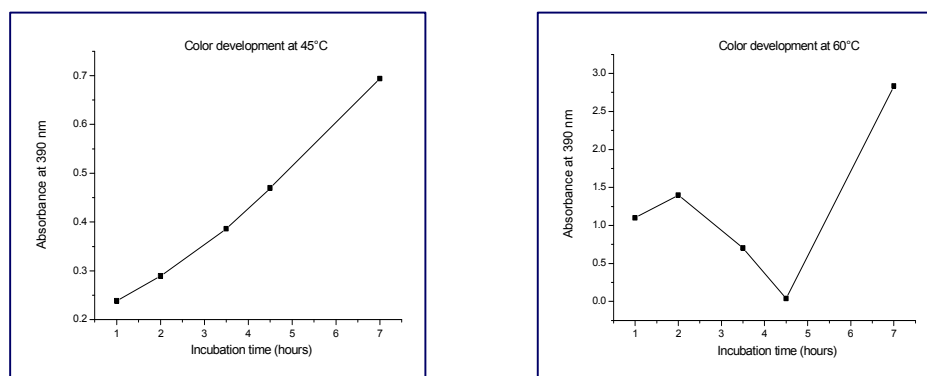
Fig 48 Study of incubation time for complete color development in the phenylhydrazine assay. Experiments were performed at 20 mM β-D-glucose, with a 0.32 ml total volume and freshly purified POx.

In a first approach, GOx was used to remove possible interference of glucose excess. No significant improvement was observed by applying this further treatment. The problem could be consisting on the high excess of the color reagent phenylhydrazine and substrate β-D- glucose concentration after scaling down the assay.

Two further experiments performed with lowered values of both color reagent and glucose confirmed this hypothesis showing good color saturation after two hours with the value keeping stable at least 1 hour showing a slight decrease after two hours.

No significant difference observed by adding GOx.
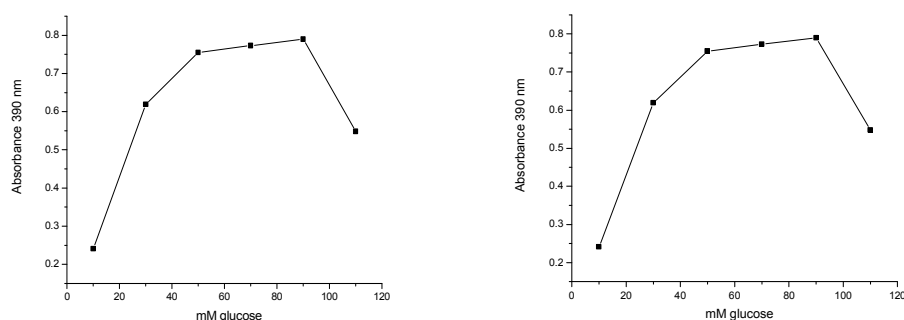
Fig 49 Substrate saturation curve of the phenylhydrazine assay system. Measurements taken after 2h and 4h of incubation time at 45°C, respectively. **GOx used for glucose excess removal**
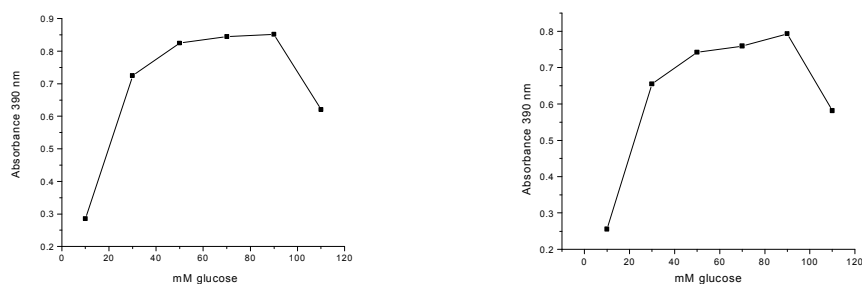
Fig 50 Substrate saturation curve of the phenylhydrazine assay system. Measurements taken after 2h and 4h of incubation at 45°C, respectively. **No GOx used for glucose excess removal**.

R= 0.94   R= 0.92
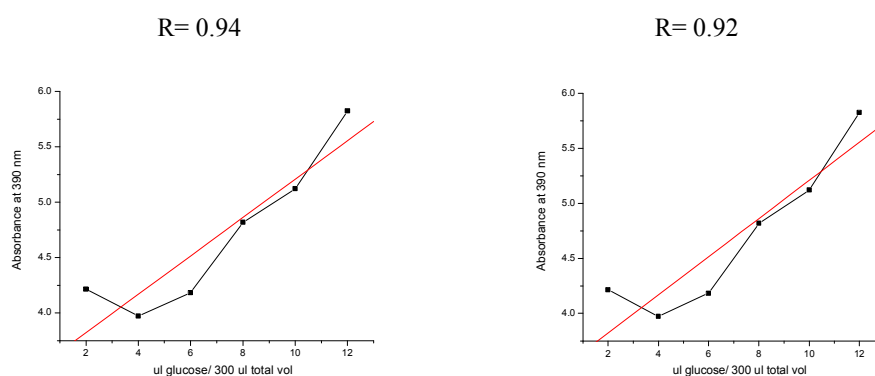
Fig 51 Study of linear dynamic range in the 96-well format of the phenylhydrazine system. Measurements taken after 3h and 5 h of incubation at 45°C, respectively. **No GOx used for glucose excess removal.**

3.11.2.2 Establishing the phenylhydrazine system as HTS assay

In order to develop the phenylhydrazine assay as an HTS system, clones of *E. coli* expressing 17b POx from *Trametes versicolor* were inoculated in 2 ml deep well multititer plates containing 1ml LB$_{amp}$ let for growth and induced. Cells were then pelleted by centrifugation, re-suspended in phosphate buffer pH 7 and disrupted by B-PER. Supernantants were then transferred to standard 96-well plate for POx activity by phenylhydrazine assay.

Replication in a deep well multititer plate using the replicator tool showed improved assay results when compared to inoculation of a certain volume of culture, which led to too high cells concentration.

Phenylhydrazine assay on the supernatants of the induced cells showed color development.
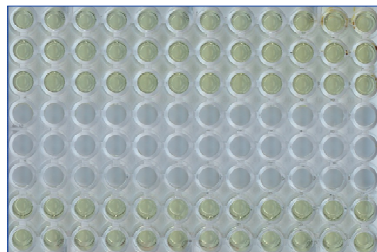
Fig 52 Color development after 3 hours for activity of POx expressed in *E. coli*. SD values are high due to the colored background

Different procedures were tried out in order to:

- minimize the time required per test
- obtain the lowest standard deviation
- gain highest color contrast between controls and samples
- achieve reasonably stable measurements

Parameters to test and optimize were:

- Time for POx reaction (ranging from 15' to 5 h)
- Time for phenylhydrazine color development reaction (ranging from 0 to 6 h)
- Order in which the reagents are added

Results showed SD values around 14 % and as a result, a protocol for Phenylhydrazine assay on supernatants could be established (Material and Methods). The ABTS assay remained preferred for screening purposes.

3.11.2.3 Testing permeabilizers

Aiming at reducing the time required per measurement comparative experiments were performed by using EDTA as permeabilizer showing that this approach was actually viable at certain concentration values and showed increased sensitivity.

In view of the results, other permeabilizers - Polyethylenimine, DHMP (dihydroximetaphosphate), Polymyxin B and EDTA - were tested. Polymyxin B performed well and was further studied testing at different concentrations ranging from 5 to 30 μM and compared to:

- using EDTA in a whole cell assay system.
- activity-test performed on supernatants after chemical lysis with B-PER

The results indicated that

> ➢ Polymyxin B acts better than EDTA as permeabilizer
> ➢ Optimum Polymyxin B concentration 5 μM
> ➢ Both permeabilizers led to increased sensitivity for POx activity detection if compared to tests on the supernantants after lysis with B-PER
> ➢ Best procedure:
> - 2 h at 45°C for POx reaction
> - centrifugation (4°C, $2,100 \times g$, 10 min)
> - phenylhydrazine solution itself (pH $\cong$ 1) for stopping the reaction
> - 3 h at 45 °C for color development reaction

A preliminary protocol for whole cell Phenylhydrazine HTS assay could be established (Materials and Methods). It was nevertheless not used for screening purposes since the values of SD remained over 20% probably due to the reagent yellow background. An improved POx variant showing a significant higher activity would allow to overcome this difficulty.

After directed evolution, a comparison experiment was run with several POx variants testing activity

A) By phenylhydrazine assay in the supernatant after chemical cell disruption

B) By phenylhydrazine assay in the whole cell using the Polymyxin B as permeabilizer
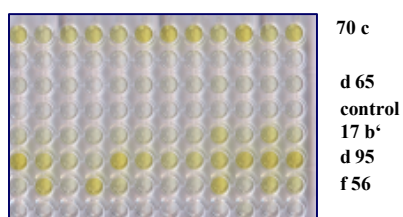
Fig 53a Color development in the supernatants after cell disruption. Phenylhydrazine assay for POx expressed in *E. coli.*
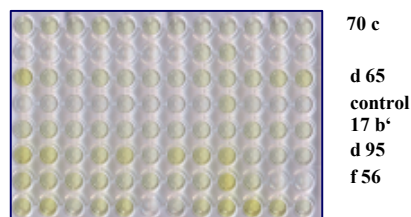
Fig53b Color development in permeabilized cells using 60 µM Polymyxin B. Phenylhydrazine assay for POx expressed in *E. coli.*

There was certain correlation for the Phenylhydrazine HTS in supernatants and using permeabilized cells, but differences were significant and prevented us from using the permeabilizer-based protocol.

3.11.3 Trying 4-hydrazino-7-nitro-benzofuranan as a candidate to develop a fluorescence-based HTS system

This compound was reported to be able of reacting with aldehyde groups to produce a strong fluorescent product (Konarzycka et al 2003). Considering it might react with the keto group in the POx product over glucose -2-keto-glucose- the possibility of developing a more sensitive assay was considered.

A series of three experiments was run. These tests considered incubation times ranging from 0 to 6 hours, fluorescence readings at excitation $\lambda= 485$ nm and emission $\lambda= 520$ nm are taken every hour and after 16h as a final point. Parallel tests were performed in whole cell samples where 60 µM polymyxin B was used as permeabilizer and in

supernatants after B-PER buffer was used for chemical lysis. No fluorescence was observed.

The use or not of GOx to remove glucose excess right after the POx reaction was also considered, with a set of experiments including a 30 min incubation step at 37°C with 5 U/ml GOx. No difference was observed.

In a last attempt, two experiments simulating a hypothetical saturation curve and a dynamic linear range study were performed in Eppendorf tubes using purified commercial POx. The results are showed below:

Glucose (mM)	0	5	10	20	30	50
Fluorescence reading	43783	38964	45746	45036	44447	45993

Glucose (µM)	0 (dye)	0 (POx)	50	100	160	205	260	325	400	500	750
Reading	10240	11165	14115	16313	15839	15980	14090	12461	16228	17166	15865

Tab 12 Results showed no difference of fluorescence between controls and samples

➢ No significant difference was observed between control and sample readings in all tests performed. The keto group might not be reacting. This occurred in both recombinant POx and purified commercial enzyme

➢ No improvement was observed by increasing the incubation time, changing the incubation temperature, modifying 4-hydrazino-7-nitro-benzofuranan concentration or glucose concentration

➢ No difference was observed between by adding GOx in an additional incubation step as to remove glucose excess. These results indicate that the aldehyde group of glucose was not interfering

The possibility of using 4-hydrazino-7-nitro-benzofuranan as a candidate for a fluoresce-based assay to assist POx directed evolution was finally discarded.

3.11.4 Developing a gluconate reductase-based assay system

In vivo substrates of POx are D-glucose, D-galactose, and D-xylose. In adition, POx also exhibits significant activity with a number of other carbohydrates, including L-sorbose, D-glucono-1,5-lactone and D-allose.

2-keto-D-gluconate reductases
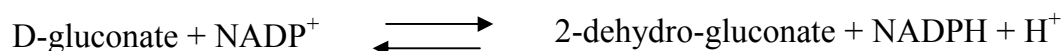
D-gluconate + NADP$^+$ $\rightleftharpoons$ 2-dehydro-gluconate + NADPH + H$^+$

2-keto-D-gluconate reductases catalize the oxidation of D-gluconate to 2-dehydro-gluconate with the concomitant reduction of the cofactor NADP$^+$ to NADPH + H$^+$. This reaction is reversible in most of the cases and can be followed by photometric reading of NADPH production at 340 nm or fluorescent emission reading at 445 nm after excitation at 340nm. My idea was to develop a novel essay in which production of 2-dehydro-gluconate via POx oxidation of the D-glucono-1,5-lactone, would be followed by decrease of the photometric/fluorescent reading values as the oxidized NADP$^+$ is being produced via 2-keto-D-gluconate reductase activity.

A scheme of this novel HTS to assay POx activity follows:

D-glucono-1,5-lactone

2KG reductase   POx

D-gluconate + NADP$^+$ $\rightleftharpoons$ **2-dehydro-gluconate + NADPH + H$^+$**

Absorbance reading at 340 nm / Fluorescence reading at 445 nm
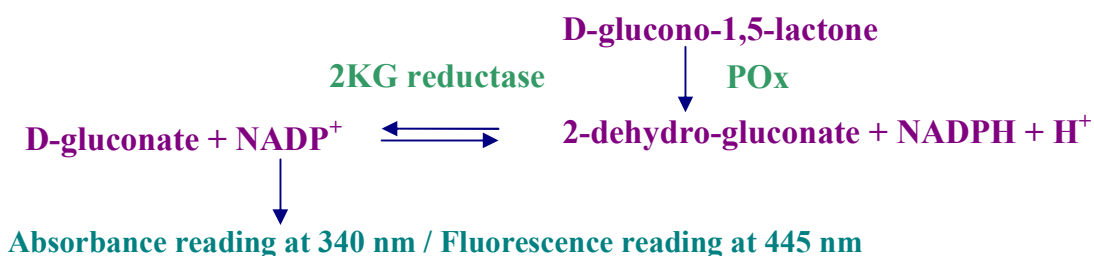
Various 2-keto-gluconate reductases from different organisms were considered. Most of them show a pH preference for either the oxidation of D-gluconate to 2-dehydro-gluconate or the opposite reductive reaction. The first is favored at pH values in the range from 10 to 12, whereas the latter occurs at lower values, in the range from 4 to 9. This feature made them suitable for testing POx activity due to two reasons: pH optimum of POx is 7 which turns advantageous in terms of sensitivity, and a pH shift for the assay would be unnecessary thus simplifying the protocol.

According to their substrate specificity, affinity over the substrate (K_m value for 2-keto-gluconate), optimum pH and temperature, as well as pH and temperature ranges of activity 2-keto-gluconate reductases from *Acetobacter ascendens* and *Acetobater rascens* seemed to be the best candidates (see the Introdution section). Unfortunately, the assay could not be tested, for neither the enzymes were commercially available nor other research groups working on 2-keto-gluconate reductases willed to share their material. Various groups involved in research with 2-keto-gluconate reductases were contacted but they showed repeatedly reluctant to transfer the expressing strain and/or the purified enzyme.

3.11.5 Ferrocenemetahnol based assay

The ferrocenemethanol assay was developed by Ziwei Zhu in a procedure described in her PhD Thesis. It involves two preliminary preparation steps:

a) Catalytic oxidation ferrocenemethanol using laccase (benzenodiol: oxygen oxidoresuctase, EC 1.10.3.2) at pH 3 with concomitant reduction of molecular oxygen to water.

b) Laccase removal: by adjusting the pH value to 8 for its inactivation and subsequent ultrafiltration.

The ferrocenemethanol assay, established after a series of tests, was based in the reaction of the oxidized form of ferrocenemethanol with reduced form of GOx in a reaction that was followed by colorimetric reading at 625 nm. Its use to screen a GOx improved variant in comparison with the ABTS assay was also presented as proof of principle in Ziwei Zhu thesis.

This ferrocenemethanol assay was further used to drive wtPOx from lysed cells extracts against two controls: 1) without POx, 2) without D-glucose. The results are plotted in the figure below:
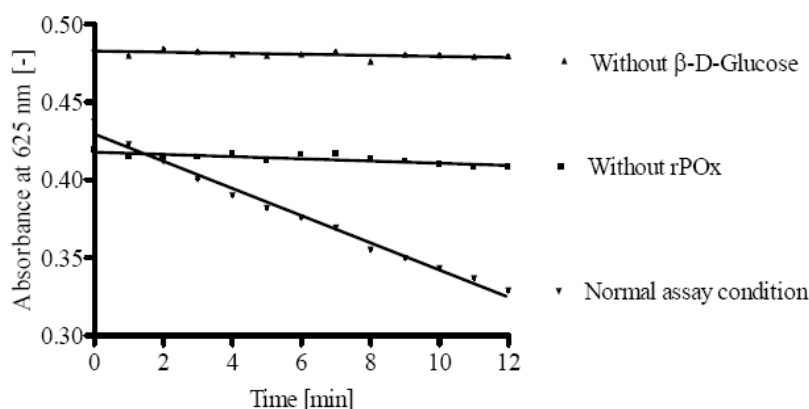
Fig 54 Ferrocenemethanol based assay on lysed cell extracts of E.coli expressing recombinant wtPOx.

These results showed promising to further develop a ferrocenemethanol assay in a 96-well format.

3.11.6 Testing pre-screening methods for clones selection

3.11.6.1 Checking a Thionine based pre-screening system

Improved variants of the second round were inoculated in petri dishes containig LB_{amp}, anhydrotetracycline as inducer and the blue dye thionine.

Initial results showed POx expressing *E. coli* as a smaller colony, clearer blue in color and the presence of a clear halo on the dark blue background. Controls containing the ATT pASK-IBA plasmid with no insert were small, dark blue and no halo was observed.

In an attempt to test a thionine based pre-screening system, which would speed up the selection of clones, a new epPCR (0.050 mM $MnCl_2$) using the extracted plasmid from 70 c variant was performed. *E. coli* was transformed with the corresponding ligation product and cells inoculated in big square plates containing LB_{amp}, anhydrotetracycline as inducer and the blue dye thionine.

Clones were selected according to colony size and color and ABTS HTS test for POx activity was performed. Results showed poor correlation between increased POx activity and color and size of the colony. The thionine based pre-screening assay was not sensitive enough to discriminate among the clones of the library.

3.11.6.2 Checking poly R 478 based pre-screening system

Similarly, improved variants of the second round were inoculated in petri dihes containig LB_{amp}, anhydrotetracycline as inducer and the red dye poly R478. Initial results showed a smaller colony of dark red color and the presence of a cleared halo for POx expressing *E. coli*.

Using the 70 c epPCR product, *E. coli* was transformed with the ligation construct and cells inoculated in big square plates containing LB_{amp}, anhydrotetracycline as inducer and the red dye poly R478. Clones were obtained and selected according to their size and color and ABTS HTS test for POx activity was performed.

No clear correlation could be established between increased POx activity and color, size and presence of a halo around the colony. A further definitive test was performed by testing improved variants 70 c on a poly R478 containing plate.

No significant difference could be observed between these clones when compared to controls containing the ATT pASK-IBA 3 plasmid with no insert. Poly R478 was discarded as a candidate for developing a pre-screening assay.

3.12 Sequence analysis of recombinant wild type POx and POx variants

Extracted plasmids of the wild type and mutants were sent for sequencing. Some of the sequencing reactions failed. A PCR using the sequencing primers was performed: those primers that succeed to amplify were used to sequence the corresponding clone. For the rest new primers were designed.
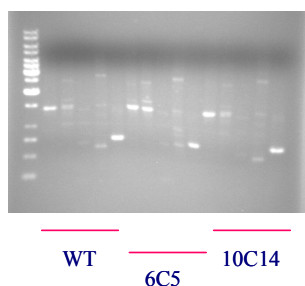
Fig 55 Checking optimal sequencing primers via PCR amplification

DNA sequences were analyzed using BioEdit. The translation tool from Expasy was used to get the amino acid sequence.

3.12.1 POx gene of T. versicolor

Amplification of the cDNA from *T. versicolor* POx yielded a 2,064-bp PCR product which included the 1,872-bp long open reading frame encoding for *T. versicolor* POx (wt POx). The cloned *T. versicolor pox* gene had a G+C content of 60 % and was predicted to encode a polypeptide of 623 amino acid residues with an estimated molecular mass of 69.4 (±0.2 KDa), which showed high similarities to other pyranose oxidases.

The specificity of the *Trametes versicolor pox* PCR product was confirmed by comparing the DNA sequence with the published sequence of cDNA of *C. versicolor* ps4a (Nishimura et al. 1996). The resulting nucleotide sequence showed 91 % identity *C. versicolor pox,* 90 % identity to *T. ochracea pox* (Vecereck et al. 2004)*,* 87 % identity to *P. gigantea pox gigantea* (Bastian et al., 2005, Danneel et al. 1993), 86 % identity to *Peniopheora sp pox* (Heckmann-Pohl et al. 2006) and 75 % identity to naturally thermostable *Ph. gigantea pox* (Schaefer et al. 1996). *T. versicolor* wtPOx amino acid sequence shared high identity with the group of POx composing the pyranose 2-oxidase group (Bannwarth et al. 2004) within the GMC oxidoreductase family (Cavener 1992).

The amino acid sequence of wtPOx showed 98 % identity to that of *T. ochracea*, its closest relative, to which it differs in only five positions: 188 (T instead of Q), 373 (V instead of I), 389 (P instead of L), 400 (S instead of E), 413 (E instead of K). When compared to *C. versicolor* POx, an additional change was observed in position 623 (V instead of E, total 96% identity). The *T. versicolor* POx amino acid sequence was 90 % identical to that of *P. gigantea.* None of these exchanged residues have yet been reported to be involved in substrate binding, catalysis, oligomerization or any other important function. In *Peniophora sp.* an A residue in position 494 is reported to constitute part of the pore that allows glucose access to the central cavity of the tetramer (Bannwarth et al. 2004). This A is absent in *T. versicolor* POx (similarly in *T. ochracea* and *C. versicolor* POxs) where the position 494 is occupied by a T residue.

Characteristic sequence motifs responsible for FAD binding were identified in the sequence of *T. versicolor* wtPOx. The segment V49VIVGSGPIG58 contained the highly conserved flavoprotein motif GXGXXG, which is responsible for the non-covalent binding of the ADP moiety of FAD (Wierenga et al. 1986). The conserved sequence S165THW168 is also present and is thought to allocate the isoalloxazine moiety of FAD via covalent bound to His167 (Bannwarth et al. 2004). The latter was shown for *T. multicolor* POx (Halada et al. 2003; Hallberg et al. 2004) and has been postulated for *P. gigantea* POx (Batian et al. 2005).

A) POx WT (clone 17b)

Differences to *Coriolus versicolor* POx referred in the literature:

644 amino acids instead of 623

6 of which are different (showed in green)

96 % similarity

Position	*Coriolus versicolor*	*Trametes versicolor* WT	
188	Q	T	Met S T S S S D P F F N F T K S S F R S A A A Q K A S A T S L P P L P G P D K K V P G Met D I K Y D V V I V G S G P I G C T Y A R E L V E A G Y K V A Met F D I G E I D S G L K I G A H K K N T V E Y Q K N I D K F V N V I Q G Q L Met S V S V P V N T L V I D T L S P T S W Q A S S F F V R N G S N P E Q D P L R N L S G Q A V T R V V G G Met S T H W T C A T P R F D R E Q R P L L V K D D T D A D D A E W D R L Y T K A E S Y F K T G T D Q F K E S I R H N L V L N K L A E E Y K G Q R D F Q Q I P L A A T R R S P T F V E W S S A N T V F D L Q N R P N T D A P N E R F N L F P A V A C E R V V R N T S N S E I E S L H I H D L I S G D R F E I K A D V F V L T A G A V H N A Q L L V N S G F G Q L G R P D P A N P P Q L L P S L G S Y I T E Q S L V F C Q T V Met S T E L V D S V K S D Met I I R G N P G D P G Y S V T Y T P G A S T N K H P D W W N E K V E N H Met Met Q H Q E D P L P I P F E D P E P Q V T T L F Q P S H P W H T Q I H R D A F S Y G A V Q Q S I D S R L I V D W R F F G R T E P K E E N K L W F S D K I T D T Y N Met P Q P T F D F R F P A G R T S K E A E D Met Met T D Met C V Met S A K I G G F L P G S L P Q F Met E P G L V L H L G G T H R Met G F D E Q E D K C C V N T D S R V F G F K N L F L G G C G N I P T A Y G A N P T L T A Met S L A I K S C E Y I K N N F T P S P F T D Q A V T H A Met V S A L G A T R S S K N N K L D L Stop
373	I	V	
389	L	P	
400	E	S	
413	K	E	
623	E	V	

Fig 56 *Trametes versicolor* recombinant POx (17b) sequence. Differences to the highly similar *Coriolus versicolor* POx, as repoted by Nishimura et al. (1996) are shown on the left.

B) POx WT (clone 18)

Clone 18 shows 7 amino acids which are different to clone 17 b (99 % similarity)

In red: amino acids in *Coriolus versicolor* POx wild type as referred in the literature

Position	*Trametes versicolor* WT clone 18	*Trametes versicolor* WT clone 17b
227	P	L
296	V	I
373	I	V
413	K	E
458	P	A
511	S	T
600	R	K

Fig 57 Differences in the sequence of the two *Trametes versicolor* recombinant POx wild type variants (Clones 17b and 18)

3.12.2 Trametes versicolor POx better expression variants

Sequencing results show the variants 6C5, 70 c and FA9 to have identical sequence to WT POx. Nonetheless, mutations are found in positions prior to Met in 6C5. 70 c and FA9 are confirmed as better expression mutants.

Mutant	3H11	FA9	GD9	AC1	6H11	GG9
Activity (fold-WT)	1.4	3-4	2	1.4	1.2	1.3

Tab 13 Relative activities of POx variants compared to recombinant POx wild type

Zymograms confirmed FA9 as a better expression mutant.

3.12.3 Clone 10C14:

624 amino acids

Two amino acids - D and L - are absent at the C-terminus of the sequence:

Met S T S S S D P F F N F T K S S F R S A A A Q K A S A T S L P P L P G P D K K V P G **Met** D I K Y D V V I V G S G P I G C T Y A R E L V E A G Y K V A **Met** F D I G E I D S G L K I G A H K K N T V E Y Q K N I D K F V N V I Q G Q L **Met** S V S V P V N T L V I D T L S P T S W Q A S S F F V R N G S N P E Q D P L R N L S G Q A V T R V V G G **Met** S T H W T C A T P R F D R E Q R P L L V K D D T D A D D A E W D R L Y T K A E S Y F K T G T D Q F K E S I R H N L V L N K L A E E Y K G Q R D F Q Q I P L A A T R R S P T F V E W S S A N T V F D L Q N R P N T D A P N E R F N L F P A V A C E R V V R N T S N S E I E S L H I H D L I S G D R F E I K A D V F V L T A G A V H N A Q L L V N S G F G Q L G R P D P A N P P Q L L P S L G S Y I T E Q S L V F C Q T V **Met** S T E L V D S V K S D **Met** I I R G N P G D P G Y S V T Y T P G A S T N K H P D W W N E K V E N H **Met** **Met** Q H Q E D P L P I P F E D P E P Q V T T L F Q P S H P W H T Q I H R D A F S Y G A V Q Q S I D S R L I V D W R F F G R T E P K E E N K L W F S D K I T D T Y N **Met** P Q P T F D F R F P A G R T S K E A E D **Met** **Met** T D **Met** C V **Met** S A K I G G F L P G S L P Q F **Met** E P G L V L H L G G T H R **Met** G F D E Q E D K C C V N T D S R V F G F K N L F L G G C G N I P T A Y G A N P T L T A **Met** S L A I K S C E Y I K N N F T P S P F T D Q A V T H A **Met** V S A L G A T R S S K N N K L **Stop**

Fig 59 Sequence of the POx mutagenesis variant 10C14. Two C-terminal amino acids –DL- are missing

3.12.4 Clones DL 2B and DL 4D

E. coli XL1-Red was used for mutant library generation over a total incubation period of seven days. Screening of the POx mutant libraries resulted in variants with increased v_{max} and lower K_m values.

The most beneficial POx mutant (trPOx) showed an adenine deletion in position 1,227. This deletion changes the reading frame of the subsequent nucleotide sequence. As a result, an early stop codon is generated at amino acid position 416 –seven codons after the adenine deletion- so that a truncated monomeric POx (trPOx) occurs. trPOx is composed of 415 amino acids compared to 626 amino acids of wtPOx. After the frame shift, seven amino acids of the wtPOx sequence (N409EKVENH415) are changed in trPOx (T409RRWRTT415). The enzymatic activity increase for the trPOx was confirmed by site-directed mutagenesis of the wtPOx gene sequence using the primer pair f1, r4 (Table 4).

WT:

tgg tgg **aa**c gag aag gtg gag aac cac atg atg cag cac cag
 W   W   N   E   K   V   E   N   H   M   M   Q   H   Q

…D W W N E K V E N H **Met Met** Q H Q E D P L P I P F E D P E P Q V T T L F Q P S H P W H T Q I H R D A F S Y G A V Q Q S I D S R L I V D W R F F G R T E P K E E N K L W F S D K I T D T Y N **Met** P Q P T F D F R F P A G R T S K E A E D **Met Met** T D **Met** C V **Met** S A K I G G F L P G S L P Q F **Met** E P G L V L H L G G T H R **Met** G F D E Q E D K C C V N T D S R V F G F K N L F L G G C G N I P T A Y G A N P T L T A **Met** S L A I K S C E Y I K N N F T P S P F T D Q A V T H A **Met** V S A L G A T R S S K N N K L D L **Stop** S E K W R T L C D I F F V C R L P L L R H G S P R A L **Stop** R R I K R G G C G G Y A Q R D R Y T C Q R P S A R S F R F L P F L S R H V R R L S P S S S K S G A P F R V

DL 2B (The same deletion is found in mutant DL 4D)**:**

tgg tgg **a**cg aga agg tgg aga acc aca **tga** tgc agc acc agg
 W W T R R W R T T - C S T R

…D W W T R R W R T T **Stop** C S T R K T R S R S H S R T P S R R S P P C S S H R T R G T L R F T A **Met** R S A T A R C S K A S T H V S L S T G A S S A A R S Q R R R T S S G S R T R S R T R T T C R S R R S T S A S Q R A A R A R R R I **Stop Stop** P T C A S C R R R L V A S C P A P S R N S W S P D L S F T S V V R T A W A S T S R R T S A A S T R T R A C S A S R I S S S A A A E T F P P R T A R T R R S P Q C R S R S R V A S T S R T T S H R A L S Q I R L **Stop** P **Met** P W S Q R L E P P A V R K I I S L T C E V K N G A H C A T F F L S A V Y R Y C V T D L H A P C S G A L S A A G V V V T R S V T A T L A S A L A P A P F A F F P S F L A T F A G F P R Q A L N R G L P L G F

These results indicate that the POx monomer is reduced from 626 amino acids in the WT to 414 amino acids in the mutants.

3.13 Zymograms

A zymogram technique was developed to identify and study higher activity mutants: normalized samples were run under non-denaturating conditions by PAGE electrophoresis:

> ➢ No SDS added
> ➢ No mercaptoethanol in the loading dye
> ➢ No heating step prior to running

Gels were then applied on paper previously impregnated in ABTS assay cocktail: 100 mM glucose, 5U/ml HRP and 25 mM ABTS solution. A green spot appeared where POx was active. Spot size and color intensity correlated well to POx activity.
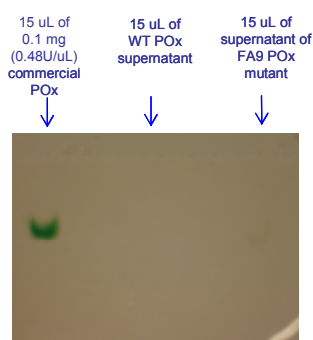
Fig 58a Zymogram development after 1h at RT
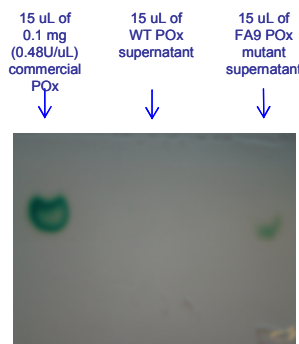
Fig 58b Zymogram development after 18h at RT

3.14 Enzymatic characterization of recombinant wild type POx and POx variants

3.14.1 Recombinant wild type POx

Recombinant wtPOx was expressed in *E. coli* XL2-Blue in sufficient amounts of soluble and catalytically active enzyme. The formation of inclusion bodies could be avoided by lowering the incubation temperature to 28°C. Significant improvements in reproducibility of POx expression (99%) and yields of enzymatic active POx (~2 fold) were made by concomitant expression of the set of chaperones GroES-GroEL.

wtPOx was purified to homogeneity and characterized (3.5 g/L of cell mass yielded 44 mg/L of pure wtPOx). Purified wtPOx produced a typical flavoprotein spectrum with absorption maxima at 280, 345 and 456 nm. Reduction of the enzyme by addition of the β-D-glucose led to disappearance of the peaks at 345 and 456 nm.

wtPOx was stable over a broad pH range (5.5-8) and up to 50°C with a maximum of activity at pH 7-7.5 and 45°C (Fig 68). By comparison to other sequence-related POxs, these values were comparable to those determined for *C. versicolor* POx (Masuda-Nishimura et al. 1999): stable in pH range 5-8, with maximum in activity at pH 7 and 50°C; to *T. matsutake* POx (Takakura and Kuwata 2003): stable in pH range 5.5-11 with maximum in activity at pH 7.5-8 and 50°C; and to *P. obtusus* POx (Janssen and Ruelius

1975): with maximum in activity at pH 7.0-7.5 and 55°C. *T. versicolor* POx activity showed no significant variation when assayed in chloride concentrations below 400 mM.

wtPOx differed in temperature optimum 45°C (Fig. 69) to the sequence-related POxs from *P. gigantea* (Daneel et al. 1993), *Ph. gigantea* (Schaefer et al. 1996) and *Peniophora sp* (Heckmann-Pohl et al. 2006) which ranged from 40°C (*P. gigantea* POx) to 55°C (*Peniophora* sp. POx) and to 65°C (naturally thermo-stable *Ph. gigantea* POx). It also differed in the pH optima: ranging from pH 6.0–6.5 (*P. gigantea* POx) to pH 5.0–6.5 (*Peniophora* sp. POx) and to pH 5.0–7.5 (*Ph. gigantea* POx).

In terms of kinetic parameters, *T. versicolor* wtPOx showed a lower apparent K_m value for D-glucose (4.5 mM) in comparison to POx of *Peniophora sp* (7.6 mM) (Heckmann-Pohl et al. 2006) and higher compared to that of C. *versicolor* (1.4 mM) (Masuda-Nishimura et al. 1999), *T. matsutake* (1.28 mM) (Takakura and Kuwata 2003), *P. obtusus* (1.18 mM) (Janssen and Ruelius 1975), *P. gigantea* (1.1 mM) (Daneel et al. 1993) and *Ph. gigantea* (1.2 mM) (Schaefer et al. 1996). *T. versicolor* POx k_{cat} value towards D-glucose (22.0 s^{-1}) was lower than *C. versicolor* POx (59.9 s^{-1}) (Masuda-Nishimura et al. 1999). The catalytic efficiency k_{cat}/K_m of wtPOx for D-glucose was higher (4.75 mM^{-1}s^{-1}) compared to *Peniophora sp* POx (1.23 mM^{-1}s^{-1}) (Heckmann-Pohl et al. 2006) and lower in comparison to *C. versicolor* POx (42.7 mM^{-1}s^{-1}) (Masuda-Nishimura et al. 1999).

3.14.2. Trametes versicolor POx variants

For further characterization, clones were inoculated and induced for POx expression. Cells were sonicated and a SDS-PAGE electrophoresis gel of the supernatants and pellets was run. ABTS assay was performed in the supernatants. The aim was to check whether the improved mutants were due to an increased expression of POx or to a real higher POx activity of the mutants. Results showed that the intensity of the 65kb band was not significantly increased in the mutants when compared to WT. This result indicated that the variants were improved in terms of POx activity and not better expression mutants.

Pellets did not show significant presence of inclusion bodies except maybe for the 6C5 variant.
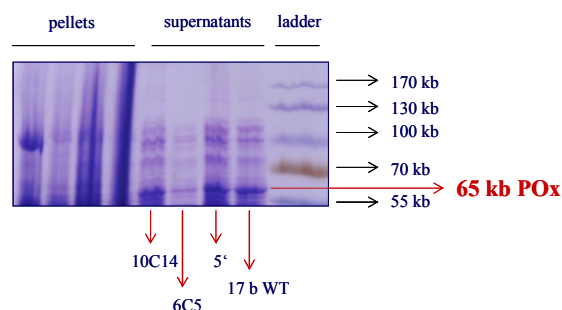
Fig 60 SDS Page electrophoresis of POx WT, 5, 6C5 and 10C14 variants

Protein determination using BCA method on purified fractions combined with Michaelis-Menten analysis of the results obtained from ABTS kinetics allowed determining the kinetic parameters of the variants

	Km (uM)	Kcat (1/sec)	Kcat/Km (1/sec*M)
6C5	527.8	52.54	99537
10C14	205.7	74.38	361571
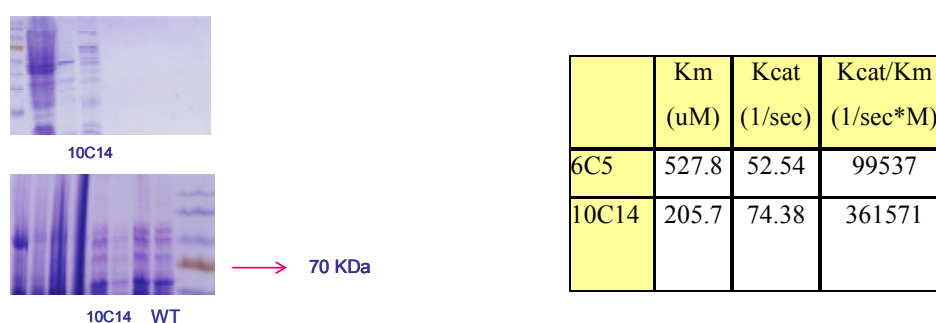
Tab 14 Kinetic parameters of C5 and 10C14 POx variants
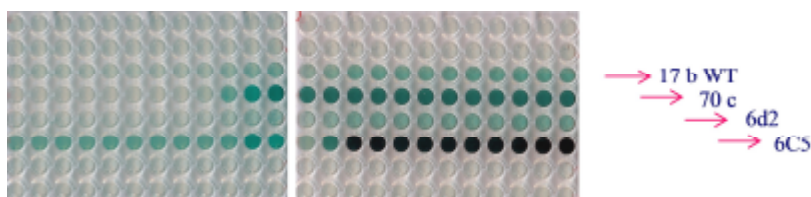
Fig 61 ABTS kinetics of purified fractions of POx variants.
Increasing glucose concentration ranging from 0 to 20 mM.

Similar ABTS kinetics assay was performed on the main and aside fractions obtained via HPLC that contained the recombinant POx variant. The intensity of the three peaks of absorbance used for POx identification (280, 435, 345 nm), did not always correlate

identically for samples showing activity, which suggested the presence of different aggregation states of POx.
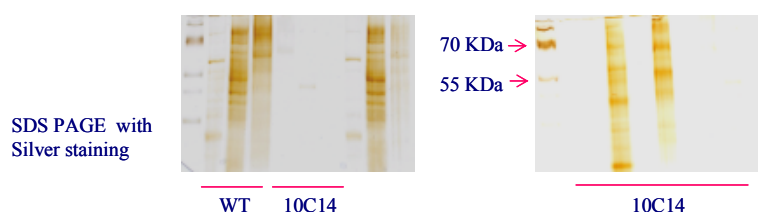
Fig 62 Silver staining SDS Page electrophoresis of POx WT, 5, 6C5 and 10C14 variants

3.14.3 trPOx

Screening of the POx mutant libraries from Mutator Strain resulted in variants with increased v_{max} and lower K_m values. The most active mutant DL 2B and Ch2 DL 4D (later named trPOx) was isolated and sequenced.
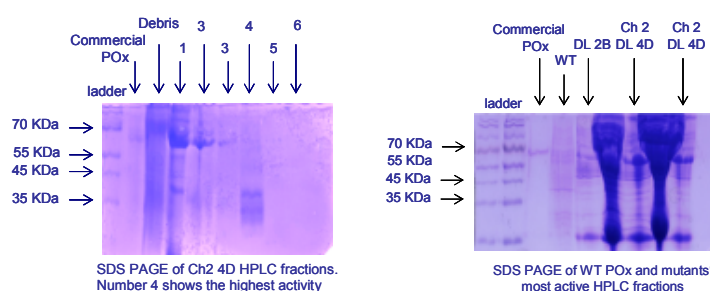
Fig 63 SDS PAGE electrophoresis of mutants samples after HPLC

trPOx cultures were prepared, POx purified and the kinetic data for glucose conversion determined. Samples were normalized and disrupted by french press. HPLC purification followed with ABTS test of the fractions. Pure active samples were checked via SDS-Page electrophoresis and stained with Comassie Blue, activity tested via ABTS and protein determined by Bradford Method.

Analysis of the gels confirmed an enhanced band at 46 KDa in the mutants' samples. Protein determination and activity tests on pure mutant POx fractions of clones DL 2B

96

and Ch2 DL 4D (L & H) indicated at least 14-fold higher turnover number than the wild-type (from 23 s-1 up to 634 s-1) considering an estimated 2-fold increased expression via chaperones.
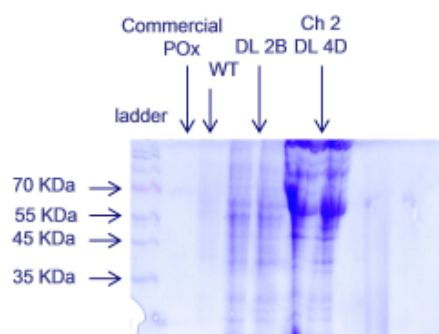
Fig 64 SDS PAGE electrophoresis of DL2B and DL4D mutants after HPLC

Activity – fold WT	2B L	2B H	CH2 4D L	CH2 4D H
Kinetics ABTS	3.75	3.58	101.76	169.86
End point ABTS (5 min)	10.0	14.3	244.3	381.7
End point ABTS (4 h)	1.9	1.5	8.0	11.2

Table 15 Relative activity of 2B and 4D mutants fractions compared to WT. H and L corresponds to higher and lower activity as observed in direct ABTS check on HPLC fractions, respectively. 4D mutant expression was assisted with chaperones

y = 0.0009x + 0.1032
R² = 0.9926
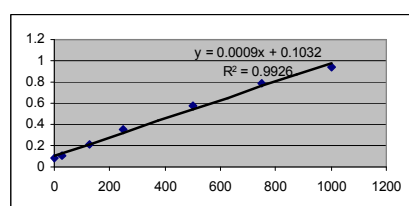
BCA calibration curve

ug/ml	1512.6	1147.0	2378.7	2227.6	284.8
sample	DL 2B L	DL 2B H	CH2 DL 4D L	CH2 DL 4D H	WT

BCA method for protein determination

Table 16 Determination of protein contents in HPLC fractions of 2B and 4D mutants, and WT. H and L corresponds to higher and lower activity as observed in direct ABTS check on HPLC fractions, respectively. 4D mutant expression was assisted with chaperones

POx Samples containing 10 mg/mL of pure POx lyophilisate were analyzed using an Agilent Bioanalyzer (Fig 65). wtPOx sample showed the expected peak at ~69 KDa and

could be quantified. This band was absent in samples containing the mutants where a peak at ~ 46 KDa occurred.

Fig 65a Agilent chromatogram of HPLC purified samples DL 2B and Ch2 DL 4D: individual normalization. Chaperones peaks GroES-GroEL appear at 10 KDa and 60 KDa respectively

Sample (fraction)	KDa	% band intensity	% on the total
Ch 2 DL 4D H	43.2	4.2	14
	46.8	9.9	
Ch 2 DL 4D L	43.6	4.7	9.5
	47.3	4.8	
DL 2B H	43.3	4.5	39
	47.6	34.3	
DL 2B L	43.0	6.0	28
	47.0	22.4	

Fig 65b Agilent chromatogram data analysis of HPLC purified samples DL 2B and Ch2 DL 4D: individual normalization. Expression of chaperones in 4D explains the lower %

Fig 65c Kinetics of HPLC purified samples DL 2B and Ch2 DL 4D compared to WT. Dilutions of the assay sample are also shown for more clarity

Further tests on quantification of the POx content and measurements of activity via ABTS assay showed a surprisingly ~14 fold increased increased k_{cat} for trPOx (trPOx k_{cat}: 78.2 s^{-1} per catalytic center compared to wtPOx k_{cat}: 5.5 s^{-1} per catalytic center). Apparent K_m value towards glucose was reduced in the truncated variant (trPOx K_m: 0.85 mM compared to wtPOx K_m: 4.5 mM). As a result, the catalytic efficiency of trPOx increases significantly (trPOx k_{cat}/K_m: 93,038 M^{-1}s^{-1} per catalytic center compared to wtPOx k_{cat}/K_m: 1,186 M^{-1} s^{-1}, a ~78 fold increase). All kinetic constants (k_{cat}) and catalytic efficiencies (k_{cat}/K_m) have been calculated per active site in order to avoid

differences that might be caused by different aggregation states of wtPOx and trPOx (monomer, dimer or tetramer).
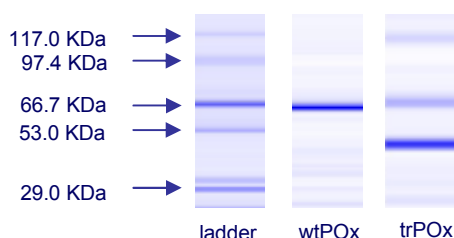
Fig 66 Size profile of wtPOx and trPOx samples analyzed in an
Agilent Bioanalyzer, Ladder, wtPOx and trPOx.

Zymograms of wtPOx and trPOx (Fig. 67) showed clear differences in electrophoretic mobility as expected for the smaller deletion variant as further proven by SDS-Page electrophoresis (wtPOx appears at 69 KDa, trPOx at around 46 KDa). wtPOx and trPOx band were cut from the zymogram, extracted in solution and the preparations used for SDS-Page electrophoresis and to quantify FAD load (Yamada et al. 1979). FAD load in *T. versicolor* wtPOx and trPOx pure samples were estimated by determination of oxidized FAD at 450 ($\varepsilon = 11.3$ mM^{-1} cm^{-1}) and by comparison of the enzyme content determined by photometric reading at 280 nm ($\varepsilon = 69.13$ mM^{-1}cm^{-1} calculated for the wtPOx monomer). trPOx showed a higher FAD load (~1.3 fold) compared to purified wtPOx due to the lower protein signal. These results are consistent with a 33 % reduced size of the trPOx monomer and considering the tetrameric structure of POx. Results were confirmed by comparison to FAD load of the commercial *C. versicolor* POx (a close homologous showing a 91 % identity to the nucleotide sequence of wtPOx). wtPOx showed a FAD load ~3 fold that of *C. versicolor* POx whereas trPOx a ~4 fold the FAD load of commercial *C. versicolor* POx.
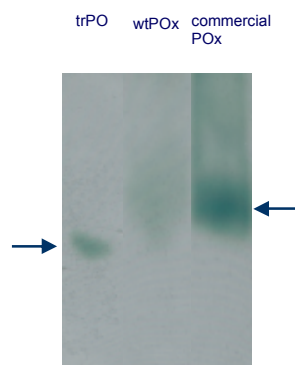
Fig 67 Zymogram of trPOx, wtPOx and *C. versicolor* commercial POx. Equal amounts of purified POxs samples are run in native PAGE gels. Color development is reached covering the gel with a cellulose membrane soaked on the ABTS assay reaction mix and incubating for 4 hours at RT. Full color development is reached after incubation overnight

Thermo-stability of wtPOx and the kinetically improved variant trPOx was found to be similar up to 55°C (Fig 68). trPOx showed higher enzymatic activity in the range of 30°C to 45°C (96 % of maximum activity compared to 82 % in wtPOx). Significant differences were found in stability at temperatures higher than 55°C (at 60 °C: trPOx shows 27 % of relative activity compared to 57 % of wtPOx).
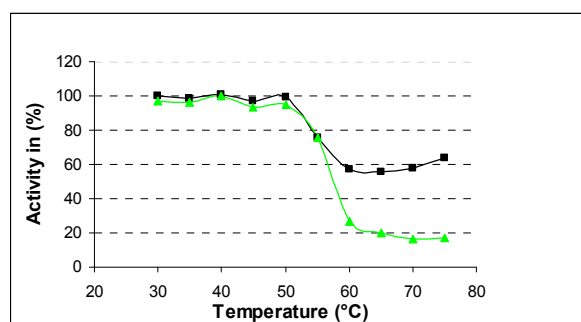
Fig 68 Effect of temperature on the stability of *Trametes versicolor* wtPOx (▪) and trPOx (▲) variant. POx samples in 100 mM potassium phosphate buffer pH 7 were incubated at diverse temperatures for 30 min. After 15 min at RT, remaining activity was measured by standard ABTS assay.

The temperature profile of trPOx was found to be shifted to lower values in comparison to wtPOx (Fig 69). In the range of 30°C-40°C, trPOx showed 94 % of its maximum activity compared to 76 % observed for wtPOx. The optimum temperature of trPOx was

40°C compared to 45°C of wtPOx. Aside of the optimum activity at 45°C, values of activity of trPOx fall to 82.3 % at 50°C and to 19 % at 60°C in comparison to a 96 % and 60 %, respectively, for wtPOx.
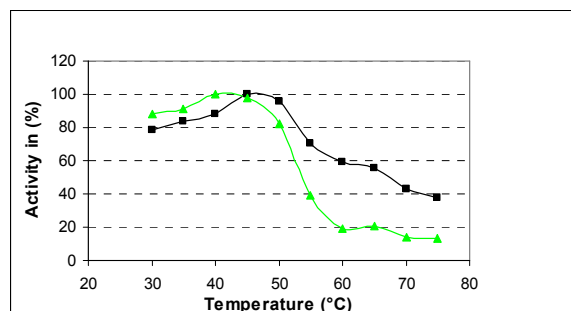
Fig 69 Effect of temperature on the activity of *Trametes versicolor* wtPOx (■) and trPOx (▲) variant. POx samples in 100 mM potassium phosphate buffer pH 7 were incubated with glucose for reaction at the given temperature. Activity was measured by standard ABTS assay.

The substrate profile of trPOx was analyzed using D-glucono-1,5-lactone and 5-thio-D-glucose. No significant increase (< 5%) of FAD catalysis was observed for trPOx over these substrates. trPOx showed a low activity for D-glucono-1,5-lactone (0.34 % compared to the activity for D-glucose) and 5-thio-D-glucose (2.5 % compared to the activity for D-glucose). Regioselective oxidation was determined by using 2-fluoro-2-deoxy-D-glucose as substrate. trPOx did not show enhanced activity compared to wtPOx. Regioselectivity of the oxidation in position 2 is preserved in trPOx (data not shown).

3.15 Improvements in the protocols

Protocols were designed in order to concentrate and better preserve POx in order to be able to further study POx expression and activity variants

3.15.1 Improved POx purification HPLC protocol

Direct and reverse salt gradients were performed and different step protocols tested. Since, some more contaminant proteins eluted showing absorption in the same three

wavelengths than POx 280, 435 and 354 nm ratios of the three wavelengths involved were considered. As a result, the following purification protocol could be established for POxs

Step purification scheme:

0 % B	**20 % B**	**40 % B**	**100 % B**
10 mM K_xPO_4 pH 7 0 M KCl	10 mM K_xPO_4 pH 7 200 mM KCl	10 mM K_xPO_4 pH 7 400 mM KCl	10 mM K_xPO_4 pH 7 1M KCl
Column wash and equilibration Injection Some proteins elute	POxs elute	Some proteins elute	Complete wash
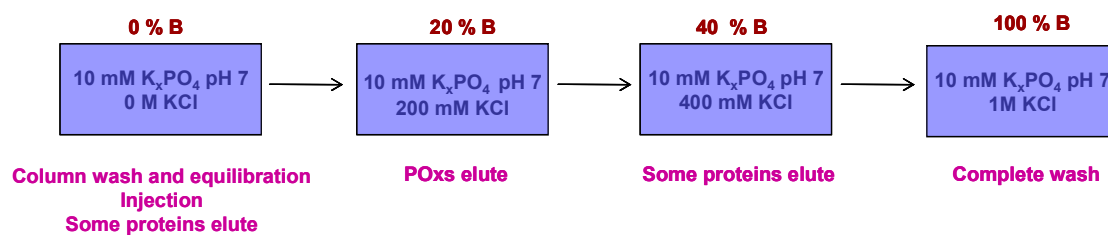
A: 10 mM KxPO4 pH 7

B: 10 mM KxPO4 pH 7- 2 M KCl

➢ Readings at 280, 435 and 354 nm for FAD

➢ Eluates are checked on the spot via ABTS assay

➢ Enriched POx samples show bright yellow color

➢ Part of the fraction is stored for subsequent tests: SDS Page, Agilent, Bradford, ABTS, Phenylhydrazine assays. The rest is lyophilisated on the same day
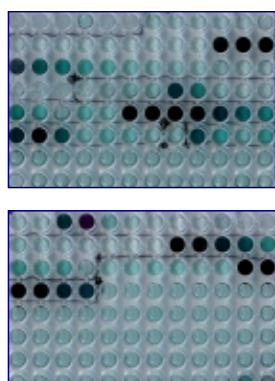
Eluate fractions tested via ABTS assay on the spot

3.15.2 Ultrafiltration after HPLC

HPLC with DEAE-650 S packed column was used to separate POx from supernatants after sonication of *E. coli*. Washes were performed with 10 mM KxPO4 pH 7 buffer. A gradient with 2 M KCl 10 mM KxPO4 pH 7 buffer revealed that POx elutes around 28 mM KCl. A simplified two steps protocol was used: 0 mM KCl, 30 mM KCl.

The POx contenting fractions were further treated by Ultrafiltration with Centricon columns 30 KDa cut-off: After 20 min of centrifugation at 4000 rpm, sample volume was not significantly reduced. Longer durations were tried out with no improvement observed. Ultra filtration was discarded as a further concentration step.

3.15.3 Recovering and concentrating POx samples

A suspension of DEAE-650 S resin in 10 mM KxPO4 pH 7 buffer was checked out as a method to store and concentrate POx from lyophilisates or excessively diluted samples. Wash outs of the resin with 10 mM KxPO4 pH 7 buffer showed no activity thus indicating that POx adsorbed to the resin particles. A reduced volume of 250 mM KCl 10 mM KxPO4 pH 7 buffer turned to be sufficient to completely recover the enzyme. This method allowed recovering POx from excessive diluted samples as well as from apparently inactive lyophilisates solutions (concentration effect).

The recovered samples should undergo ulterior desalting process. Detailed protocols have been developed.

3.15.4 Optimal conditions for POx storage

3.15.4.1 Lyophilisation

Recombinant POx lyophilisates activity was compared to that of samples stored in frozen or refrigerated solution. The comparison was made in terms of kinetics parameters and

enzymatic efficiency. ABTS assay was used for kinetics, BCA method was used for determining protein content. Activity loss was significantly higher in refrigerated or frozen solutions.

Enzymatic efficiency loss of the lyophilisates when stored at –20C was studied subsequently. Two lyophilisates were prepared: Lyoph 1 corresponded to a sample that had previously been kept refrigerated in solution for 10 days. Lyoph 2 corresponded to a fresh sample that underwent lyophilisation directly after HPLC.

	Activity (umol glu/sec*mg prot)	Kcat (1/sec)	Kcat/Km (1/sec*M)	Efficiency loss (%)
Lyoph 1	0.24	61.75	241870	13.45
Lyoph 2	0.18	47.19	38394	32.85

Enzymatic efficiency loss within 9 days of storage at –20 C in a 14 days old POx lyophilisate

	Activity (umol glu/sec*mg prot)	Kcat (1/sec)	Kcat/Km (1/sec*M)	Efficiency loss (%)
Lyoph 1	0.50	129.85	96974	65.30
Lyoph 2	0.22	56.85	37903	33.71

Enzymatic efficiency loss within 16 days of storage at –20 C in a 21 days old POx lyophilisate

Table 17 Study of optimal storage conditions for recombinant POx. Refrigerated and frozen samples are compared to lyophilised samples. In a second experiment fresh and delayed lyophilisation are compared

As a conclusion, lyophilisation reduced activity loss of POx when compared to frozen or refrigerated stored solutions. Still the loss of activity efficiency was pronounced (around 30% within 15 days). This effect was minimized with lyophilisation of the POx containing fractions performed directly after HPLC.

3.15.4.2 Use of additives

The use of EDTA and PMSF as additives during lyophilisation was studied:

Recombinant POx	Day 0	Day 2
6c5	1.92	2.07
6c5 (1 mM EDTA + PMSF)	1.44	0.76
6c5 (1 mM EDTA + 0.1mM PMSF)	1.28	0.75
10c14	1.00	1.25
10c14 (1 mM EDTA + 0.1 mM PMSF)	0.99	0.79
10c14 (1 mM EDTA + 0.1mM PMSF)	1.07	1.28

Table 18 Test of recombinant POx stability by using additives

6C5 POx lyophilisates showed better stability when free of additives. No significant difference was observed for 10C14 POx (Tab 18). This result turned to be very positive since POx samples are thought for the anodic compartment of biofuel cells and for this purpose they need eventually be free of both additives and salts.

3.15.4.3 Samples absorbed on DEAE-650 S resin suspension

ABTS assay on recovered fractions indicated the suspension of DEAE-650 S resin in 10 mM KxPO4 pH 7 buffer as a good method to store POx. This method allowed recovering POx from excessive diluted samples as well as from apparently inactive lyophilisates solutions -concentration effect-.

	Activity (umol glu/sec*mg prot)	Kcat (1/sec)	Kcat/Km (1/sec*M)
6C5 DEAE recoveries	0.20	52.54	99537
10C14 DEAE recoveries	0.28	74.38	361571
6C5 lyophilisate DEAE recoveries	0.30	78.79	149280

Table 19 Activity of recombinant POx samples recovered from DEAE-650 S resin

3.16 Improvements in the HTSs

3.16.1 ABTS assay

The increased active POx expression obtained with groES-groEL proteins allowed us to use an alternative, faster ABTS assay, in which the POx reaction and the color development reaction occur simultaneously. This improvement was tested using various intermediate variants and testing the activity by the two protocols. The good correlation allowed using rapid ABTS assay for screening purposes.

Activity – fold WT	2B	11D	CH2 2C	CH2 4D
Fast - end point ABTS (2 h)	17.15	3.70	0.88	1.09
End point ABTS (4 h)	31.27	8.52	0.74	1.14

Table 20 Validation of rapid ABTS assay

3.16.2 Improvement of SD in the phenylhydrazine assay:

Developing HTS systems which are independent from H_2O_2 formation was one of the major goals of the project. This could allow us to design oxygen independent POxs as well as improving electron transfer interface from electrode to POxs. Numerous tests previously depicted while developing the Phenylhydrazine assay showed a major handicap: the detection limit could not be reduced from 48 mM glucose what made it insufficient for screening purposes, and the standard deviation could not get reduced from 30 %.

By using a better expression mutant (FA9) the Phenylhydrazine HTS showed an increased color development and reduced SD, with values around 15 %.

FA9 mutant library. SD: 19,15 %

FA9 mutant library. SD: 15,86 %
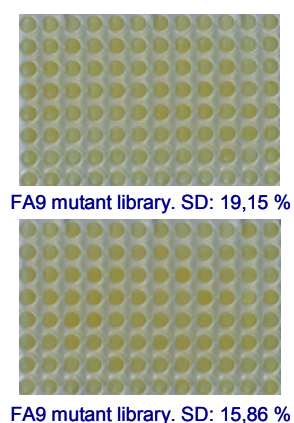
Fig 70 FA9 expression mutant allows reducing SD in Phenylhydrazine system

3.16.3 Phenylhydrazine assay correlation to the ABTS assay

Mutants were used to test the correlation of Phenylhydrazine and ABTS assays. Correlation between the two assay systems got improved especially in clones that co-expressed POx with chaperones (GroES-GroEL)

Activity – fold WT	2B	11D	CH2 2C	CH2 4D
End point Phenylhydrazine	5.17	1.31	0.65	1.17
End point ABTS	31.27	8.52	0.74	1.14
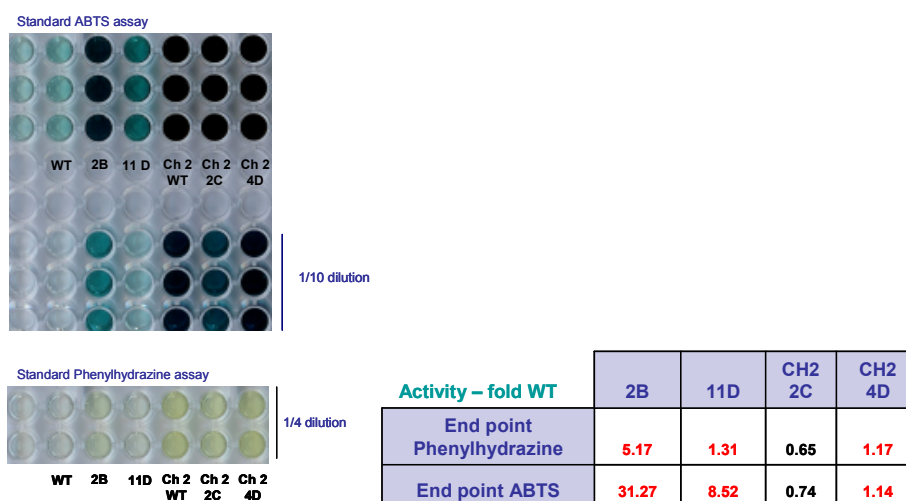
Fig. 71 Study of ABTS and phenylhydrazine systems correlation using POx expression assisted by chaperones. Test were performed on POx WT and in improved variants

3.17 Other experiments tried out

> Killing site to reduce religation: incubation with NcoI, EcoRI, KpnI, BamHI set of enzymes, various inactivation T and t of incubation tested, several digestion buffers and protocols tried. Protocols got complicated and religation still occured.

> Saturation Mutagenesis of position Phe 454, whose side chain shows steric hindrance with active site. A SM library of 600 clones did not show any variant with significant increased activity.

> Clone WT POx and mutant in the pETM 11 plasmid to facilitate purification via His-tag at the N-terminus followed by protease digestion.

> To co-express the GroEL-GroEs proteins with POx in pETM 11 cloning system for increased active expression of POx.

4. DISCUSSION

According to the objectives of this PhD work, *pox* from *Trametes versicolor* was cloned and POx actively expressed in *E. coli*. Characterization of the enzyme and comparison to related enzymes proved *T. versicolor* POx a good candidate to be used in the anodic compartment of biofuel cells. Tools of Directed Evolution were adapted and optimized to tailor POx. The utility of various assay system to screen POx mutant libraries was tested and, as a result, the ABTS assay was developed to a highthroughput screening system. A novel assay based on phenylhydrazine was also proposed and throughoutly studied. Preliminary tests on ferrocenemethanol assay over *T. versicolor* POx showed promising and suggested that ferrocenemethanol assay could be developed in a 96-well format.

Using a mutator strain to generate mutations in the *pox* gene, a truncated POx variant showing 14 fold increased k_{cat} –trPOx- was obtained. trPOx is a shortened enzyme which does not act as an indiscriminate oxidant and keeps D-glucose as preferred substrate. These treats make trPOx very interesting for industry but also for further studies, since it could provide evolutionary clues on POxs and other members of the GMC family.

The increased activity values showed by trPOx also allowed establishing the novel phenylhydrazyine assay as a highthrouput screening assay. The combination of ABTS and phenylhydrazine assays will allow correlating POx activity and O_2-independecy in future POxs studies.

4.1 Gene Cloning

From naturally occuring *Trametes versicolor* fruiting bodies, RNA was prepared for construction of a cDNA library. The library yielded two active wtPOxs, named clone 17b and clone 18, respectively, with a 99% sequence similarity between them and only seven amino acids differences. Similar results have been reported by other authors working with *Tricholoma matsusake* POx (Takakura and Kuwata, 2003). As explained in their work, the genetic backgrounds of individual fruiting bodies may not be uniform and

therefore the protein sequences deduced from cDNA might reflect slight genetic alteration among fruiting bodies originated from different progenies.

For clone 17b, further referred to as *pox,* cloning, expression, purification, and characterization of a novel pyranose oxidase was achieved. *T. versicolor pox* is identical from 86 to 91 % to other *poxs* like those from *C. versicolor* (Nishimura et al., 1996)*, T. ochracea* (Vecereck et al., 2004), *P. gigantea* (Bastian et al., 2005, Danneel et al, 1993), and *Peniophora sp.* (Heckmann-Pohl et al, 2006) in descendant order of similarity. *T. versicolor pox* is less related to the thermo-stable *Ph. gigantea pox* (Schaefer et al. 1996) with an identity value of 75 %.

During the generation of *pox* mutagenesis libraries, the classical ligation method showed rather low transformation efficiency and a high percentage of religation. A ligase-free method based upon generating customized overhanging sequences, which were complementary to the plasmid, led to an increase of the number of clones that contained the POx expressing vector. This method thus avoided self-religation of both, the plasmid and the insert. By implementing an additional gel extraction step to further remove residual self-ligated vector, the quality of the libraries was considerably improved.

Although error-prone PCR was the main tool used to generate genetic variety, our results additionally showed the feasibility of „*in vivo*" mutagenesis: Applying the Mutazyme II Polymerase Kit in combination with XL1-Red Competent Cells, both from Stratagene, yielded the most promising POxs variants. Particularly XL1-Red Competent Cells, which contain a deficient Polymerase III, which adds mutations, allowed the generation of numerous libraries within a few days.

It is also remarkable that applying different polymerase-based methods may have reduced mutational biases: epPCR is based use of Taq Polymerase only whereas Mutazyme II combines Polymerase I and Polymerase III, and XL1-Red Competent Cells function with a triple deficient Polymerase III, capable of producing a wider range of genetic diversity at a high rate.

4.2 Expression system

First experiments on expression of wild type POx in *E. coli* showed no activity of the enzyme, although SDS PAGE electrophoresis indicated the presence of a 69-kDa protein band corresponding to POx. These results suggested that overexpression of POx was either leading to the formation of inclusion bodies, which aggregated in the membrane fraction, or that the expressed protein was non-functional. Lack of protein function might have been due to lack of cofactors and false folding of the protein in the heterologous host. Lowering the growth temperature from 37°C to 30°C led to a significant reduction of inclusion body formation, which was corroborated by detecting some POx activity in the samples.

POx expression remained variable, which, given the intrinsic low values of POx activity, represented a serious obstacle for the directed evolution approach. However, the set-up of the novel screening assay, the screening of the mutant libraries, and the characterization of obtained protein variants required a high POx expression rate, which needed to be improved.

Overexpressing a recombinant protein in an expression host such as *E. coli* may compromise its resources for a proper protein processing. Molecular chaperones, for instance, had been demonstrated to be involved in assisting protein folding by various mechanisms. Thus, expression systems of five different sets of chaperones were tested in combination with recombinant POx expression. From them, groES-groEL proteins, encoded in plasmid pGro7 carrying an origin of replication derived from pACYC and a chloramphenicol resistance gene provided relevant improvements in assisting POx expression.

The expression system of groES-groEL chaperones, with the corresponding genes situated downstream of the araB promoter, allowed to separately express them prior to expression of POx, which in turn was mediated by the tet promoter. This system combination proved optimal for POx expression: a two-fold increase of POx expression

was obtained and the results of expression experiments became strictly reproducible. Consequently, this system combination was further used to express all POx variants and to establish the phenylhydrazine assay.

4.3 Production of recombinant POx from T. versicolor

The amino acid sequence of wtPOx showed 98 % identity to that of *T. ochracea* POx. It differs to its closest relative in only five positions: 188 (T instead of Q), 373 (V instead of I), 389 (P instead of L), 400 (S instead of E), 413 (E instead of K), with an additional change in position 623 (V instead of E) (total 96% identity) compared to *C. versicolor* POx. None of these residue exchanges have yet been reported to be involved in substrate binding, catalysis, oligomerization, or any other important function.

According to the sequence analysis, *T. versicolor* POx belongs to the pyranose 2-oxidase enzyme family (Bannwarth et al., 2004) within the GMC oxidoreductase family (Cavener 1992). However, there are differences in the substrate binding mode of the flavoenzymes within the family and catalytically relevant residues are not always located at the corresponding positions. Mutational refinements in the course of evolution might have led from a hypothetical original enzyme capable of catalysis over various substrates to the nowadays highly specific enzymes in the family, with distinct functions (Albrecht and Lengauer, 2003).

The characteristic sequence motif, S165THW168, responsible for FAD binding via covalent bound to His167 (Bannwarth et al. 2004), and the motif V49VIVGSGPIG58, which contains the highly conserved flavoprotein motif GXGXXG, responsible for the non-covalent binding of the ADP moiety of FAD (Wierenga et al. 1983), were identified in the wtPOx sequence of *Trametes versicolor*. The residue T was also present at position 169 both in wtPOx and trPOx as well as in the other variants. This amino acid residue has recently been reported by different authors to be important for substrate and flavinyl oxidation, during reductive and oxidative half-reactions, respectively (Pitsawong et al. 2010; Spadiut et al. 2007).

T. versicolor wtPOx was stable over a broad pH range (5.5-8) and up to 50°C with a maximum of activity at pH 7-7.5 and 45°C. These values are comparable to those determined for the phylogentically related *C. versicolor* POx (Masuda-Nishimura, 1999) and *T. matsutake* POx (Takakura and Kuwata, 2003). The later ones were stable at a pH range of 5.5-8 (down to pH 5 for *C. versicolor* POx, up to pH 11 for *T. matsutake* POx). These POxs have maximum enzyme activities within the pH range 7-8 and with a temperature range of 45-55°C.

WtPOx differed in temperature (45°C) and pH optima (pH 5.5-8) to the POxs isolated from *P. gigantea* (40°C, pH 6.0–6.5) (Bastian et al., 2005, Danneel et al, 1993) and *Peniophora sp* (55°C, pH 5.0–6.5) (Heckmann-Pohl et al. 2006). It also differed from the distantly related, naturally thermo-stablePOx of *Ph. gigantea* (65°C, pH 5.0–7.5) (Schaefer et al. 1996). *T. versicolor* wtPOx enzymatic activity showed no significant variation when assayed in chloride concentrations below 400 mM.

In terms of kinetic parameters, *T. versicolor* wtPOx showed a lower apparent K_m value for D-glucose (4.5 mM) in comparison to POx from *Peniophora sp* (7.6 mM) (Heckmann-Pohl et al. 2006) and higher apparent K_m value for D-glucose as compared to those of C. *versicolor* (1.4 mM) (Masuda-Nishimura, 1999), *T. matsutake* (1.28 mM) (Takakura and Kuwata, 2003), *P. obtusus* (1.18 mM) (Jansenn and Ruelius, 1975), *P. gigantea* (1.1 mM) (Danneel et al. 1993), and *Ph. gigantea* (1.2 mM) (Schaefer et al. 1996). The *T. versicolor* wtPOx k_{cat} value towards D-glucose (22.0 s^{-1}) is lower than that of *C. versicolor* POx (59.9 s^{-1}) (Masuda-Nishimura et al. 1999). The catalytic efficiency k_{cat}/K_m of wtPOx for D-glucose was higher (4.75 $mM^{-1}s^{-1}$) compared to *Peniophora sp* POx (1.23 $mM^{-1}s^{-1}$) (Heckmann-Pohl et al. 2006) and lower in comparison to the respective enzyme of *C. versicolor* (42.7 $mM^{-1}s^{-1}$) (Masuda-Nishimura et al. 1999).

4.4 Relevant POxs variants

Screening of *T. versicolor* POx mutant libraries resulted in several clones exhibiting increased POx activity. Sequencing results for the improved variants obtained via epPCR confirmed clones 6C5, 70c, and FA9 as improved expression mutants. Screening of *T. versicolor* POx mutant libraries created via "*in vivo*" mutagenesis resulted in an additional variant with increased enzymatic activity. Sequencing results for this enzyme variant showed a deletion of an adenine residue at position 1,227, which changed the reading frame for the subsequent five amino acids. This change resulted in an early stop codon at amino acid position 416, which led to a truncated monomeric POx variant (trPOx). trPOx had 415 amino acid residues compared to 623 of wtPOx as corroborated by the divergent SDS-PAGE band pattern: wtPOx appeared at 69 kDa whereas trPOx migrated at around 46 kDa. In addition, trPOx showed a five-amino-acid tail that differed from the wild type protein sequence.

Thermostability of wtPOx and the kinetically improved trPOx variant was found to be similar (55°C) with a maximum of activity at 45°C (Fig 68). trPOx showed a higher enzymatic activity in the temperature range of 30 to 45°C exhibiting 96 % of its maximum activity compared to 82 % observed for wtPOx. Significant differences were found for the protein stability at temperatures higher than 55°C. At 60°C activity of trPOx dropped to 27 % compared to 57 % observed in wtPOx (Fig 68). The temperature profile of trPOx shifted to lower values compared to wtPOx (Fig 69). In the range of 30-40°C, trPOxt showed 94 % of its maximum activity compared to 76 % observed for wtPOx. The optimum temperature of trPOx was 40°C compared to 45°C for wtPOx. Aside of the optimum activity at 40°C, values of activity of trPOxt fell to 82.3 % at 50°C and to 19 % at 60°C in comparison to a 96 % and 60 %, respectively, for wtPOx (Fig. 69).

trPOx showed a ~14 fold increased k_{cat} (78.2 s^{-1} per catalytic center compared to a wtPOx k_{cat} of 5.5 s^{-1} per catalytic center) and an improved apparent K_m value (0.85 mM) compared to that of wtPOx (K_m: 4.5 mM). trPOx catalytic efficiency was ~78 fold

improved (trPOx k_{cat}/K_m: 93,038 $M^{-1}s^{-1}$ per catalytic center compared to wtPOx k_{cat}/K_m: 1,186 $M^{-1}s^{-1}$ per catalytic center).

The substrate profile analyses of wtPOx and trPOx for FAD catalysis showed that trPOx did not act as an indiscriminate oxidant. trPOx showed low activities for D-glucono-1,5-lactone (0.34 % compared to the activity for D-glucose) and for 5-thio-D-glucose (2.5 % compared to the activity for D-glucose). These results suggested that D-glucose acted as the preferred substrate for trPOx. Alternatively, the decreased values for these two substrates could be explained by the overall increased activity of the trPOx variant. Assays performed with 2-fluoro-2-deoxy-D-glucose as substrate demonstrated that trPOx preserved its regioselectivity. Similarly to wtPOx, trPOx oxidized preferably at position 2 of D-glucose.

The kinetic parameters of trPOx (k_{cat}: 78.2 s^{-1} per catalytic center, K_m: 0.85 mM, and k_{cat}/K_m: 93,038 $M^{-1}s^{-1}$ per catalytic center) make this shorted POx variant reacting faster than the following POx variants engineered by other authors: POx from *P. gigantea* (Bastian et al. 2005), which included amino acid substitutions K312E, E540K and a C-terminal His$_6$-tag (K_m: 0.4 mM; k_{cat}/K_m: 269.08 $mM^{-1}s^{-1}$ per tetrameric enzyme), and POx from *Peniophora sp.* (Heckmann-Pohl et al. 2006), with substitutions T158A, E540K and a C-terminal His$_6$-tag (k_{cat}: 133.5 s^-1; Km: 0.47 mM, k_{cat}/K_m: 284.03 $mM^{-1}s^{-1}$ per tetrameric enzyme).

Considering the high sequence similarity of *T. versicolor* POx to native *T. multicolor* POx (Hallberg et al. 2004) and *Peniophora sp.* POx (Bannwarth et al., 2004; Bannwarth et al., 2006), whose structural data are available, trPOx possesses an unaffected catalytic domain whereas the substrate binding area would be severely changed. In fact, a significant POx part of around five antiparallel β-sheets with central residues 436-448-472-363-539 had been removed. These amino acids interact with other regions of the POx monomer and bind D-glucose (Bannwarth et al., 2004).

These conflicting results raise questions about the actual binding and catalysis of D-glucose. Native zymographic analysis demonstrated clear differences in the electrophoretic mobility of wtPOx and trPOx but confirmed the correct folding and increased enzymatic activity of the truncated variant. FAD load quantification of *T. versicolor* POx samples extracted from the zymogram bands was consistent with these findings. The increased FAD load found in trPOx can be quantitatively explained when considering an unaffected FAD load and binding of the cofactor to the monomer, but a significantly reduced protein complex signal as expected from a complex formed by smaller polypeptide subunits. trPOx showed a ~1.3-fold higher FAD load compared to that of purified wtPOx. These results were consistent with a 33 % reduced size of the trPOx monomer and considering the tetrameric structure of POx. These results were furthermore confirmed by comparison to the FAD load in commercial *C. versicolor* POx (a close homologous showing 91 % identity at the nucleotide sequence to that of wtPOx): wtPOx showed a FAD load, which was ~3 fold higher than that of *C. versicolor* POx whereas trPOx and ~4 fold higher than that of commercial *C. versicolor* POx.

Increased values of activity of trPOx might also be explained when considering reported structural limitations in terms of accessibility of the substrate. First of all, most of the amino acids that form the glucose-sized pores leading from the spacious central cavity formed in the tetramer to the four catalytic centers (Bannwarth et al., 2004) were absent in the *T. versicolor* trPOx. This could imply that diffusion of glucose might not be a limiting trait per se as reported previously (Bannwarth et al., 2004). Secondly, the highly mobile loop 454-461 at the active center, which is assumed to function as a gatekeeper to make way for the sugar to pass into the active center, was absent in the trPOx variant. The active-site loop has been reported to block the entrance to the substrate-binding pocket and thus monosaccharide binding (Hallberg et al. 2004). This would have consequences for the reaction rate, since a dynamic change in wtPOx is necessary during the reductive half-reaction to allow binding of the carbohydrate. The removal of this loop in the trPOx variant could explain a faster catalytic process. The strictly conserved and mobile Phe454 within the loop was also deleted in trPOx. This amino acid residue could be affecting POx oxidation rate as it had been reported to move away during sugar access

to the active site, close like a lid, and push D-glucose towards the FAD still bound to His167 (Bannwarth et al., 2006).

Bannwarth et al. (2006) suggested that the α-anomer of D-glucose is unlikely to be accepted by the enzyme, since the hydroxyl group would severely collide with Val546 and Phe474, thus making a prior mutarotation reaction necessary in the tetramer central cavity. In trPOx these impediments do not exist. Similarly, it had previously been reported that prior to active-site access the substrate must enter the tetramer void through any of the four solvent channels leading from the external surface of the tetramer into the void (Bannwarth et al., 2004; Hallberg et al. 2004). Possible carbohydrate-binding residues that line the channel have been proposed and include: Glu421, His419, Gln418, Phe428 and Glu429 (near the external opening); Asp101, Ser465, Glu432 and Arg451 (inside the channel); Gln461, Asn99, Ser113, Glu542 (near the internal opening) (Hallberg et al. 2004); or Ile100, Pro248, Glu429, and Ser465 of Subunit A and Asn140 and Ala494 of Subunit B (Brannwarth et al. 2004). Making oblivious the differences between the authors, many of these residues were absent in the trPOx, with the exception of three, Asp 101, Asn99, and Ser113, out of the thirteen proposed in the first model (Hallberg et al. 2004); or two, Ile100 and Pro248, out of six proposed in the second one (Brannwarth et al. 2004). In any case, and assuming with caution the proposed models, structural limitations in terms of accessibility of the substrate seem to be reduced in *T. versicolor* trPOx.

A mostly hydrophobic portion that stretches within the wtPOx protein structure and corresponds to the substrate binding area – three strands of the six antiparallel β-sheets fold with central residues 237-436-448-472-363-539 (Bannwarth et al., 2004; Hallberg et al. 2004) have been removed in trPOx. As a result, the trPOx monomer might exhibit easier access to the active site.

Amino acid residues 368-430 form a protrusion of the monomer structure with a rather flat surface rich in T and S residues. This surface might allow the enzyme to attach to the outer membrane or to other POxs and might therefore be involved in POx

oligomerization (Hallberg et al. 2004). Due to the change in the reading frame at position 1,227, an early stop codon was generated at amino acid position 416 in trPOx. Downstream of the frame shift, seven amino acid residues of the wtPOx protrusion sequence (N409EKVENH415) were changed in trPOx (T409RRWRTT415). Additionally, 15 amino acids from the sequence that forms the head protrusion in wtPOx (M416MQHQEDPLPIPFED430) were lost in trPOx. These changes likely hampered trPOx interactions and limited the formation of oligomerized POx. Cooperative effects such as stabilization of the POx structure might further be lost in the trPOx as indicated by its altered temperature profile. The fact that the deleted portion is mostly hydrophobic supported this assumption especially since some of the removed amino acids were previously reported to be involved in weak interactions of the dimer structure (Hallberg et al. 2004).

The different sets of possible monomer–monomer interfaces are differentially stable with one dimer pair (A–B or C–D) exhibiting the smallest exposed surface area and the largest degree of polar interactions (Hallberg et al. 2004). Sub-domain F (Rossmann domain) does not directly take part in oligomerization and sub-domain H2 (conserved in trPOx) appears to be the principal determinant for dimerization. The monomer pairs A–D and B–C feature hydrophobic packing interactions and a small number of hydrogen bonds mediated by the oligomerization arm. The weakest interaction surfaces are observed at the interfaces of the A–C and B–D pairs and are mainly hydrophobic packing contacts between residues in the sub-domain segment H8-B6 of each monomer (residues 508 to 528 and 532 to 540, respectively) (Hallberg et al. 2004). H8-B6 and a significant part of the hydrophobic surface of the monomer are absent in trPOx.

trPOx is the smallest active POx yet described. The increased activity, functional expression in *E.coli* and preserved regioselectivity render trPOx an attractive industrial catalyst. In the future, further directed evolution approaches should be applied to increase trPOx activity and expression.

Finally, it might be interesting from an evolutionary point of view to further investigate trPOx. Various authors suggested that POxs together with the entire GMC family were derivatives of a primordial FAD-binding domain that developed large insertions at the same positions – such as glutathione reductase and numerous other members of the family (Bannwarth et al. 2004; Dym and Eisenberg, 2001). trPOx might represent such a primordial FAD-binding domain, which evolved to eventually constitute enzymes like tetrameric POx. Therefore, further research on trPOx could provide evolutionary clues on POxs and other members of the GMC family.

4.5 Screening methods

4.5.1 Pre-screening assays

Agar plate-based pre-screening assays could simplify and speed up the directed evolution experiments. In this work, recombinant wtPOx instrinsically low activity posed a major problem to develop the proposed pre-screening assays, which were based on thionine and poly R 478 as substrates, respectively. Working with trPOx, which has a significantly increased activity, as a starting point could allow surpassing this obstacle and further develop improved and more sensitive pre-screening assays.

Based on this work, additional considerations are advisable: In the pre-screening assays performed, the inducer for POx expression –anhydrotetracycline - was included in the agar preparation in order to homogenize its concentration and thus the degree of induction amongst the colonies. Adding inducer solution at a later step would not warrant equal distribution. However, this early induction of the protein expression could have somehow negatively affected expression of the active form of POx. As deduced from experiments carried out with liquid media, optimum levels of active POx expression were obtained when colonies were left to grow until an OD_{578} value of 0.4 before proceeding with POx gene induction. Likewise, the significant improvement of POx expression observed during the co-expression with chaperones strongly recommends their further

use. However, this would mean introducing another inducer – arabinose – in the agar plate preparation and, consequently, another early induction. According to our experiences, this additional inducer could stress the cells and therefore hinder the process of expression of active POx. In fact, induced expression of chaperones 2 h prior to induction of POx expression demonstrated optimum results. Therefore, finding a way to sequentially induce chaperones and POx without compromising equal distribution of the inducers in the agar medium could be advisable for an optimum pre-screening assay of trPOx – or other increased activity variant libraries.

4.5.2 Novel assay systems

4.5.2.1 Phenylhydrazyine assay

Developing high through-put systems independent from H_2O_2 formation could allow us to design oxygen independent POxs as well as to improve the electron transfer interface from electrode to POxs. In contrast to the ABTS assay, the phenylhydrazyne method detects the product 2-keto-glucose and allows improving bioelectrochemical properties of POxs for their use in the anodic compartment of biofuel cells, where they are not reoxidized by molecular oxygen.

Initial tests while developing the phenylhydrazine assay showed that the detection limit could not be improved from 48 mM glucose and that the standard deviation of 30 % was unsatisfactory and insufficient for screening purposes. By using the better expression mutant FA9 an increased color development was achieved for the phenylhydrazine system and the standard deviation was reduced to values of ~15 %. Moreover, the protocol was simplified by using a permeabilizer –Polymixin B- so that cell disruption and several subsequent separation and washing steps were made unnecessary. These results were corroborated in libraries of the increased activity variant trPOx and were furthermore improved by co-expression of the chaperones GroES-GroEL. Overall, a very significant improvement was achieved for the temporal duration of the screening process.

A good correlation of phenylhydrazine and ABTS assays was demonstrated. Consequently, the phenylhydrazine assay can be further used to tailor POxs and specially oxygen independent POxs.

4.5.2.2 Ferrocenemethanol assay

Ferrocenemethanol served to develop an additional colorimetric assay with a detection range from 0 to 700 µM in a 96-well microtiter plate and a standard deviation of 16% or less, which was validated by standard hydrogen peroxide detection via ABTS assay (Ziwei Zhu PhD Thesis). This newly established assay was also used to detect POx activity of cell extracts of *E. coli* expressing wtPOx. The ferrocenemethanol assay has therefore the potential to serve for screening POxs and other FAD containing oxidases.

SUMMARY

Pyranose 2-oxidase (POx) is a H_2O_2-producing flavoenzyme that participates in ligninolytic processes by wood-degrading basidiomycete fungi. Unlike glucose oxidase (GOx), POx catalyzes the oxidation in position 2 of D-glucose and other aldopyranoses (D-xylose, D-galactose, and L-arabinose) to the corresponding 2-keto derivatives. Since its first characterization, the importance of POx for various biotechnical applications has been recognized with special emphasis on bio-transformations of carbohydrates to produce various important sugar-derived intermediates for the synthesis of rare sugars, fine chemicals, and drugs. A novel application, subject of study of this PhD work, is the potential application of POxs in biofuel cells.

In D-glucose based biofuel cells, GOx has become the prime enzyme used in the anodic compartment due to its high specificity and efficiency. Prolonging the life span for such a biofuel battery, which would be very attractive for diverse applications, is the main goal at developing implanted miniature biofuel cells. Electrical output could be improved by tailoring GOx to optimally function at 37°C and pH 7; or, alternatively, by using pyranose oxidase (POx), a very promising candidate. POxs show a broader substrate profile, a significantly higher affinity towards glucose and no anomeric preference. Their pH range of activity varies from 5 to 8, and at values superior to 7, the kinetics of the reaction over D-glucose is barely affected by the buffer composition. However, the catalytic efficiency of POxs needs to be improved. Moreover, POxs are specially challenging since – in contrast to GOxs - there is little knowledge about POx structures, their structure-function relationships, electrochemical properties, and enzymatic stabilities. Only few relevant publications have been released in recent years and the first resolved POx structure was reported in 2004.

According to the objectives of this PhD work, *pox* from *Trametes versicolor* was cloned from a cDNA library and was expressed in *Escherichia coli* as an intracellular active recombinant enzyme. Characterization of the enzyme and comparison to related enzymes proved *T. versicolor* POx a good candidate to be used in the anodic compartment of

biofuel cells. Tools of Directed Evolution were adapted and optimized to tailor POx aiming to improve its catalytic efficiency and to search for O_2 independent POx variants. The utility of various assay systems to screen POx mutant libraries was tested and, as a result, the ABTS assay was developed to a high throughput screening system. A novel assay based on the phenylhydrazine reaction with 2-keto-glucose, the enzymatic product of POxs over D-glucose, was also proposed and carefully studied. Preliminary tests on ferrocenemethanol assay over *T. versicolor* POx showed promising and suggested that ferrocenemethanol assay could be developed in a 96-well format.

Using a mutator strain to generate mutations in the *pox* gene, a truncated POx variant showing 14 fold increased k_{cat} –trPOx- was obtained. trPOx is a shortened enzyme which does not act as an indiscriminate oxidant and keeps D-glucose as preferred substrate. These treats make trPOx, which is the smallest POx yet described, very interesting for the industry but also for further studies, since it could provide evolutionary clues on POxs and other members of the glucose-methano-choline family of enzymes.

The increased activity values showed by trPOx also allowed establishing the novel phenylhydrazyine assay as a high throughput screening assay. The combination of ABTS and phenylhydrazine assays will allow correlating POx activity and O_2-independecy in future POxs studies.

Results of this study proved the applied directed evolution strategy to be successful at optimizing catalytic activities of POxs. Directed evolution could be further used to tailor other properties of these enzymes for the anodic compartment of implanted miniature biofuel cells.

Appendix

Oxidized ferrocenemethanol preparation

Ferrocenemethanol preparation [reduced (red), 6mM] was partially dissolved under stirring in phosphate buffer (100 mM; pH 3, RT). This yellow suspension exhibits an absorbance maximum at 430 nm. Ferrocenemethanol (red) was enzymatically oxidized by adding laccase from *Trametes versicolor* (Fluka, 7.2 U/mL in 50 mM phosphate buffer, 1h). During the oxidation the yellow suspension fully dissolves: ferrocenemethanol (ox) is at pH 3 a blue solution with absorbance maximum at 625 nm. After 90% conversion, the laccase catalyzed oxidation of ferrocenemethanol was stopped by adjusting the pH to 8 (0.2 M NaOH). Laccase was subsequently removed from the oxidized ferrocenemethanol solution by ultrafiltration using a stirred cell (200 mL, Amicon 8200, Millipore, Schwalbach, Germany) with a 30-kDa cut-off membrane (PBTK, Millipore).

Determination of molar extinction coefficient of ferrocenemethanol

6mM oxidized ferrocenemethanol was diluted to a concentration range 0-6 mM using 100 mM pH 8 phosphate buffer (316 mM ionic strength). The absorbance was measured at 625 nm using a FLASHScan S12 microplate reader (Analytik Jena, Jena, Germany). The absorbance values of oxidized ferrocenemethanol at different concentrations were then plotted and molar extinction coefficient ξ (M-1cm-1) was calculated using the following formula: $\xi = A/C*l$ (A: absorbance at 625 nm; l: pathlength; C: molar concentration of oxidized ferrocenemethanol).

Linear detection range of ferrocenemethanol based assay

Ferrocenemethanol was used as an electron acceptor for reduced form of glucose oxidase to determine the linear detection range under screening conditions in 96-well format. Various concentrations of ferrocenemethanol (0-2 mM final concentration) were pippeted into 100 µL of phosphate buffer (100 mM, pH 8) in 96-well microtiter plate. A solution consisting of 100 µL of 1 M D-glucose in phosphate buffer (100 mM, pH 8) was mixed with ferrocenemethanol and finally 100 µL of wtGOx added to initiate the reaction . Bubbles were removed using a Bunsen burner and absorbance was measured at 625 nm for 30 min to quantify the reaction kinetics using a a FLASHScan S12 microplate reader (Analytik Jena, Jena, Germany).

REFERENCES

Adachi, O., T. Chiyonobu, E. Shiganawa, K. Matsushita, and M. Ameyama. 1978. Crystalline 2-ketogluconate resuctase from *Acetobacter Ascendens*, the second instance of crystalline enzyme in genus *Acetobacter. Agric. Biol. Chem.* **42**:2057-2062.

Albrecht, M., and T. Lengauer. 2003. Pyranose oxidase identified as a member of the GMC oxidoreductase family. *Bioinformatics* **19**:1216-1220.

Ameyama, M., and O. Adachi. 1982. 2-Keto-D-gluconate reductase from acetic acid bacteria. *Methods Enzymol.* **89**: 203-210.

Ander, P. 1994. The cellobiose oxidizing enzymes CBQ and CbO as related to lignin and cellulose degradation - a review. *FEMS Microbiol. Rev.*13:297-311.

Ander, P., C. Mishra, R. L. Farrell, and K. E. L. Eriksson. 1990. Redox reaction in lignin degradation, interaction between laccase, different peroxidases and cellobiose quinone oxidoreductase. *J. Biotechnol.* **13**:189-198.

Artolozaga, M. J., E. Kubatova, J. Volc, and H. M. Kalisz. 1997. Pyranose 2-oxidase from *Phanerochaete chrysosporium*-further biochemical characterisation. *Appl. Microbiol. Biotechnol.* **47**:508-514.

Bamminger, U., R. Ludwig, C. Galhaup, C. Leitner, K. D. Kulbe, and D. Haltrich. 2001. Continuous enzymatic regeneration of redox mediators used in biotransformation reactions employing flavoproteins. *J . Mol. Catal. B-enzym.* **11**:541-550.

Bannwarth, M., S. Bastian, D. Heckmann-Pohl, F. Giffhorn, and G. E. Schulz. 2004. Crystal structure of pyranose 2-oxidase from the white-rot fungus *Peniophora sp. Biochemistry* **43**:11683-11690.

Bannwarth, M., D. Heckmann-Pohl, S. Bastian, F. Giffhorn, and G. E. Schulz. 2006. Reaction geometry and thermostable variant of pyranose 2-oxidase from the white-rot fungus *Peniophora sp. Biochemistry* **45**:6587-6595.

Bastian, S., M. J. Rekowski, K. Witte, D. M. Heckmann-Pohl, and F. Giffhorn. 2005. Engineering of pyranose 2-oxidase from *Peniophora gigantea* towards improved thermostability and catalytic efficiency. *Appl. Microbiol. Biotechnol.* **67**:654-663.

Bateman, R. C. J., and J. A. Evans. 1995. Using the glucose oxidase - peroxidase system in enzyme kinetics. *J. Chem. Ed.* **72**:240-241.

Baute, R., and M. A. Baute. 1984. Ocurrance among macrofungi of the bioconversion of glucosone to cortalcerone. *Phytochemistry* **23**:271-274.

Baute, R., M. A. Baute, and G. Deffieux. 1987. Proposed Pathway to the Pyrones Cortalcerone and Microthecin in Fungi. *Phytochemistry* **26**:1395-1397.

Bolon, D. N., C. A. Voigt, and S. L. Mayo. 2002. De novo design of biocatalysts. *Curr. Opin. Chem. Biol.* **6**:125-129.

Bourdillon, C., C. Demaille, J. Moiroux, and J. M. Saveant. 1993. New insights into the enzymatic catalysis of the oxidation of glucose by native and recombinant glucose-oxidase mediated by electrochemically generated one-electron redox cosubstrates. *J. Am. Chem. Soc*. **115**:2-10.

Cadwell R. C., and G. F. Joyce. 1992. Randomization of genes by PCR mutagenesis. *PCR Methods Appl.* **2**:28-33.

Camps M., J. N., B. P. Johnson, and L. A. Loeb. 2003. Targeted gene evolution in *Escherichia coli* using a highly error-prone DNA polymerase. PNAs **100**:9727–9732.

Cass, A. E. G., G. Davis, G. D. Francis, H. A. O. Hill, W. J. Aston, I. J. Higgins, E. V. Plotkin, L. D. L. Scott, and A. P. F. Turner. 1984. Ferrocene-mediated enzyme electrode for amperometric determination of glucose. *Analytical Chemistry* **56**:667-671.

Cavener, D. R. 1992. GMC oxidoreductases. A newly defined family of homologous proteins with diverse catalytic activities. *J. Mol. Biol.* **223**:811-814.

Cedrone, F., A. Menez, and E. Quemeneur. 2000. Tailoring new enzyme functions by rational redesign. *Curr. Opin. Struc. Biol*.**10**:405-410

Chance, B., and A. C. Maehly. 1955. Assay of catalases and peroxidases. *Methods in Enzymology* II:764-817.

Chiyonobu, T., E. Shiganawa, K. Matsushita, O. Adachi, and M. Ameyama. 1976. Purification, crystallization and properties of 2-ketogluconate reductase from *Acetobacter Rancens. Agric. Biol. Chem.* **40**:175-184.

Christensen, S., S. F. Lassen, and P. Schneider. 2000. Nucleic acids encoding polypeptides having pyranose oxidase activity. *US Patent* **6**,146,865.

Chusney, G. D., M. Philippa, and J. C. Pickup. 1995. Comparison of microenzymatic and high-performance liquid chromatography methods for the assay of serum 1,5-anhydroglucitol. *Clin. Chim. Acta* **235**:91-99.

Cox, E. C. 1976. Bacterial mutator genes and the control of spontaneous mutation. *Annu. Rev. Genet.* **10**:135-156.

Daniel, G. 1992. Use of electron microscopy for aiding our understanding of wood degradation. *FEMS Microbiol. Rev.* **13**:199-233.

Daniel, G., J. Volc, and E. Kubatova. 1994. Pyranose Oxidase, a Major Source of H_2O_2 during Wood Degradation by *Phanerochaete chrysosporium*, *Trametes versicolor*, and *Oudemansiella mucida*. *Appl. Environ. Microbiol.* **60**:2524-2532.

Danneel, H. J., E. Rossner, A. Zeeck, and F. Giffhorn. 1993. Purification and characterization of a pyranose oxidase from the basidiomycete *Peniophora gigantea* and chemical analyses of its reaction products. *Eur. J. Biochem.* **214**:795-802.

de Koker, T. H., M. D. Mozuch, D. Cullen, J. Gaskell, P. J. Kersten. 2004. Isolation and purification of pyranose 2-oxidase from *Phanerochaete chrysosporium* and characterization of gene structure and regulation. *Appl. Environ. Microbiol.* **70**:5794–5800.

Dym, O., and D. Eisenberg. 2001. Sequence-structure analysis of FAD-containing proteins. *Protein Sci.* **10**:1712-1728.

Eberhardt, A. 1999. Prozesskontrolle Versfaelschungsnachweismittles HPLC-Biosensor Kopplung: Analytic von Kohlenhydraten. PhD Thesis, TU Braunschweig.

Eriksson, K. E., B. Petersson, J. Volc, and V. Musilek. 1986. Formation and partial characterization of D-glucose, a H_2O_2-producing enzyme in *Panerochaete crysosporium*. *Appl. Microbiol. Biotechnol.* 23:257-262.

Freimund, S., A. Huwig, F. Giffhorn, and S. Kopper. 1998. Rare keto-aldoses from enzymatic oxidation: Substrates and oxidation products of pyranose 2-oxidase. *Chem. Eur. J.* **4**:2442-2455.

Fukumura, Y., S. Tajima, S. Oshitani, Y. Ushijima, I. Koyabashi, F. Hara, S. Yamamoto, and M. Yabuuchi. 1994. Fully enzymatic methods for determining 1,5-anhydro-D-glucitol in serum. *Clin. Chem*. **40**:2013-2016.

Funcke, W., C. Vonsonntag, and C. Triantaphylides. 1979. Detection of the Open-Chain Forms of D-Fructose and L-Sorbose in Aqueous-Solution by Using C-13-Nmr Spectroscopy. *Carbohydr. Res.* **75**:305-309.

Giffhorn, F. 2000. Fungal pyranose oxidases: occurrence, properties and biotechnical applications in carbohydrate chemistry. *Appl. Microbiol. Biotechnol.* **54**:727-740.

Giffhorn, F., S. Köpper, A. Huwig, and S. Freimund. 2000. Rare sugars and sugar-based synthons by chemo-enzymatic synthesis. *Enzyme Microbiol. Technol*. **27**:734–742.

Halada, P., C. Leitner, P. Sedmera, D. Haltrich, and J. Volc. 2003. Identification of the covalent flavin adenine dinucleotide-binding region in pyranose 2-oxidase from *Trametes multicolor. Anal. Biochem.* **314**:235-242.

Hallberg, B. M., K. E. Eriksson, B. Petersson, and C. Divne. 2002. Crystal structure of the flavoprotein domain of the extracellular flavocytochrome cellobiose desydrogenase. *J. Mol. Biol.* **315**:421-434.

Hallberg, B. M., C. Leitner, D. Haltrich, and C. Divne. 2004. Crystal structure of the 270 kDa homotetrameric lignin-degrading enzyme pyranose 2-oxidase. *J. Mol. Biol*. **341**:781-796.

Hallberg, B. M., C. Leitner, D. Haltrich, and C. Divne. 2004. Crystallization and preliminary X-ray diffraction analysis of pyranose 2-oxidase from the white-rot fungus *Trametes multicolor*. Acta Crystallogr., Sect D: Biol. Crystallogr. **60**:197-199.

Haltrich, D., C. Leitner, W. Neuhauser, B. Nidetzky, K. D. Kulbe, and J. Volc. 1998. A convenient enzymatic procedure for the production of aldose-free D-tagatose. *Ann. N. Y. Acad. Sci*. **864**:295-299.

Heckmann-Pohl, D. M., S. Bastian, S. Altmeier, and I. Antes. 2006. Improvement of the fungal enzyme pyranose 2-oxidase using protein engineering. *J. Biotechnol.* **124**:26-40.

Huwig, A. 1997. Untersuchungen zur enzymatischen Synthese von Carbonylzuckern mit der Pyranose-2-oxidase aus *Peniopora gigantea.* PhD Thesis, University of the Saarland.

Izumi, Y., Y. Furuya, and H. Yamada. 1990a. Isolation of a new pyranose oxidase producing basidiomycete. *Agric. Biol. Chem.* **54**:799-801.

Izumi, Y., Y. Furuya, and H. Yamada. 1990b. Purification and properties of pyranose oxidase from basidiomycetous fungus No 52. *Agric. Biol. Chem.* **54**:1393-1399.

Janssen, F. W., and H. W. Ruelius. 1975. Pyranose oxidase from *Polyporus obtusus*. Method Enzymol. **41**:170-173.

Kelley, R. L., and C. A. Reddy. 1986b. Characterization of glucose oxidase-negative mutants of a lignin degreding basidiomycete *Phanerochaete crysosporium*. *Arch. Microbiol.* **144**:254-257.

Kelley, R. L., and C. A. Reddy. 1986a. Identification of glucose oxidase activity as the primary source of hydrogen peroxide production in ligninolytic cultures of *Phanerochaete crysosporium. Arch. Microbiol.* **144**:248-253.

Kelley, R. L., and C. A. Reddy. 1986c. Purification and characterization of glucose oxidase activity from ligninolytic cultures of *Phanerochaete crysosporium*. *J. Bacteriol.* **166**:269-274.

Kiba, N., S. Itagaki, K. Fukumura, K. Saegusa, and M. Furusawa. 1997. Highly sensitive flow-injection determination of glucose in plasma using an immobilized pyranose oxidase and a chemiluminometric peroxidase sensor. *Anal. Chim. Acta* **354**:205-210.

Konarzycka, M., and U. Bornscheuer. 2003. A high-throughput-screening method for determining the synthetic activity of hydrolases. *Angew. Chem. Int.* Ed:1418-1420.

Koths, K., R. Halenbeck, and M. Moreland. 1992. Synthesis of the antibiotic cortalcerone from D-glucose using pyranose 2-oxidase and a novel fungal enzyme, aldos-2-ulose dehydratase. *Carbohydr. Res*. **232**:59-75.

Laemli, U. K. 1970. Cleavage of Structural Proteins during the Assembly of the Head of Bacteriophage T4. *Nature* **227**:680 - 685.

Leitner, C., P. Halada, D. Haltrich, E. Kubatova, M. Kujawa, C. Peterbauer, P. Sedmera, and J. Volc. 2003. Pyranose dehydrogenase, a novel quinone-dependent sugar oxidoreductase of lignocellulose-degrading litter fungi. *Abstr. Pap. Am. Chem.* S. **225**:U279-U279.

Leitner, C., D. Haltrich, B. Nidetzky, H. Prillinger, and K. D. Kulbe. 1998. Production of a novel pyranose 2-oxidase by basidiomycete *Trametes multicolor. Appl. Biochem. Biotechnol.* **70**-72:237-248.

Leitner, C., W. Neuhauser, J. Volc, K. D. Kulbe, B. Nidetzky, and D. Haltrich. 1998. The cetus process revisited: A novel enzymatic alternative for the production of aldose-free D-fructose. *Biocatal. Biotransform.* **16**:365-382.

Leitner, C., J. Volc, and D. Haltrich. 2001. Purification and characterization of pyranose oxidase from the white rot fungus *Trametes multicolor. Appl. Environ. Microbiol.* **67**:3636-3644.

Liden, H., J. Volc, G. Marko-Varga, and L. Gorton. 1988. Pyranose Oxidase Modified Carbon Paste Electrodes for Monosaccharide Determination. *Electroanal* **10**:223-230.

Luong, J. H. T., C. Masson, R. S. Brown, K. B. Male, and A. L. Nguyen. 1994. Monitoring the activity of glucose oxidase during the cultivation of *Aspergillus niger* using novel amperometric sensor with 1,1'-dimethylferricinium as a mediator. *Biosen. and Bioelectron.* **9**:577-584.

Machida, Y., and T. Nakanishi. 1984. Purification and properties of Pyranose Oxidase from *Coriolus versicolor. Agric. Biol. Chem.* **48**:2463-2470.

Maresova, H., B. Vecerek, M. Hradska, N. Libessart, S. Becka, M. H. Saniez, and P. Kyslik. 2005. Expression of the pyranose 2-oxidase from *Trametes pubescens* in *Escherichia coli* and characterization of the recombinant enzyme. *J. Biotechnol.* **120**:387-395.

Masuda-Nishimura, I., T. Minamihara, and Y. Koyama. 1999. Improvement in thermal stability and reactivity of pyranose oxidase from *Coriolus versicolor* by random mutagenesis. *Biotechnol. Lett.* **21**:203–207.

Mohanty, J. G., J. S. Jaffe, E. S. Schulman, and D. G. Raible. 1997. A highly sensitive fluorescent micro-assay of H_2O_2 release from activated human

leucocytes using a dihydroxyphenoxazine derivative. *J. Inmunol. Methods* **202**:133.

Moser, I., T. Schalkhammer, E. Mannbuxbaum, G. Hawa, M. Rakohl, G. Urban, and F. Pittner. 1992. Advanced immobilization and protein techniques on thin film biosensors. *Sensors Actuators* **7**:356-362.

Namba, N., F. Watanabe, M. Tokuda, M. Mino, and E. Furuya. 1994. A method of quantititing serum and urinary levels of 1,5-anydroglucitol in insulin-dependent Diabetes mellitus. *Diabetes Res. Clin. Pract*. **24**:55-61.

Nesterenko, M. V., M. Tilley, and S. J. Upton. 1994. A simple modification of Blum's silver stain method allows for 30 minute detection of polyacrylamide gels. *J. Biochem. Biophys. Methods* **28**:239-242.

Nishihara, K., M. Kanemori, H. Yanagi, and T. Yura. 2000. Overexpression of Trigger Factor Prevents Aggregation of Recombinant Proteins in *Escherichia coli. Appl. Environ. Microbiol.* **66**:884-889.

Nishihara, K., M. Kanemori, M. Kitagawa, H. Yanagi, and T. Yura. 1998. Chaperones Coexpression Plasmids: Differential and Synergistic Roles of DnaK-DnaJ-GroE and GroEL-GroES in Assisting Folding of an Allergen of Japanese Cedar Pollen, Cryj2 in *Escherichia coli. Appl. Biochem. Biotech.* **64**:1694-1699.

Nishimura, I., K. Okada, and Y. Koyama. 1996. Cloning and expression of pyranose oxidase cDNA from Coriolus versicolor in *Escherichia coli. J. Biotechnol.* **52**:11-20.

Olsson, L., C. F. Madenius, E. Kubatova, and J. Volc. 1991. Immobilization of pyranose oxidase (*Phanerochaete chrysosporium*): Characterization of the enzymic properties. *Enzyme Microb. Tech.* **13**:755-759.

Petřivalský, M., S. P, M. L, and V. J. 1994. Amperometric Enzyme Electrodes for Substrates of Immobilized Pyranose Oxidase. *Coll Czech Chem. Commun.* **59**:1226-1234.

Pishko, M., I. Katakis, S. E. Lindquist, L. Ye, B. A. Gregg, and A. Heller. 1990. Direct electrical communication between graphite-electrodes and surface absorbed glucose oxidase - redox polymer complexes. *Angew. Chem. Int. Ed.* **29**:82-89.

Pitsawong, W., J. Sucharitakul, M. Prongjit, T. Tan, O. Spadiut, D. Haltrich, C. Divne, and P. Chaiyen. 2010. A conserved active-site Threonine is important for both sugar and flavin oxidations of Pyranose oxidase. *J. Biol. Chem.* **258**:9697-9705.

Pitt, D., and M. J. Mosley. 1985. Enzymes of gluconate metabolism and glycolysis in *Penicillium notatum* Antoine Van Leeuwenhoek. *J. Microbiol.* **51**:353-364.

Radman, M. 1980. Progress in Environmental Mutagenesis. *M. Alecivic Ed.*:121-130.

Roeper, H. 1991. Selective oxidation of D-glucose: chiral intermediates for industrial utilization. Lichtenhaler FW (ed) Carbohydrates as organic raw material. Verlag Chemie, Weinheim:267-288.

Rossmann, M. G., A. Liljas, C. I. Brändén, and L. J. Banaszak. 1975. Evolutionary and structural relationships among dehydrogenases. *In The Enzymes* **11**:61–102.

Sambrook, J., E. F. Fritsch, and T. Maniatis. 1989. *Molecular cloning: a laboratory manual. 2nd ed.*

Schäfer, A., S. Bieg, A. Huwig, G. W. Kohring, and F. Giffhorn. 1996. Purification by immunoaffinity chromatography, characterization, and structural analysis of a thermostable pyranose oxidase from the white rot fungus *Phlebiopsis gigantea*. *Appl. Environ. Microbiol.* **62**:2586-2592.

Schenk A., H. Weingart, and M. S. Ullrich. 2008. Extraction of high-quality bacterial RNA from infected leaf tissue for bacterial in planta gene expression analysis by multiplexed fluorescent Northern hybridization. *Mol. Plant Pathol.* **9**:227-235.

Scheuermann, R., S. Tam, P. M. J. Burgers, C. Lu, and H. Echols. 1983. Identification of the epsilon-subunit of *Escherichia coli* DNA polymerase III holoenzyme as the dnaQ gene product: a fidelity subunit for DNA replication. *Proc. Natl. Acad. Sci. USA* **80**:7085-7089.

Schulz, G. E., R. H. Schirmer, and E. F. Pai. 1982. FAD-binding site of glutathione reductase. *J. Mol. Biol.* **160**:287-308.

Schulz, G. E., R. H. Schirmer, W. Sachsenheimer, and E. F. Pai. 1978. The structure of the flavoenzyme glutathione reductase. *Nature* **273**:120-124.

Shiganawa, E., T. Chiyonobu, K. Matsushita, O. Adachi and M. Ameyama. 1978. Distribution of gluconate reductase dehydrogenase and ketogluconate reductases in aerobic bacteria. *Agric. Biol. Chem.* **42**:1055-1057.

Shin, K. S., H. D. Youn, Y. H. Han, S. O. Kang, and Y. C. Hah. 1993. Purification and characterization of D-glucose oxidase from white-rot fungus *Pleurotus ostreatus. Eur. J. Biochem.* **215**:747–752.

Spadiut, O., C. Leitner, T. Tan, R. Ludwig, C. Divne, and D. Haltrich. 2008. Mutations of Thr169 affect substrate specificity of pyranose 2-oxidase from Tametes multicolor. *Biocatalysis and Biotransformations* **26**:120-127.

Suye, S., and S. Inuta. 1991. A glucose sensor using pyranose oxidase from *Polyporus obtusus* ATCC-26733. Denki Kagatu, **59**:152-156.

Taguchi, T., K.Ohwaki, and, J. Okuda. 1985. Glucose-2-oxidase (*Coriolus versicolor*) and its application to D-glucose colorimetry. *J. Appl. Biochem.* **7**:289-295.

Takakura, Y., and S. Kuwata. 2003. Purification, characterization, and molecular cloning of a pyranose oxidase from the fruit body of the basidiomycete *Tricholoma matsutake. Biosci. Biotechnol. Biochem.* **67**:2598-607.

Tanabe, T., Y. Umegae, Y. Koyashiki, Y. Kato, K. Fukahori, S. Tajima, and M. Yabuuchi. 1994. Fully automated flow-injection system for quantifying 1,5-anhydroglucitol in serum. *Clin. Chem.* **40**:2006-2012.

ten Have, R., and P. J. M. Teunissen. 2001. Oxidative mechanisms involved in lignin degradation by white-rot fungi. *Chem. Rev.* **101**:3397-3413.

Thomas, J. G., A. Ayling, and F. Baneyx. 1997. Molecular Chaperones, Folding Catalysts, and the Recovery of Active Recombinant Proteins from *E. Coli. Appl. Biochem. Biotech.* **66**:197-238.

Vandamme, E. J., and W. Soataert. 1995. Biotechnical modification of carbohydrates. *FEMS Microbiol. Rev*.**16**:163-186.

Vecerek, B., H. Maresova, M. Kocanova, and P. Kyslik. 2004. Molecular cloning and expression of the pyranose 2-oxidase cDNA from Trametes ochracea MB49 in *Escherichia coli. Appl. Microbiol. Biotechnol.* **64**:525-530.

Volc, J., and K.-E. Eriksson. 1988. Pyranose 2-oxidase from *Phanerochaete chrysosporium. Methods Enzymol.* **161**:316–322.

Volc, J., N. P. Denisova, F. Nerud, and V. Musilek. 1985. Glucose-2-oxidase activity in mycelial cultures of basidiomycetes. *Folia Microbiol.* (Praha) **30**:141-147.

Volc, J., E. Kubatova, G. Daniel, and V. Prikrylova. 1996. Only C-2 specific glucose oxidase activity is expressed in ligninolytic cultures of the white rot fungus *Phanerochaete chrysosporium. Arch. Microbiol.* **165**:421-424.

Volc, J., E. Kubatova, G. Daniel, P. Sedmera, and D. Haltrich. 2001. Screening of basidiomycete fungi for the quinone-dependent sugar C-2/C-3 oxidoreductase, pyranose dehydrogenase, and properties of the enzyme from *Macrolepiota rhacodes. Arch. Microbiol.* **176**:178-186.

Volc, J., E. Kubatova, P. Sedmera, G. Daniel, and J. Gabriel. 1991. Pyranose Oxidase and Pyranosone Dehydratase - Enzymes Responsible for Conversion of D-Glucose to Cortalcerone by the Basidiomycete *Phanerochaete-Chrysosporium. Arch. Microbiol.* **156**:297-301.

Volc, J., E. Kubatova, D. A. Wood, and G. Daniel. 1997. Pyranose 2-dehydrogenase, a novel sugar oxidoreductase from the basidiomycete fungus *Agaricus bisporus. Arch. Microbiol.* **167**:119-125.

Volc, J., C. Leitner, P. Sedmera, P. Halada, and D. Haltrich. 1999. Enzymatic formation of dicarbonyl sugars: C-2 oxidation of 1 - 6 disaccharides gentiobiose, isomaltose and melibiose by pyranose 2-oxidase from Trametes multicolor. *J. Carbohyd. Chem.* **18**:999-1007.

Volc, J., P. Sedmera, V. Havlicek, V. Prikrylowa, and G. Daniel. 1995. Conversion of D-glucose to D-erythro-hexos-2,3-diulose (2,3-keto-D-glucose) by enzyme preparations of the basidiomycete *Oudemansiella mucida*. Carbohydr. Res. **278**:59–70.

Volc, J., P. Sedmera, P. Halada, P. Dwivedi, and M. Costa-Ferreira. 2003. Conversion of D-galactose to D-threo-hexos-2,3-diulose by fungal pyranose oxidase. *J. Carbohyd. Chem.* **22**:207-216.

Wierenga, R. K., J. Drenth, and G. E. Schulz. 1983. Comparison of the three-dimensional protein and nucleotide structure of the FAD-binding domain of p-

hydroxybenzoate hydroxylase with the FAD- as well as NADPH-binding domains of glutathione reductase. *J. Mol. Biol.* **167**:725-739.

Wierenga, R. K., P. Terpstra, and W. G. Hol. 1986. Prediction of the occurrence of the ADP-binding beta alpha beta-fold in proteins, using an amino acid sequence fingerprint. *J. Mol. Biol.* **187**:101-107.

Yabuuchi, M., M. Masuda, K. Katoh, T. Nakamura, and H. Akanuma. 1989. Simple enzymatic method for determining 1,5-anhydro-D-glucitol in plasma for diagnosis of diabetes mellitus. *Clin. Chem.* **35**:2039–2043.

Yamada, H., k. Ikuza, K. Aida, and T. Uerama. 1967. Enzymatic studies on the oxidation of sugars and sugar alcohols.III. Purification and properties of L-sorbose oxidase. *J. Biochem.* **62**:223-229.

Yamada, H., N. Mori, and Y. Tani. 1979. Properties of Choline Oxidase of Cylindrocarbon-Didymum-M-1. *Agric. Biol. Chem.* **43**:2173-2177.

Yamanouchi, T. I., E. Ogata, A. Kashiwabara, N. Ogata, N. Sekino, T. Yoshimura, K. Ichiyanagi, and T. Kawasaki. 2001. Post-load glucose measurements in oral glucose tolerance tests correlate well with 1,5-anhydroglucitol, an indicator of overall glycaemic state, in subjects with impaired glucose tolerance. *Clin. Sci.* **101**:227–233.

Yum, D. Y., B. Y. Lee, D. H. Hahm, and J. G. Pan. 1998. The yiaE gene, located at 80.1 minutes on the *Escherichia coli* chromosome, encodes a 2-ketoaldonate reductase. *J. Bacteriol.* **180**:5984-5988.

Yum, D. Y., S. S. Bae, and J. G. Pan. 1998. Purification and characterization of the 2-ketoaldonate reductase from *Brevibacterium ketosoreductum* ATCC2191. *Biosc. Biotech. Bioch.* **62**:154-156.

Zhou, M., Z. Diwu, N. Panwuck-Voloshina, and R. P. Haughland. 1997. A stable non-fluorescent derivative of resofurine for the fluorometric determination of trace hydrogen peroxide: applications in detecting the activity of phagocyte NADPH oxidase and other oxidases. *Anal. Biochem.* **253**:162-168.

Zhou, M., and Z. Hatahet. 1995. An improved ligase-free method for directional subcloning of PCR amplified DNA. *Nucleic Acids Res.* **23**:1089–1090.